DEVELOPMENT OF THE FULL HEIGHT TRUSS FRAME

A Thesis
Presented to
The Academic Faculty

By

Joel Christopher Gordon

In Partial Fulfillment
Of the Requirements for the Degree
Master of Science in Civil Engineering

Georgia Institute of Technology
August 2005

DEVELOPMENT OF THE FULL HEIGHT TRUSS FRAME

Approved by:

Dr. Stan D. Lindsey, Chair
School of Civil and Environment Engineering
Georgia Institute of Technology

Dr. Roberto T. Leon
School of Civil and Environment Engineering
Georgia Institute of Technology

Dr. David W. Scott
School of Civil and Environment Engineering
Georgia Institute of Technology

Date Approved: May 5. 2005

ACKNOWLEGEMENT

First, I give thanks to God, without whom I would not have had the ability or the opportunity to attempt this thesis. I thank my advisor, Dr. Stan Lindsey, for the priceless mentoring he has given me during this research and my stay at Georgia Tech. I also give thanks to Dr. David Scott for answering my questions and offering his guidance these past semesters and to Dr. Roberto Leon for improving the quality of my work. My parents, Sherry and Robert Meade and Richard Gordon, deserve ample thanks for the sacrifices they have made on my education and the patience they have shown me throughout my life. Lastly, I thank my beautiful, soon to be wife, Sarah Malone, whose part in my own success is so vast I cannot measure.

TABLE OF CONTENTS

LIST OF TABLES

LIST OF FIGURES

SUMMARY

The full height truss frame (FHTF) is an exciting new residential framing system in response to the need for low floor-to-floor steel construction. The FHTF has the potential to provide low floor-to-floor heights, a column free first floor area, an integrated frame that uses the entire height to resist loads, and the capacity to resist both gravity and lateral loads.

Because of its configuration, the full structural height can be used to resist loads. A FHTF is made up of stacked floor trusses that result in one full height truss spanning the entire width of the building. The FHTF is constructed in a conventional manner one floor at a time. The strength, inertia, and truss height will increase as each floor is added. Therefore, the construction sequence (stages) will affect the final stresses in the members.

The purpose of this thesis was to analyze and design two prototype FHTFs, to compare the economy of the prototypes with similar staggered truss frames, and to develop an approximate method to calculate staged member stresses. Each prototype was analyzed according to ETABS Nonlinear v8.4.3 (CSI, 1984-2004), a computer program that is commonly used by practicing engineers, and designed according to the 2001 American Institute of Steel Construction (AISC) Load and Resistance Factor Design (LRFD). The prototypes were used to assess the strength and serviceability of the structures, and the results of the staged analysis were used to validate the numerical method developed to approximate a staged loading sequence based on the non-staged dead load results.

The results of the analysis and design of the prototypes was the initial step in confirming the viability of the FHTF for use in the residential multistory market. FHTFs can be designed with preexisting procedure, and are capable of offering low floor-to-floor heights. The prototypes exhibited excellent lateral stiffness against wind loads. The numerical method for estimating the staged dead load accurately approximated the results of the analysis preformed by ETABS. The numerical method can be used to simulate a variety of sequences in order to optimize the stages. Lastly, the FHTF was shown to be competitive with the staggered truss systems in terms of material usage, fabrication, and construction.

CHAPTER 1

INTRODUCTION

There are a variety of structural steel systems available for use in multi-story residential construction. Typical examples include convention beams and girders, Girder-Slab™, staggered truss, and stub girder. Conventional beams and girders are not typically used in multi-story residential construction due to the depth and large weight of the members that would be required. The Girder-Slab is a patented framing and floor system developed in the 1990's to compete with the cast-in-place concrete industry. The staggered truss is a non-patented efficient framing system developed in the 1960's, but has never seen widespread use. However, the system has recently gained attention as it has been used to build a number of mid-rise hotels, apartments, and dormitories (Brazil, 2000; Faraone, 2003; Faraone and Marstellar, 2002; Levy, 2000; Pollak, 2003). AISC published a Design Guide Series on the staggered truss in 2002. The stub girder system was developed in the early 1970's primarily for office construction, but it no longer competes economically in today's construction market due to high labor costs and was never successfully used in residential construction due to the large floor depths. Each of these systems is shown in Figure 1.1.

The staggered truss is the only practical non-patented structural steel framing system offering low floor to floor heights. In the majority of regions, post-tensioned or conventionally reinforced flat plate concrete construction usually costs less than the staggered truss solution. Thus, there is a need for new, economical non-patented steel

systems to compete with the flat plate structures that currently dominate the residential market.

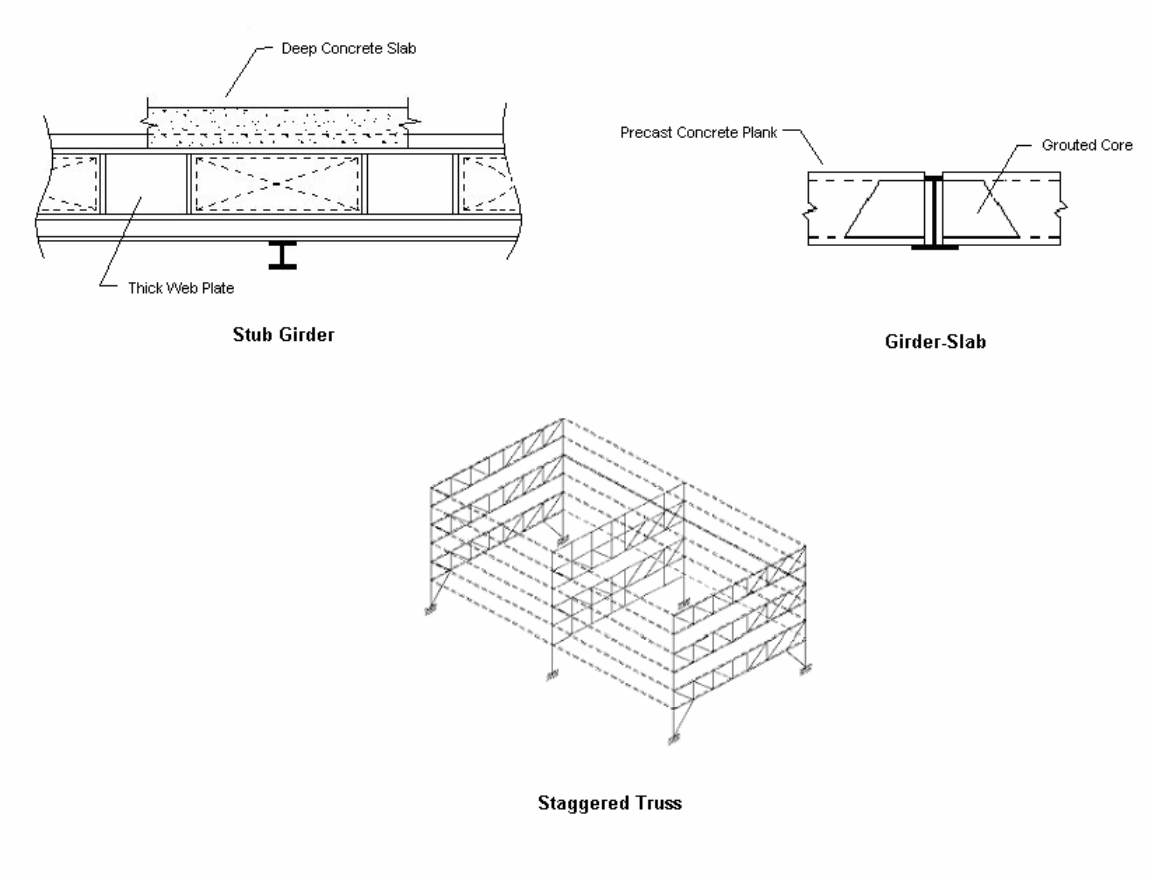

Figure 1.1 Steel Framing Systems

The major benefits of concrete flat slab construction include low floor to floor heights due to a shallow slab thickness, the use of the underside of the slab as a ceiling, and large column free areas. Also, the flat slab system provides the required fire rating, minimizes floor vibration, and absorbs sound. Efficient steel framing systems can offer the same advantages plus other benefits. If the steel framing system is appropriately used, the structural frame can blend to the building plan without interfering with the buildings use. Steel framing typically results in significantly lighter structures and faster construction.

These translate to a savings in foundation size, a reduction in seismic load, and less overall construction time. The owner gets a less expensive structure, and he gets it faster, meaning greater economy.

The Full Height Truss Frame (FHTF) is one solution to the steel industry's need. The FHTF can provide low floor to floor heights, a column free first floor area, a frame that uses the entire height to resist loads, and the capacity to resist both gravity and lateral loads without addition structural elements. In its simplest form, the FHTF is a combination of floor high trusses with Vierendeel panels (Taranath, 1997) in the center and diagonals running from floor to floor on either side as depicted in Figure 1.2. Essentially, each of the two sections with diagonals leans on the other, and the Vierendeel panel ties them together. All the connections are pinned except the Vierendeel panels and exterior columns. The layout of the frame easily lends itself to the architectural configurations of residential and hotel buildings.

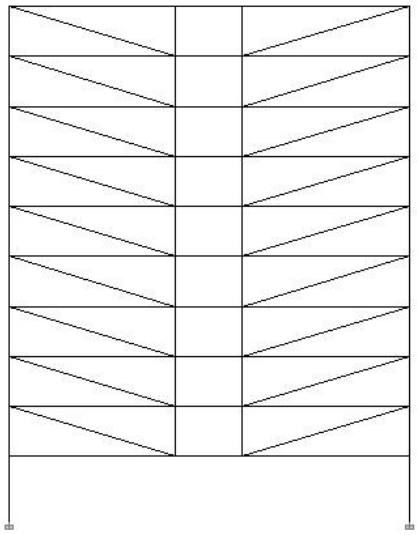

Figure 1.2 Typical Full Height Truss Frame

The FHTF is able to match the staggered truss in economy and floor height. Unlike the staggered truss that requires the trusses to transfer lateral loads to other lateral resisting systems, the FHTF can be designed to resist these loads. The staggered truss system creates a two-bay column free space at the cost of large diaphragm forces between the trusses and large lateral forces at the lowest column. For many residential systems, the two-bay column free space is unneeded. The FHTF uses stacked floor trusses that when fully erected result in one full height truss spanning the entire width of the building. Because of this configuration, large diaphragm forces between frames are not created and the full structural height can be used to resist loads.

The FHTF is constructed in a conventional manner one level or a group of level at the same time. The lowest section spans the complete width of the building, and it would be designed to support its weight and the weight of the first group of floor trusses that are erected before that addition of the floor system. Temporary erection bracing would be used between adjacent bays while the floor system was placed. The temporary bracing could be reused as more truss levels are added. The strength, inertia, and truss height will increase as each floor is added. This is illustrated in Figure 1.3. Therefore, the distribution of forces follows a staged analysis for the self weight of the frame and flooring system; however, all the superimposed dead and live loads, as well as lateral loads, will be resisted by the full height of the building.

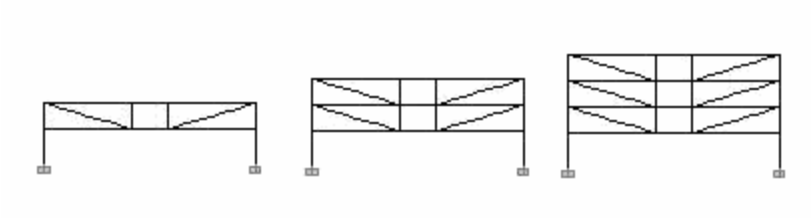

Figure 1.3 Example Construction Sequence of a FHTF

The FHTF is a combination of valid structural concepts that forms an innovative scheme. Floor high trusses have been used in framing systems before, most notably the staggered truss. Sequential design and construction are used in high-rise projects, and many commercially available computer programs are capable of staged analysis. High-rise buildings typically use multi-story systems to resist both gravity and lateral loads. The goal of this research is to develop analysis approaches and design models to develop the FHTF such that it can be implemented by the design community.

1.1 Research Objectives

The purpose of this thesis is to research and develop guidelines for the analysis and design of the full height truss frame and validate its viability to compete in the residential multi-story market. Specifically:

- Develop relationships between sequential analysis and full height analysis that will allow a safe and economical design.
- Address serviceability concerns, including drift, member deflection, truss deflection, and appropriate camber.

- Establish an economical configuration of members for the heights, spans, and loading.
- Develop an accurate analysis model that can be used with LRFD design procedure.
- Evaluate lowest external column configuration for force levels in columns.

The outcome of this research will provide the basic analysis and design procedure for the FHTF.

Two FHTF prototypes are designed and analyzed: a 10 story and a 25 story frame. The layout is the same for each frame. The plan consists of a 12 foot wide corridor with 30 foot wide residential units on either side, creating a 72 foot span for the floor trusses. The bay arrangement is typical for high rise residential construction, but the overall span of 72 feet is longer than many residential or hotel structures. Typical spans generally do not exceed 60 to 62 feet. A span of 60 feet would lead to greater economy of material usage due to the shorter exterior beam span. Because these beams are loaded under combined flexural and large axial compression at the lower levels, their capacity is closely related to their buckling length and span. The longer span was chosen to illustrate the economy of the FHTF. The first floor height is twelve feet with all the above floors having a height of nine feet. The members used in the prototypes were sized based on the analysis results and the guidelines of LRFD (AISC, 1992; AISC, 2001).

Full height and sequential analysis were preformed on each of the prototypes using ETABS Nonlinear v8.4.3 (CSI, 1984-2004). ETABS was chosen to perform the analysis because it is a commonly used design program by practicing engineers. Like most analysis programs, ETABS is capable of analyzing sequential construction loads while considering the deformed shape at each stage. ETABS can also account for nonlinear effects as specified by the user.

This design is for areas of low seismic activity. Due to limited data, a seismic response modification factor, R, of 3 can be conservatively taken as 3 in these areas, meaning no special seismic detailing is required. This is consistent with the approach that is recommended for the staggered truss system (AISC, 2002). For areas of high seismicity, the system should be evaluated. The FHTF will probably behave as a combination of a braced and moment resisting system, implying an R value much greater than 3.

1.2 Thesis Organization

Chapter two is a review of the structural concepts and considerations of the FHTF. A brief discussion of the following topics are addressed: force resisting systems of tall buildings, the leaning concept behind the FHTF model, other residential framing systems including the staggered truss and the Girder-Slab, staged analysis based on construction sequence, and column stability concerns. Chapter three focuses on the design and analysis procedure for the prototype structures. Chapter four and five discuss the design results of the prototypes; Chapter four is devoted to the 10 story frame and Chapter five

to the 25 story. Chapter six presents the conclusions of this study, including a list of additional research that can be done to further the understanding of FHTF systems.

CHAPTER 2

REVIEW OF THE STRUCTURAL CONCEPTS BEHIND THE FHTF

In building design, it is not uncommon for the gravity loads to be carried by one structural system and the lateral loads by another. Conventional steel gravity systems consist of columns and beams. The floor system transfers the gravity loads to a beam or girder which takes it to the columns through bending action. The lateral loads are resisted through a series of rigid connections between the beams and the columns, a separate bracing system, or a combination of lateral force resisting elements.

The Full Height Truss Frame (FHTF) once constructed carries both the vertical loads and lateral loads through the action of the entire frame. When any floor is loaded, all diagonals are stressed to resist the load. The diagonals transfer the gravity load directly to the exterior columns. The lateral load is carried down the frame through the diagonals. At the bottom level where there is no diagonal, the lateral load is transferred to the column as shear and into the foundation through bending. The overturning moment is resisted by the tension and compression couple between the columns. Because most members transfer the loads in direct axial stress, the FHTF is notably stiff.

This Chapter outlines the concepts behind the FHTF, how they have been used before, and their effectiveness. These concepts are crucial to understanding the behavior of the system, and the behavior is crucial to its analysis and design.

2.1 Tall Buildings: Force Resisting Systems

Structures must be able to resist two directions of loading: vertical (gravity) and lateral (wind and earth quake). Lateral load resisting systems resist the loads similar to a cantilever beam. The lateral load tries to push the structure over; therefore, the system must resist the bending and shear by cantilevering from the foundation. The ideal system to resist these effects would be one with a continuous vertical element located at the furthest extremity from the geometric center of the structure: a solid perimeter tube. Optimized lateral steel systems are skeletal framing schemes that mimic this ideal where the entire structure is designed to act as one unit to resist the lateral loads.

The framed tube system is an example of this idea put to practice (Taranath, 1997). This system was developed by Fazlur Khan in the 1960's for application to buildings over forty stories. The system consists of closely spaced columns and deep beams around the facade of the building causing it to act as a tube. A variety of improvements have been made on the original system, but the driving concept behind the modifications remains a beam and column approach. The lateral loads are carried by the columns and beams around the perimeter of the building, while part of the gravity loads are supported on framing around and in the core. This type of arrangement is not efficient because the gravity loads should be carried by the lateral system to counter the tensile stress in the columns caused by the lateral loads. This inefficiency led to the transfer floor concept. Here gravity loads are transferred at an interval of stories to the columns of the lateral force resisting system. This transfer allows the lateral system to be used to carry most of the gravity loads (Connor and Pouangare, 1995).

The beam and column approach relies on the stresses to be carried through the bending action of the members. However, forces are more efficiently resisted through axial stresses. This concept is illustrated in Figure 2.1. Consider structure 1, member AB carries a portion of the load in shear, while member BC carries the rest in direct stress. The portion each carries is related to the square of the radius of gyration, r, and the length of the members, L. The relationship is:

$$P_{BC} = F\left(\frac{1}{1+\frac{3r^2}{L^2}}\right) \tag{2-1}$$

$$V_{AB} = F\left(\frac{\frac{3r^2}{L^2}}{1+\frac{3r^2}{L^2}}\right) \tag{2-2}$$

where

F = force acting on structures at point B

P_{BC} = axial force in member BC

V_{AB} = Shear force in member AB

For typical steel structural shapes $r^2/L^2 << 1$. For example, two W8x10, $r = 3.22$ inches, with a length of 12 feet in the configuration of Structure 1 would result in member BC carrying more than 660 times the axial load than that carried by member AB in shear.

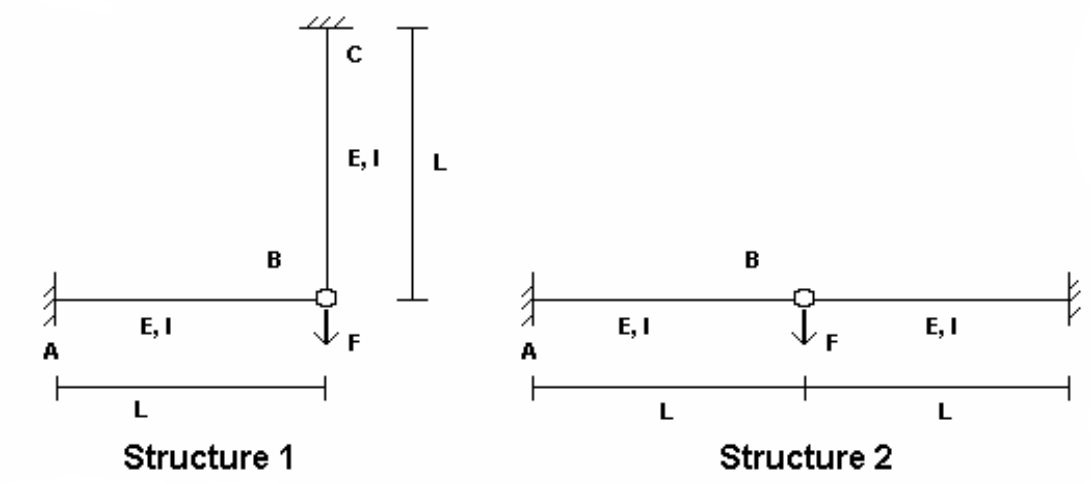

Figure 2.1 Illustration of the Efficiency of Direct Stress Compared to Bending

Now consider structure 2 with similar members and lengths. Structure 2 is identical to Structure 1 except member BC is changed from an axial member to a bending member. By symmetry, each member carries half the load to the support through bending action. When member BC is an axial member (Structure 1), it will carry nearly double the amount of force than its counter part in Structure 2. When BC is changed to a flexural member (Structure 2), the deflection at point B will increase over 330 times under the same load. This behavior advantage of axial members is the foundation for cable-stayed and space-truss bridge systems used for over a hundred years.

Space-truss systems are 3-dimensional trusses made up of planer (exterior) and interspatial (interior) diagonals. By carrying both the vertical and lateral loads axially, space-truss systems are extremely stiff. But because of the extensive usage of diagonals, the implementation of space-truss into building design has been slow (Connor and Pouangare, 1995).

Space-truss building design is an evolution, from the framed tube, to allow building heights greater than one thousand feet. The interior and exterior diagonals form a cantilever space-truss with extraordinary vertical and horizontal stiffness capable of resisting high lateral loads. Space-truss systems are made of multistory modules. Each module is comprised of four large perimeter columns and multiple interior columns all interconnected by exterior and interior diagonals. An example of a module is shown in Figure 2.2. These modules are then stacked on one another to create the complete structure. These modules resist both the gravity and lateral loads almost entirely in direct axial stress, and the diagonals force the gravity load to flow towards the perimeter columns. The major draw back is the interior diagonals that can limit the use of the plan (Connor and Pouangare, 1995).

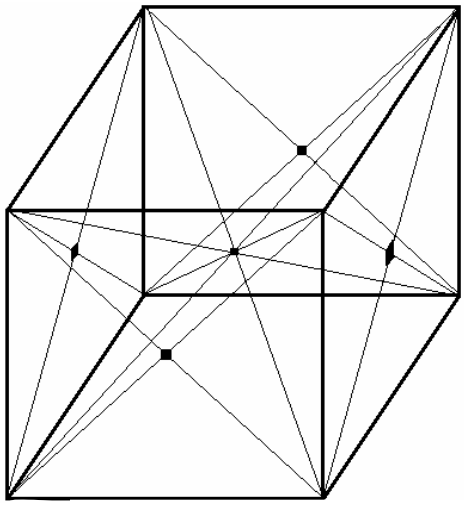

Figure 2.2 Space-Truss Interior and Exterior Diagonals

The Bank of China Tower in Hong Kong utilizes a space-truss system to carry the majority of lateral and gravity loads. A cross-braced space truss supports almost the full

weight of the seventy story structure and resists the entire wind load. The truss transfers these loads to large composite columns at the four corners of the building (Taranath, 1997).

Once a building reaches a certain height, the design is controlled more by the lateral loading than the gravity loads. Tube and space-truss systems allow buildings to reach such a height that the deflection and stiffness requirements of the lateral load control the design. The FHTF's best application occurs where vertical loading contributes to the majority of the design, but the FHTF still incorporates many of the aspects that make the truss tube and space-truss system economical: carrying the majority of loads in direct axial stress, directing vertical loads to the outer columns, and using one system to carry both the vertical and lateral loads.

2.2 Leaning Concept: the Origin of the FHTF

The fundamental behavior of the FHTF is based on a simple leaning model. The two outer bay panels of the frame "lean" on each other when loaded with gravity loads as shown in Figure 2.3 (a). The horizontal corridor frame members then provide the stabilizing force to the exterior bay panels shown in Figure 2.3 (b). A diagonal is then used to stiffen the bay panel against gravity and lateral load. These diagonals provide virtually all the vertical and lateral stiffness of the frame. Typically the span of the exterior bays is larger than the interior corridor bay. With the presence of the diagonals, the panels form a truss. The connections of the outer panel members are designed to be flexible, but the inner panel, where there is no diagonal, must be moment connected

because the lateral force is transferred by the bending of the Vierendeel panel. Essentially, the three panels are part of a story deep truss that spans the width of the building.

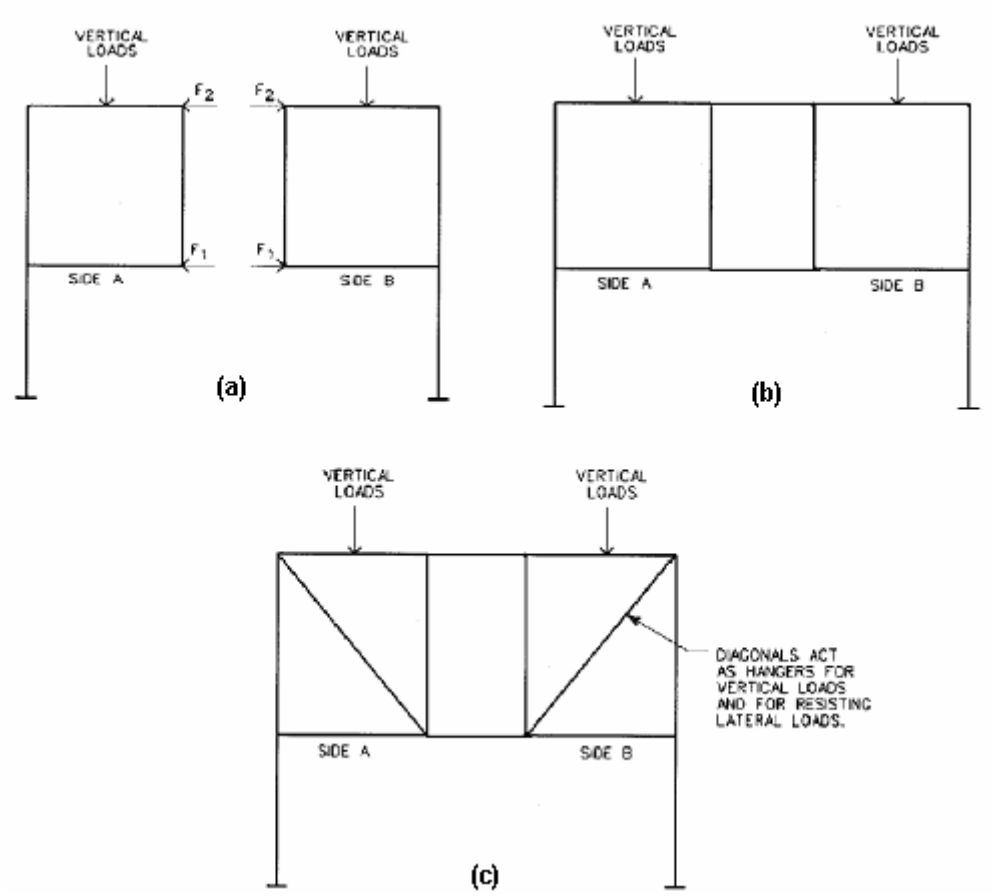

Figure 2.3 Evolution of the "Leaning" Concept

This type of story deep truss is very similar to the staggered truss model. But the basic truss from these framing systems will typically have more panels that span smaller distances. The most notable difference between the trusses of the FHTF compared to the staggered truss is that the story deep trusses of a FHTF will "stack", and the depth of the final truss will be the complete height of the building.

2.3 Staggered Truss System

The staggered truss was originally developed at MIT in the 1960's. The system is efficient for mid-rise residential buildings, but has seen limited use. It was designed to efficiently distribute wind loads while providing a versatile floor layout with large column free areas. It uses alternating story-high trusses that span the complete width of the building. This creates column free areas the size of two bays. An example of the staggered truss is illustrated in Figure 2.4.

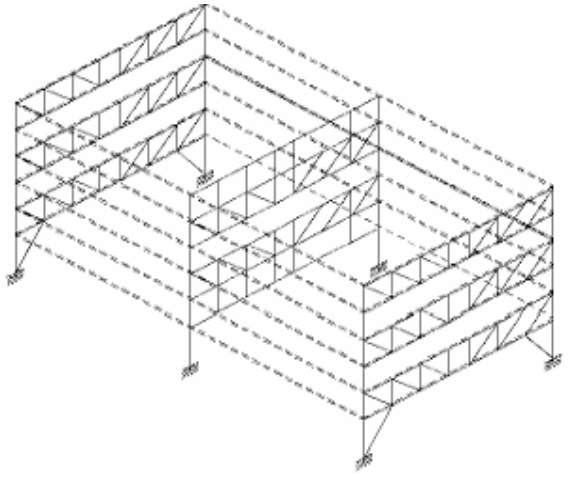

Figure 2.4 Staggered Truss Frame

Typically, there is a Vierendeel panel at the middle of the truss that serves as a corridor. Because there is no diagonal, the shear forces are carried through the bending of the panel members. If other openings are required, they can be provided at the expense of slightly weakening the structural system (the absence of a diagonal) and increasing its cost (rigidly connecting an additional panel).

The staggered truss employs story high trusses spanning in the transverse direction between exterior columns. The trusses are arranged in a staggered pattern, meaning that the floor system spans between the top chord of one truss to the bottom chord of the adjacent truss. The floor system transfers the gravity loads to trusses at both the top chord and bottom chord panel points. From the truss, the load is carried to the exterior columns. The force flow from the truss to column and column to foundation is largely direct axial stress (Cohen, 1986).

When loaded laterally, the floor system must act as a diaphragm to transfer loads between the trusses. The lateral loads are then resisted by the truss diagonals which transfer the loads directly to the columns; therefore, most columns do not develop bending moments. This allows for the column's web to be oriented perpendicular to the trusses which eliminates local bending due to the connection. This also allows for the strong-axis of the column to resist bending in the longitudinal direction (Taranath, 1997).

At the lowest level, the exterior columns connected to the second story truss must carry the lateral load collected over two bays to the foundation through bending unless an additional lateral system is used. Because the trusses are staggered, half the base columns are not loaded laterally, while the other half would carry double the load of a non staggered configuration. This usually necessitates an additional lateral system at the lowest level trusses and exterior columns to transfer the lateral forces to the foundation. The additional lateral element shown in Figure 2.4 is the extra brace from the lowest truss to the foundation along the exterior frames.

Basically, the staggered truss resists lateral loads in the transverse direction by the entire frame acting as a cantilever beam. The exterior columns act as the flange, and the trusses that span between are the web. The stiff floor diaphragm transfers the loads between adjacent trusses. This creates double-planar cantilever action which minimizes the bending in the columns (Scalzi, 1971).

The floor system must be able to collect and transmit the gravity loads to the trusses and columns and to provide adequate diaphragm action between the bottom chord of one truss to the top chord of the adjacent. Precast concrete planks are a particularly good solution for the flooring system because of their ease of erection, economy, and minimal finish required to be used as an exposed ceiling. Typically, the trusses should span at least forty-five feet to be economical (Taranath, 1997). For a typical residential building, using the staggered truss over a conventional moment-connecting frame can reduce the steel requirement by up to forty percent (Taranath, 1997).

The Staggered Truss has proven to have many advantages over a moment-connected (portal) frame. The bending action in the columns is minimized by the trusses, and the columns' strong-axis can be used to resist lateral loads in the longitudinal direction. Also the floor system can span short distances while providing two bay column free areas. Live load reduction can be maximized due to the large tributary area of the truss. Because the truss spans the full building width, the base level is column free, and the foundation can be made up of strips lying along the exterior column lines. The framing

system is resistant to drift and can fully take advantage of high strength steel members due to the majority of load being carried in direct axial stress. All of these advantages result in a significantly lighter structure when compared to steel moment-connected frames (Scalzi, 1971).

Constructing the staggered truss also has advantages over conventional frames. The reduction in steel tonnage results in smaller and easier to construct foundations resulting in greater economy. Construction can be completed quicker and with cost savings because there are fewer components to erect due to the prefabrication of trusses. The staggered truss can be erected under most weather conditions. Precast planks are lighter and more cost effective than similar flat-slab concrete floors. In addition, the low floor to floor heights reduce the buildings overall height and increase facade and structural material savings (AISC, 2002).

The staggered truss's advantages have been proven to work under real-life conditions. The staggered truss was recently implemented with great success in the Mystic Marriot Hotel and Spa located in Groton, Connecticut (Faraone, 2003). Design and construction of the New York City Embassy Suites hotel employed the staggered truss after originally trying a concrete flat-slab system (Brazil, 2000). There are many examples of the success of the staggered truss, but despite its accomplishments as a framing system, it has not seen the widespread use in high-rise residential construction that its creators initially envisioned.

2.4 Girder-Slab™ System

The Girder-Slab™ System was developed by Girder-Slab Technologies, L.L. with the goal of replacing bearing wall and plank systems with a steel and plank design (Girder-Slab Technologies, 2005). The system utilizes an open-web dissymmetric beam or D-Beam ™ that supports 8" precast hollow core concrete planks. The planks are supported on the bottom flange while the web and top flange of the D-Beam are hidden within the plane of the concrete planks as shown in Figure 2.5. This forms a composite slab that provides low floor to floor heights in a similar fashion as concrete flat-plate construction.

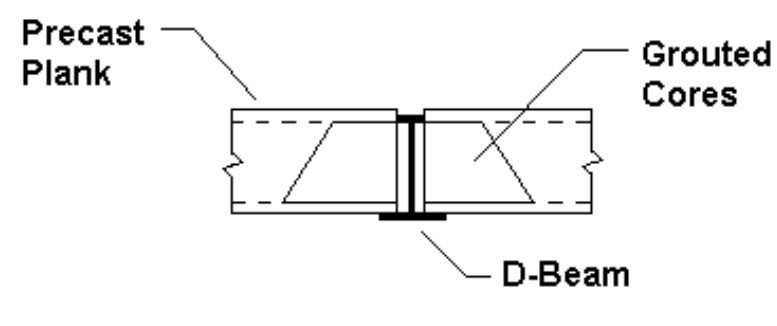

Figure 2.5 Cross-sectional View of a D-Beam

After the planks are in place, grout is injected through the web openings into the hollow cores developing composite action between the girder and the slab. Each end of the hollow core planks are capped with 8" knockouts. The knockouts are broken on site and pushed into the cores to form a dam. Steel reinforcing bars are then set between the openings in the web and grouted into place. A variety of composite D-beams have been laboratory tested; all test samples after being grouted have show composite action was achieved (Naccarato,1999). Figure 2.6 illustrates how composite action is achieved by

the D-Beam and the planks. The D-Beam typically spans 16'-0 while the precast planks are capable of spans up to 28'-0. A system of "goosenecking" the columns can allow the D-Beams to span as much as 22'. The goosenecks are extensions of the D-Beam that are moment connected to the columns and bolted to the D-Beam. An example of a goosenecked column is shown in Figure 2.7 (Veitas, 2002).

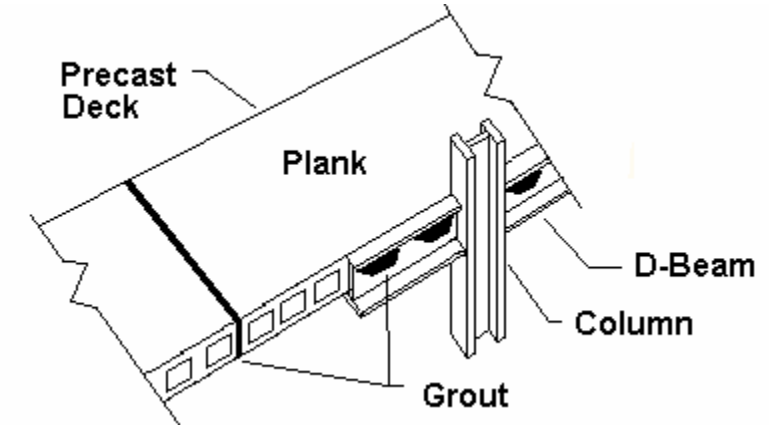

Figure 2.6 Composite Action between D-Beam and Precast Deck

The composite floor system is designed to resist all the gravity loads. Lateral Loads must be resisted by separate rigid steel frames, bracing, or both. A typical lateral system could include lateral bracing in the direction of the D-Beams and rigid connections between the columns and wide flange spandrel beams in the longitudinal direction.

The Girder-Slab System can be built quickly at low cost with prefabricated materials while maintaining low floor to floor heights (Cross, 2003; Naccaroto, 1999, 2001, 2000; Veitas, 2002). It is specifically targeted for mid to high-rise hotels, dormitories, condos, hotels, and other multi-story residential buildings. The relatively short spans of the D-

Beams are appropriate for residential construction (Naccarato, 2001). While residential units vary from floor to floor, they are typically stacked vertically for structural consistency and economy of the utilities. This feature of residential construction allows for regularly spaced partition walls that conceal the columns and cross-bracing. The Girder-Slab System can be built quickly at low cost with prefabricated materials while maintaining low floor-to-floor heights. It is, however, patented; this can cause a limitation on competition - a major drawback to the system.

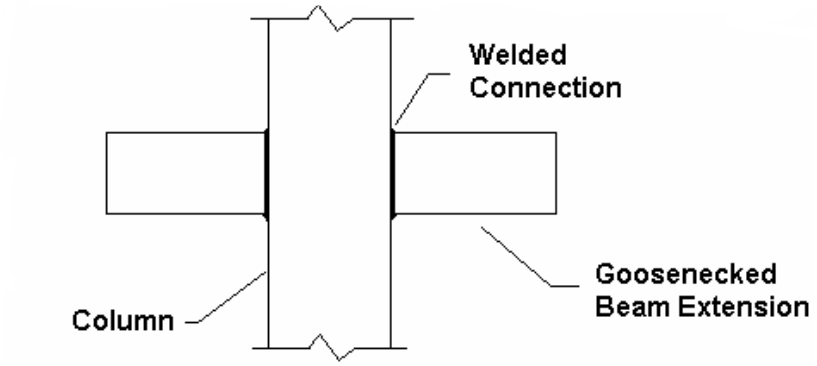

Figure 2.7 Goosenecked Beam Extension

Ultimately it is a combination of factors that determines which structural system is the best for a particular project. While height, shape, and usage lead the engineer to consider a proven system, there are undoubtedly a variety of unique considerations that will affect the structural system. Architectural constraints, owner requirements, and building location can render a structural system unacceptable for its application to a specific project. There are numerous factors that influence the selection process. These include availability of materials and labor cost, construction schedule, regional design loads,

building behavior as it relates to occupant comfort and usage, and site-specific foundation considerations. No structural framing system is the solution to all designs.

2.5 Staged Analysis

The structural analysis and design of the FHTF differs from conventional steel structures. As additional levels are built on top of the previous, the strength and stiffness increase, and the distribution of the gravity loads adjusts to the change in the number of diagonals. Therefore, it is necessary for a staged analysis to accurately determine the dead load stresses in the members. An analysis that does not consider this will underestimate the stresses in the lower members and overestimate the stress in the upper members.

The construction sequence and the application of dead load affect the force distribution and deformations of the completed structure. The stiffness and total gravity load will change as each story is added. Typically, an ordinary analysis of a conventional multistory frame under dead load will result in an exaggeration of the differential column shortening. The overstated differential shortening between the columns is a result of loading the entire structure instantly. Due to construction methods, for a conventional frame the deformations of the floor below do not affect the floor being built. Multistory Frame analysis should consider the sequential change in stiffness, configuration, gravity load, and effects of the deformed shape at each stage (Choi and Kim, 1985).

An instantaneous frame analysis of a multi-story moment frame under gravity load would result in a maximum differential shortening between the interior and exterior columns at

the top story. When the structure is fully loaded in an instant, the elastic deformations of the columns collect from the bottom to upper levels. Generally, it can be assumed that the interior columns carry approximately double the load of the exterior columns under gravity loading. In many cases, exterior columns are designed with similar cross-sections as interior columns in order to resist lateral loads. This causes significant differential shortening between the columns because the exterior columns carry significantly less axial force but have a similar cross-sectional area ($\delta = PL/AE$). The difference in shortening will cause bending moments in the rigidly connected beams at the beam-column joints. As the complete structure is instantaneously loaded, differential shortening and the induced bending moments in the columns would collect from the bottom to a maximum at the top. In reality, this is not the case (Choi and Kim, 1985).

During the construction of a typical moment frame, the structure is built either one floor or multiple floors at a time. Each floor is built on top of a previous floor which has already been loaded and gone through column shortening due to dead weight. Because each floor is leveled during its construction, the deformation that occurred in the frame before the floor's construction is irrelevant to the future floor. Using these concepts, Chang-Koon Choi and E-Doo Kim developed a method of analysis to calculated differential shortening between columns and the additional bending moments at each floor (Choi and Kim, 1985).

Their model analyzes the behavior of the frame using a sequence in the opposite order of construction - starting at the top floor and moving down. Each story of the frame is

separated into one of three categories: “active”, “inactive”, and “deactivated”. The “active” level is the one currently being analyzed, the “inactive” levels are those below the “active”, and the “deactivated” are those above the “active”. The behavior of a floor is determined using the stiffness equation:

$$P = K \Delta \tag{2-3}$$

where

K = stiffness matrix of the frame between the “active” and ground level

P = load from levels above the “active” and the self weight of the “active”

Δ = the nodal displacements

Each floor is analyzed in a similar way until all the column displacements are found (Choi and Kim, 1985). An example of this technique is illustrated in Figure 2.8. This method has been simplified by an empirical correction factor that yields similar results to the rigorous step-by-step analysis (Choi et. al, 1992; Choi and Chung, 1993).

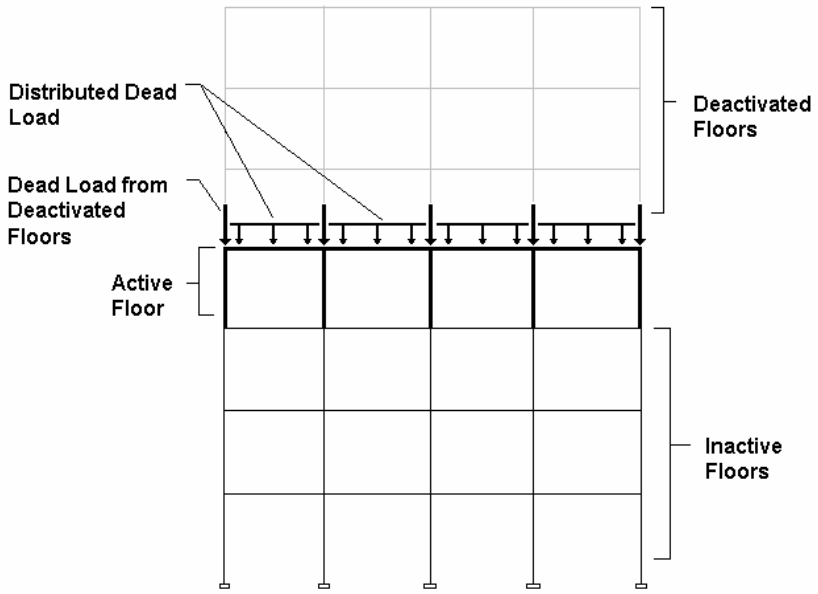

Figure 2.8 Choi and Kim’s Model for Sequential Application of Dead Load

This type of sequential analysis would not be adequate for the FHTF. Choi and Kim's model was designed for conventional framing systems where differential shortening between columns could increase the gravity load moments. There are no interior columns at the base level because a full height truss spans the complete transverse distance between exterior columns. Differential shortening between the exterior columns and vertical Vierendeel members will not induce bending moments because the beams spanning between them are designed as flexible connections. Unlike conventional frames, the staged analysis must be done in the same sequence as construction because each floor becomes part of the truss to carry the gravity loads.

The FHTF under dead load should be analyzed from the first stage of construction to the final. Because the frame acts like a truss, the distance between the bottom and top chord increases as each floor is added, changing the distribution of stresses between all the members for each stage of construction. Using this method, the first stage would be loaded and the member forces, moments, and deflected shape would be determined. The second level is then put on the deformed and stressed shape of the first and loaded. Once the results of the second stage are complete, the third level is added and loaded. This process is repeated until the structure is complete. For frames with multiply stages, the computations involved are rigorous, but there are a variety of computer programs capable of doing this. For this research, ETABS Nonlinear v8.4.3 (CSI, 1984-2004) was used.

A staged analysis was performed on the prototype frames. Comparing a full height analysis of a FHTF with a staged of the same frame reveals significant differences in the

force distribution. Typically, when sequential effects were not considered there was a more uniform distribution of axial stress. Under staged dead loading, member forces in previous stages are "locked" in and will only increase as new levels are added. This causes a disproportionate level of stress in the lower stories of the frame. A discussion of the results of sequential analysis for both the 10 story and 25 story will follow in Chapter four and Chapter five.

2.6 Column Design Considerations

Stablility is another structural consideration of the FHTF. Current methods usually begin by classifying the frame as either braced or unbraced. If the frame is designed as braced, it is assumed that there is no sidesway. If the frame is designed as unbraced, it is assumed that the frame is sidesway uninhibited. An effective length factor to estimate the buckling shape of the column is then calculated based on these assumptions.

At all levels except the lowest, the diagonals of the FHTF provide significant restraint. Traditionally, a frame with proper diagonal bracing can be considered completely braced if the stiffness of the brace at a story is greater than or equal to the critical buckling load of the column divided by its height (Cheong-Siat-Moy, 1997). The column is modeled as being restrained by a spring with its stiffness equal to that of the brace, as shown in Figure 2.9. But this would not accurately model the FHTF due to the lack of a diagonal from the lowest column to the foundation. Also, studies have shown that even when a bracing system's stiffness is greater than the critical buckling load of a column divided by its height, the resulting no sway column design can be unconservative due to an

overestimation of the K factor and buckling load of the columns (Cheong-Siat-Moy, 1997).

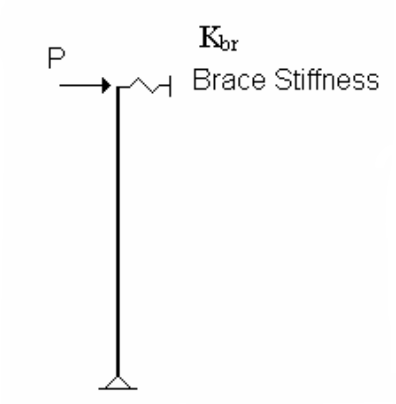

Figure 2.9 Lateral Restraint Model for a Braced Column

In order to accurately estimate the stability effects, an alternative method was used for analysis: the Direct Analysis Approach. The Direct Analysis Approach models the parameters that accurately determine frame and individual member strength within an elastic analysis thus eliminating the need for approximate methods for design such as the effective length (AISC, 2004a; AISC, 2004b; Maleck and White, 2003a; Maleck and White, 2003b; Maleck and White, 2003c). The parameters accounted for by the Direct Analysis Approach include residual stresses, initial imperfections of the members, and boundary condition effects. An inelastic stiffness reduction is applied to the stiffness, flexure (EI) or axial (EA), of members that contribute to the frame's lateral stability. For slender members this reduction is a product of a factor of safety, 0.9, and the reduction factor from the AISC column curve equation for elastic buckling E2-3, 0.877 (AISC, 2001). When applied to non slender columns, the 0.8 reduction factors accurately

accounts for inelastic softening under combined bending and compression (AISC, 2004b). An additional stiffness reduction, τ_b, is applied to the flexural stiffness of members carrying a compression load exceeding half of the yield load. An additional lateral load, the notional load, based on the gravity load is added at each level to account for the initial out-of-plumbness of the frame. These notional loads are to be considered in all load combinations based on the factored gravity load. The reduction in stiffness is only applicable to strength considerations of the analysis. The purpose of the stiffness reduction is to more accurately calculate the stresses in the member due to a second order analysis; therefore, the unreduced stiffness should be used to calculate nominal member capacities. Serviceability limitations are checked using the unreduced stiffness values; however, the notional loads are still added because they account for the frame member imperfections (Maleck and White, 2003a; Maleck and White, 2003c).

In order for the Direct Analysis Approach to accurately model the strength and stability of the frame, a second order analysis must be performed. Both the second order frame drift and the individual member deflection effects are to be accounted for unless it can be shown that the member stability effects are minimal. This approach is not recommended for frames where the second-order displacement is six times that of the first-order displacement. But for frames that do have a second-order displacement amplification factor greater than six, the changes in second-order forces due to additional notional load are large and can be excessive (Maleck and White, 2003a; Maleck and White, 2003c). The FHTF falls well within this criteria due to its lateral stiffness.

CHAPTER 3

PROTOTYPE STRUCTURES

Two prototype frames were used to assess the response of the Full Height Truss Frame (FHTF) to gravity and lateral load and to evaluate its economy compared to the staggered truss. The two prototypes were a 10 and 25 story 2-D interior frame sharing identical configuration, member connection, and dimension. The design process was iterative and performed with an advanced analysis and design program. The design loads were applied to generic members then resized according to the stress in the member. This was repeated until the analysis model matched the design model.

The gravity and wind loads were obtained from the *Minimum Design Loads for Buildings and Other Structures*, ASCE 7-02, (ASCE, 2003) and an additional notional load was calculated according to Appendix 7 of the draft *Specification for Structural Steel Buildings* (AISC, 2004a). A second order analysis was performed to determine the axial load, shear force, and moment in each frame member. The design of the columns, beams, and braces was done in accordance with the American Institute of Steel Construction (AISC) *Manual of Steel Construction: Load and Resistance Factor Design* (LRFD) Third Edition (AISC, 2001), and the analysis of the frames was performed according to Appendix 7 of the draft *Specification for Structural Steel Buildings* (AISC, 2004a).

3.1 Description of Structures

The 10 story and 25 story prototypes are interior frames of a three bay residential building spaced at 25 feet in the North-South direction. The FHTFs carry the lateral load in the East-West direction, and a separate lateral system carries the North-South direction. The North-South lateral system could be made up of a series of braces along the exterior, the corridor, or a combination of the two. The frames consist of three bays in the East-West direction: two outer bays and one interior bay spaced at 26 and 20 feet. The first story is 12 feet tall; each succeeding story height is 9 feet. The configuration lends itself to a typical residential building. The 30' x 25' (750 sq ft) area across the exterior bay and part of the interior bay are the resident units and the remaining area of the interior bay, 12' X 25', is the corridor. This configuration is shown in Figure 3.1.

The units are separated along the column line allowing the outer brace and beam to be hidden in the wall. This allows the outer bay beams to be as deep as the architectural constraints allow. At the frame line, a minimum clearance of 7'-0" must be provided along the corridor. The floor system consists of 8" precast hollow core planks and an additional 2" of concrete topping that span the 25 feet between adjacent frames. This allows the corridor beam to be up to 14" deep and still maintain the 7 feet of clearance necessary as shown in Figure 3.2.

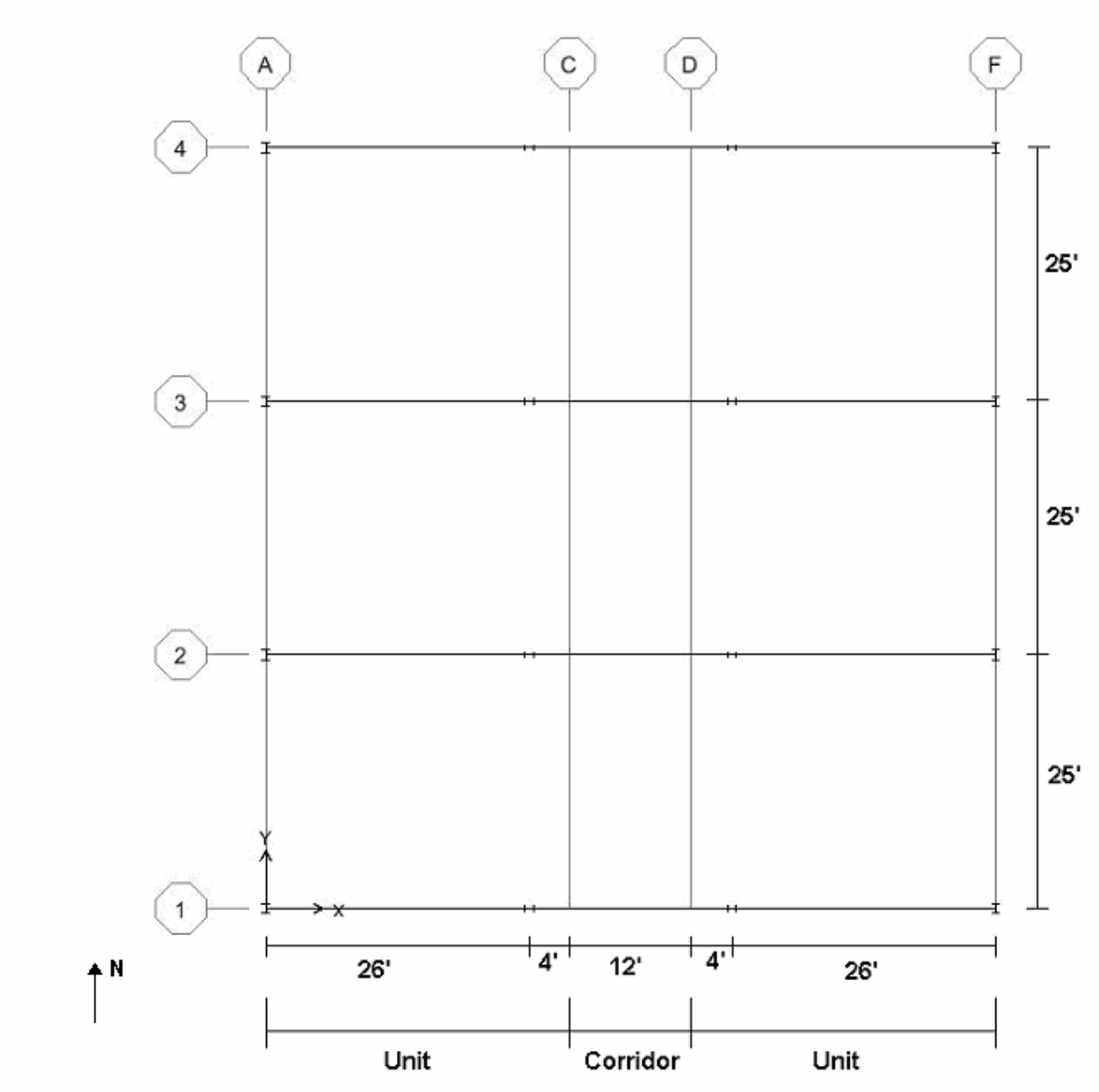

Figure 3.1 Plan and Column Orientation of Prototype Above the First Story

The prototype frames were designed to carry the lateral load without an additional lateral system at the lowest level; however, the exterior FHTFs of the building could be braced at the lowest level in the East-West direction without disrupting the column free space. This additional bracing would brace both the interior and exterior FHTFs due to the rigid diaphragm of the floor system. In this way, the bending and deflection of the lower level columns could be reduced.

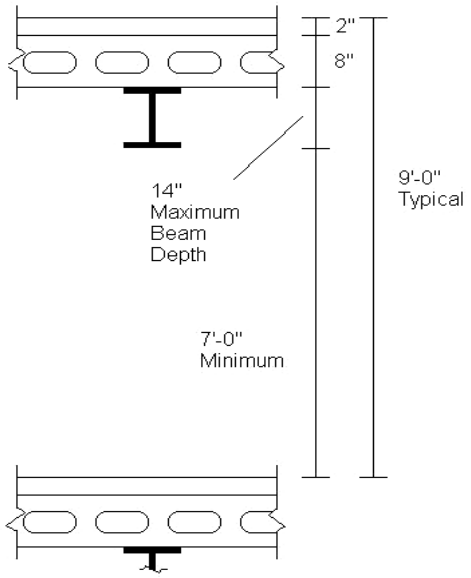

Figure 3.2 Floor Height at Cross-section of Corridor Beam

The interior and exterior beam spans are tailored to optimize the design considering a 14" deep corridor beam. This beam must span at least the required corridor width. Increasing the span of the exterior beams will allow for a shallower interior beam, but at the cost of deeper and heavier exterior beams. Because the interior beam is fixed on either end, less design bending stress is introduced compared to a pinned beam of similar span. Because the exterior beams are pinned on both ends, the span of the interior beam

should be as long as the maximum depth criterion economically permits. This will result in a lighter frame.

The span dimension of both the prototypes was chosen to be 72 feet to consider the longest extreme expected for residential hotel construction. The span is approximately 10 feet longer than typical spans of commercial configurations. The longer span of the FHTF prototypes illustrates that even with the extended span the structures remain lightweight and economical. When comparing a FHTF to the staggered truss, the FHTF is more sensitive to span increases. Typically a staggered truss will have many more panels than a FHTF, thus the spans are divided among more panels and the span of each panel is less.

All the members in the prototype frames are conventional steel W-shapes, except the first stage exterior columns of the 25 story prototype. These columns were designed as encased W-shapes in high strength concrete. Composite sections were used because of the large axial stresses in these columns and to increase the stiffness of the lowest column without increasing steel tonnage and steel section depth. The flexural stiffness of these columns used in the analysis was based on an effective moment of inertia of the equivalent steel section. All of the columns share an identical depth to avoid impractical framing between the column members; therefore, if the lowest column's depth was increased to gain flexural stiffness, all of the other column depths would be similarly increased. Preferably, the depth of the columns should be minimized; therefore large

composite columns at the first four levels are more practical than an increase in section depth of columns at every level.

The diagonals were designed as W-shapes to simplify the prototype models. Because the diagonals carry tension exclusively, steel plates, angles, channels, or HSS shapes of equal area can be used to minimize the width of these members. Depending on the direction of the lateral load, one side of diagonals is compressed, while the other side is tensioned. Compression can be introduced into the diagonals by the lateral loads, but this compression is countered by the tension caused by the gravity loads resulting in a net tensile force in the diagonals – one of the advantages of the FHTF.

When the east-west lateral load is applied to the frame, the loads are carried in direct stress to the lowest truss chord by the diagonals and then into the foundation by the bending action of the lowest exterior column. This lateral load is transferred to the column as shear by the lowest chord member of the truss. All of the exterior columns above the first story are vertical load carrying elements, thus their major axis can be oriented to resist bending normal to the truss plane. This can create a perimeter lateral force resisting system in the orthogonal direction.

The frame geometry and member configuration is symmetrical. The outer bay beams and diagonals are pinned on both ends to the exterior column and interior panel. The interior panel is comprised of the two interior columns and beams welded together to form a rigid Vierendeel truss shown in Figure 3.3. Parts of these panels could be welded by the

fabricator to reduce the number of members connected in the field and to ensure the quality of the rigid connections. A shop fabricated center panel is shown in Figure 3.4. The simple frame layout, conventional member shapes, and traditional connections reduce costs and increase the ease of construction.

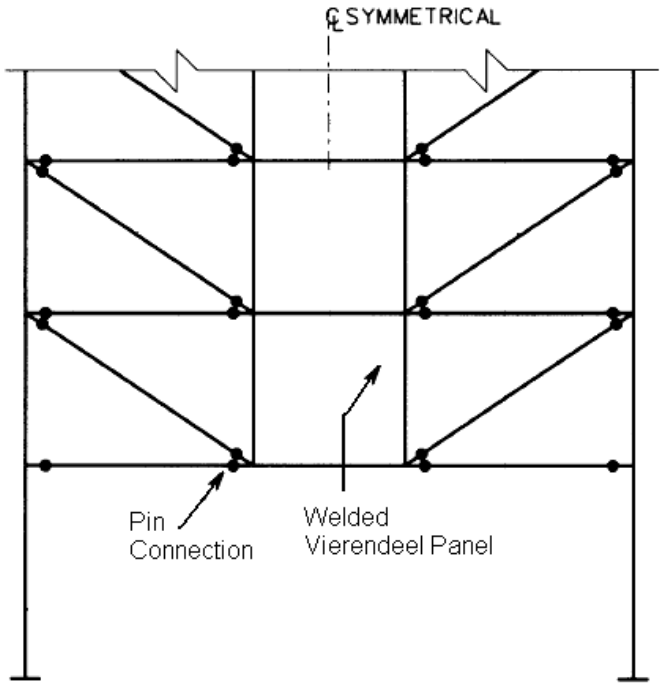

Figure 3.3 Prototype Frame Member Configuration and Connections

The erection of the FHTF follows conventional construction practices. The lowest truss section is built. For both prototype structures, all frame elements up to the fourth story comprised this first truss section. A lesser number of levels for the first truss could also be used depending on the structure. Then the levels of this first section are planked. After the first stage, each additional construction stage included the next three levels of

frame elements and then each new floor being planked. Again, the number of levels could be modified as desired.

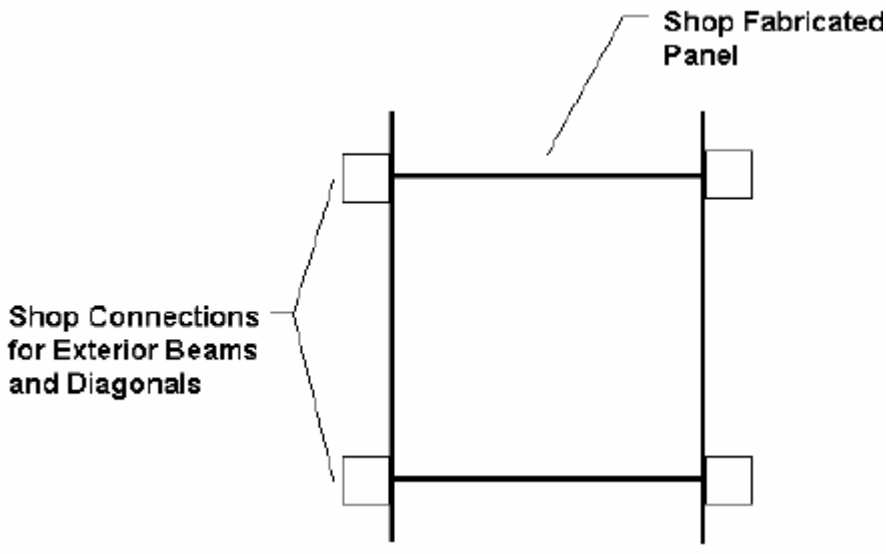

Figure 3.4 Shop Fabricated Center Panel

This type of construction sequence can be described as "static stages". Both the prototypes were erected in this manner until the full height was reached. Different construction sequences result in different economy. More frame levels present at each stage results in a more equal distribution of gravity load to the diagonals once the building is fully erected; therefore, the first stage should consist of as many levels as possible to prevent the buildup of force in the lower levels.

An alternate construction sequence to the static stages can be described as "dynamic stages". Due to limitations of ETABS, this type of sequential construction model was not used. The lowest truss section is built, and then the first floor is planked. After

planking, one or more stories of frame elements are added before the next level is planked. In this manner, the frame stays a number of stories "ahead" of the planking level until the structure is complete. The more stories the frame is "ahead" of the planking, the deeper the truss will be at each construction stage. This will bring the staged construction distribution of axial force more in line with a full height instantaneous analysis. When the staged analysis results are similar with the full height analysis, a greater economy of material usage can be achieved. Therefore if feasible, a FHTF should be constructed with the frame as many stories ahead of the planking as possible.

3.2 Gravity Loads and Load Combinations

The loading of the prototype frames was done in accordance with ASCE 7-02 for typical residential buildings. The dead load (DL) applied to the frame is made up of the weight of the floor system and the steel frame. The 8" precast hollow core planks weigh 55 psf and the additional 2" topping weighs 25 psf assuming normal weight concrete (150 pcf). The weight of the steel frame is based on the self weight of the design members. The roof dead load (D_{roof}) was 25 psf. For the partition walls, mechanical, electrical, HVAC, etc., a 15 psf superimposed dead load (SD) was applied. The nominal live load for private residential units (L_{unit}) was 40 psf. Similarly, a nominal live load ($L_{corridor}$) of 100 psf corresponded to the corridor area. The roof live load (L_{roof}) was 20 psf. For live load reduction at each level the truss was treated as one member similar to the method of live load reduction for design of the staggered truss as outlined in the *Steel Design Guide Series 14: Staggered Truss Framing Systems* (AISC, 2002). The tributary area of the

truss at each level is then 72 ft x 25 ft or 1800 sq feet. The tributary area (A_T) of the exterior columns at each level is 36 ft x 25 ft or 900 sq feet. This allows for the roof live load to be reduced to 12 psf. The other reduced live loads can then be found by:

$$LL_{reduced} = LL\left(0.25 + \frac{15}{\sqrt{K_{LL}A_T}}\right) \qquad \text{(3-1) ASCE 7-02 Eq. 4.1}$$

where

K_{LL} = Live load element factor

= 4 for exterior columns

A_T = tributary area, ^{in2}

The truss can be treated as an interior beam with a live load element factor of 2. This allows for a live load reduction of 50% to both columns and truss members. Because the columns support all the levels above, the actual tributary area is based upon the 900sq feet of all the levels the column supports. ASCE 7-02 allows for a maximum reduction of 60% for the members that support more than one story. A "compensating force" method to adjust for the difference in the live load applied to the columns and that applied to the beams is widely accepted and used (Ziemian and McGuire, 1992). This extra 10% of reduction applicable to the columns was neglected in order to simplify the analysis model. It can be argued that the full height truss supports a tributary area based upon every story of the truss. This would allow the full 60% reduction to be applied to all truss members. For the prototypes, the more conservative 50% reduction was used.

The ASCE 7-02 and LRFD guidelines for load factors and combinations were used. The load combinations are based on probability models to establish realistic strength limits that could act on the building throughout its life cycle. The following load combinations from ASCE 7-02 Sec 2.3.2 were chosen as:

1.4D	(3-2, Combination 1)
$1.2D + 1.6L + 0.5L_{roof}$	(3-3, Combination 2)
$1.2D + 1.6L_{roof} + (0.5L \textit{ or } 0.8W)$	(3-4, Combination 3)
$1.2D + 1.6W + 0.5L + 0.5L_{roof}$	(3-5, Combination 4)
0.9D +1.6W	(3-6, Combination 5)

3.3 Wind Loads

The wind loads were calculated following the procedure outline in ASCE 7-02 Section 6.5. First, the velocity pressure, q_z, was calculated at each level by:

$$q_z = 0.00256 K_Z K_{zt} K_d V^2 I \qquad \text{(3-7) ASCE 7-02 Eq. 6-15}$$

where

K_z = velocity pressure exposure coefficient evaluated at height z (ASCE 7-02 Tables 6-4 & 6-5)

K_{zt} = topographical factor (ASCE 7-02 Sec 6.5.4.4)

K_d = wind directionality factor (ASCE 7-02 Sec 6.5.4.4)

V = basic wind speed, miles per hour (ASCE 7-02 Fig 6-1)

I = importance factor (ASCE 7-02 Table 6-1)

For the design of the prototype structures, only the East-West wind force is applied to the 2-D frame model. For both prototype frames, a wind velocity, V, of 90mph; exposure C; a topographical factor, K_{zt}; an importance factor, I, equal to 1; and a wind directionality factor, K_d, of 0.85 were assumed.

Next the pressure at each story level is calculated by:

$$p_z = q_z G_f C_p \qquad \text{(3-8) ASCE Eq. 6-1X}$$

where

$G_f = 0.85$ = gust effect factor

C_p = external pressure coefficient (ASCE 7-02 Fig 6-3)

C_p equals 0.8 on the windward side and -0.5 on the leeward side. In order to calculate the wind force applied at each column floor node, the wind pressure is assumed constant over each level. Then each column floor node received the wind force based on its tributary area - half the story above and below for half the bay length on either side. Since the leeward force is a suction force, both the windward and leeward act in the same direction; therefore, the leeward can be added to the windward for analysis purposes. Table 3.1 contains for the velocity pressure exposure coefficient, velocity pressure, wind pressure, and wind loads at each story.

Table 3.1 Wind Loads (kips) for Interior FHTF at Each Story Level

			25 Story			10 Story		
Story	Story Height (ft)	q (lb/ft^2)	F wind (k)	F Lee (k)	Wind Load (k)	F wind (k)	F Lee (k)	Wind Load (k)
25	9	26.42	2.43	1.52	3.94			
24	9	26.20	4.83	3.03	7.86			
23	9	25.98	4.79	3.03	7.82			
22	9	25.76	4.75	3.03	7.78			
21	9	25.52	4.71	1.52	6.22			
20	9	25.28	4.66	3.03	7.70			
19	9	24.99	4.62	3.03	7.65			
18	9	24.68	4.56	3.03	7.59			
17	9	24.39	4.50	3.03	7.54			
16	9	24.16	4.46	3.03	7.49			
15	9	23.88	4.41	3.03	7.44			
14	9	23.49	4.35	3.03	7.38			
13	9	23.09	4.28	3.03	7.31			
12	9	22.69	4.20	3.03	7.24			
11	9	22.30	4.13	3.03	7.16			
10	9	21.96	4.06	3.03	7.10	2.02	1.26	3.28
9	9	21.54	3.99	3.03	7.03	3.99	2.52	6.51
8	9	20.97	3.90	3.03	6.93	3.90	2.52	6.42
7	9	20.34	3.79	3.03	6.82	3.79	2.52	6.31
6	9	19.71	3.68	3.03	6.71	3.68	2.52	6.20
5	9	19.04	3.56	3.03	6.59	3.56	2.52	6.08
4	9	18.22	3.42	3.03	6.45	3.42	2.52	5.94
3	9	17.27	3.26	3.03	6.29	3.26	2.52	5.78
2	9	16.00	3.05	3.03	6.09	3.05	2.52	5.57
1	12	14.98	3.30	3.54	6.84	3.30	2.94	6.24

3.4 Notional Load

In accordance with the draft *Specification for Structural Steel Buildings* (AISC, 2004) Appendix 7, an additional lateral load was added due to the geometric nonlinearities, imperfections, and inelasticity of the members used. The lateral load was applied in the same direction as the wind forces to have the most destabilizing effects. Appendix 7, outlines the Direct Analysis Method for frame stability analysis and design. The method eliminates the need for effective length factors to calculate the member buckling loads; therefore, all members are designed with an effective length factor equal to 1. A second order analysis considering both the effects due to story drift and the effects due to member deflection must be performed. The method has been verified to more accurately estimate the internal frame forces than the conventional buckling solution (Maleck and White, 2003a, 2003b, 2003c).

The additional lateral load at each level is based on the factored gravity load applied at the same level. For the notional load calculation, an average steel weight of 5 psf from the self weight of the frame was assumed to act at each level in addition to the other dead loads. The unfactored notional load contributions from the dead, live, and super dead are shown in Table 3.2:

$$N_i = 0.002Y_i \qquad \text{(3-9) AISC Eq. A-7-4}$$

where

N_i = notional lateral load applied at level I, kips

Y_i = gravity load from the LRFD load combination acting on level i, kips

Table 3.2 Notional Loads Applied at each Level

	Notional Loads (k) 25 Story Prototype			Notional Loads (k) 10 Story Prototype		
Story	**Dead**	**SDead**	**Live**	**Dead**	**SDead**	**Live**
25	0.09	0	0.0432			
24	0.306	0.054	0.09			
23	0.306	0.054	0.09			
22	0.306	0.054	0.09			
21	0.306	0.054	0.09			
20	0.306	0.054	0.09			
19	0.306	0.054	0.09			
18	0.306	0.054	0.09			
17	0.306	0.054	0.09			
16	0.306	0.054	0.09			
15	0.306	0.054	0.09			
14	0.306	0.054	0.09			
13	0.306	0.054	0.09			
12	0.306	0.054	0.09			
11	0.306	0.054	0.09			
10	0.306	0.054	0.09	0.09	0	0.0432
9	0.306	0.054	0.09	0.306	0.054	0.09
8	0.306	0.054	0.09	0.306	0.054	0.09
7	0.306	0.054	0.09	0.306	0.054	0.09
6	0.306	0.054	0.09	0.306	0.054	0.09
5	0.306	0.054	0.09	0.306	0.054	0.09
4	0.306	0.054	0.09	0.306	0.054	0.09
3	0.306	0.054	0.09	0.306	0.054	0.09
2	0.306	0.054	0.09	0.306	0.054	0.09
1	0.306	0.054	0.09	0.306	0.054	0.09

Because the flexural stiffness of the lowest two exterior columns and Vierendeel panels contribute to the lateral stiffness of the frame, they were reduced according to:

$$EI^{*} = 0.8\tau EI \qquad \text{(3-10) AISC Eq. A-7-2}$$

where

E = modulus of elasticity = 29,000 ksi

I = moment of inertia about the axis of bending, in^4

$$\tau = 1.0 \text{ for } \frac{P_r}{P_y} < 0.5 \qquad (3\text{-}11)$$

$$\tau = 4\left[\frac{P_r}{P_y}\left(1 - \frac{P_r}{P_y}\right)\right] \text{ for } \frac{P_r}{P_y} \geq 0.5 \qquad (3\text{-}12)$$

P_r = required axial compressive strength under LRFD load combination, kips

$P_y = A_s F_y$ = member yield strength, kips

A_s = area of cross-section, in^2

F_y = yield strength of steel section, ksi

Although the 2005 Specification does not address the use of composite sections with the direct analysis method, this analysis method can be used with composite structures (AISC, 2004b). The unreduced stiffness used in the analysis is based on an equivalent section of steel. While the stiffness reduction is not appropriate for the composite columns, equation 3-10 was applied. In the case of the composite columns, the member yield strength, P_y, was replaced with the nominal axial compressive strength without any buckling consideration:

$$P_0 = A_s F_y + A_{sr} F_{yr} + 0.85 A_c f_c^{'} \qquad (3\text{-}13)$$

where

A_{sr} = area of continuous reinforcing bars, in^2

F_{yr} = specified minimum yield strength of reinforcing bars, ksi

A_c = area of concrete, in^2

f_c' = specified minimum concrete compressive strength, ksi

Similarly, because the axial stiffness of the diagonals, exterior bay beams, and other exterior column contributes to the lateral stiffness of the frame, they were reduced according to:

$$EA^* = 0.8EA \qquad \text{(3-14) AISC Eq. A-7-3}$$

3.5 Second Order Effects

It is necessary to consider the second order effects on the structure due to the gravity loads in order to accurately calculate the magnitude of the internal forces of the frame. As the building sways due to lateral load, the out of plumbness of the gravity load relative to the frame causes moment amplification at joints. This is commonly referred to as the P-Δ effect. Bending of the members between joints can cause an increase in moments of individual members, known as the P-δ effect. These effects are illustrated in Figure 3.5. A second order analysis must be preformed on the structural system to account for the deformations of the structure (LeMessurier, 1976; LeMessurier, 1977; Lui, 1988).

ETABS performs an iterative analysis based on a user defined P-Δ load combination. The user determines the maximum number of iterations and the relative displacement convergence tolerance. This is the ratio of the maximum change in displacement to the largest displacement in either iteraton. The P-Δ load combination used for the analysis in both the 10 and 25 story prototype was:

$$1.2D + 0.5L + 0.5L_{roof} \tag{3-14}$$

This gravity load combination accurately accounts for moment amplification due to the overall sway of the frame from combination four (3-6), while conservatively estimating the effect in combination three (3-5) and five (3-7). For combination one (3-2) and two (3-3), the secondary effects are negligible because the only lateral load present is a small notional load with a magnitude more than 20 times less than the wind load

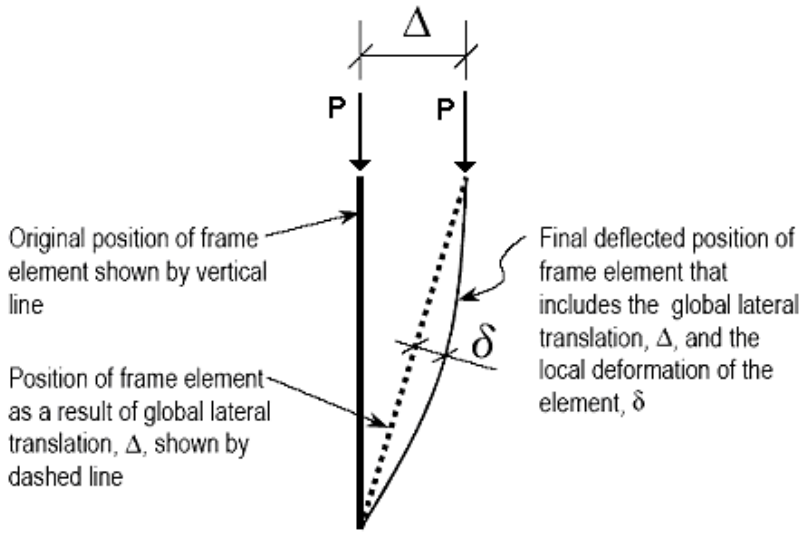

Figure 3.5 Second Order Effects on Frame Element (CSI, 1984-2004)

The P-δ effect on members between joints was not directly calculated in the analysis. ETABS second order analysis is based on an iterative approach (CSI, 1984-2004). While this method can accurately model P-Δ effects, it will not accurately capture P-δ effects unless the elements are subdivided (White and Hajjar, 1991). ETABS does not recommend subdividing elements for analysis; therefore, this effect is accounted for by factors in the design. The ultimate design moment for the members was determined according to AISC LRFD Manual (AISC, 2001):

$$M_u = B_1 M_{nt} + B_2 M_{lt} \qquad \text{(3-15) AISC Eq. C1-1}$$

where

M_{nt} = required flexural strength in member assuming there is no lateral translation of the frame, kip-in

M_{lt} = required flexural strength in member as a result of lateral translation of the frame only, k-in

$$B_1 = \frac{C_m}{1 - P_u / P_{e1}} \geq 1 \qquad \text{(3-16) AISC Eq. C1-2}$$

$$P_{e1} = \frac{\pi^2 EI}{(KL)^2} \qquad \text{(3-17)}$$

C_m = a coefficient based on elastic first-order analysis assuming no lateral translation of the frame whose value shall be taken as follows:

a) For compression members not subject to transverse loading between their supports in the plane of bending,

$$C_m = 0.6 - 0.4(M_1 / M_2) \qquad \text{(3-18) AISC Eq C1-3}$$

where M_1/M_2 is the ratio of the smaller to larger moments at the ends of that portion of the member unbraced in the plane of bending under consideration. M_1/M_2 is positive when the member is bent in reverse curvature, negative when bent in single curvature.

b) For compression members subjected to transverse loading between their supports, the value of C_m shall be determined either by rational analysis or by the use of the following values:

For members whose ends are restrained $C_m = 0.85$

For members whose ends are unrestrained $C_m = 1.00$

$$B_2 = \frac{1}{1 - \sum P_u \left(\frac{\Delta_{oh}}{\sum HL} \right)} \qquad \text{(3-19) AISC Eq. C1-4}$$

ΣP_u = required axial strength of all columns in a story, kips

Δ_{oh} = lateral inter-story deflection, in.

ΣH = sum of all story horizontal forces producing Δ_{oh}, kips

L = Story height, in.

M_{nt} is associated with the member deflection, and the amplification factor B_1 approximates the P-δ effect. M_{lt} is associated with the frame sway deflection, and ETABS directly calculates the effect of this deformation; therefore, ETABS sets B_2 equal to one (CSI, 1984-2004). The stiffness, EI, used to calculate B_1 is the reduced stiffness in accordance with Section 3.5 (AISC, 2004b). In this way, the second order effects are accounted for in frame design.

The members most influenced by their instability (P-δ effects) are unrestrained members carrying both transverse loads between supports and large axial loads. The only members of the FHTF that are transversely loaded are the interior and exterior beams. The interior beams are restrained at both ends, and the majority of these beams will not have significant axial compression. However, the exterior beams, especially in the lower levels, carry both large axial and transverse loads. The other frame members will not be notably influenced by member instability. The diagonals are only loaded in tension, while the exterior columns and Vierendeel columns under the no-sway condition develop end moments in reverse curvature, reducing C_m. The B_1 factors calculated by ETABS for each frame member are shown in Table 3.3.

These B_1 factors calculated by ETABS were verified using MASTAN2 (Ziemain and McGwire, 2000). Three of the 25 story prototype's exterior beams were modeled in MASTAN2 as shown in Figure 3.6 and subdivided into six elements. 1st and 2nd order elastic analyses were performed, and the moment amplification factor at the center span tabulated. The 2nd order analysis was a simple step method of 100 increments each with a size of 0.01. The results are shown in Table 3.4.

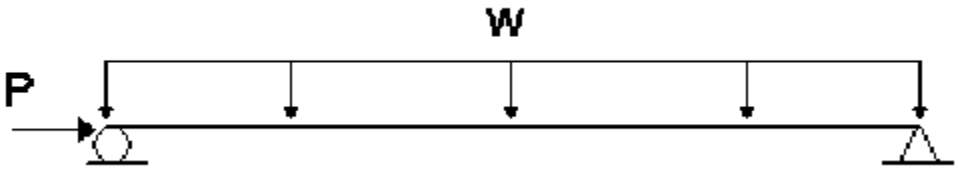

Figure 3.6 Exterior Beam Analysis Model

Table 3.3 ETABS Calculated B_1 Factors for Prototype Members

	Diagonal		Exterior Column		Veirendeel Column		Interior Beam		Exterior Beam	
Story	25 story	10 Story	25 Story	10 Story	25 Sory	10 Story	25 Sory	10 Story	25 Story	10 Story
25	1		1		1		1		1.037	
24	1		1		1		1		1.024	
23	1		1		1		1		1.025	
22	1		1		1		1		1.03	
21	1		1		1		1		1.031	
20	1		1		1		1		1.032	
19	1		1		1		1		1.041	
18	1		1		1		1		1.042	
17	1		1		1		1		1.043	
16	1		1		1		1		1.054	
15	1		1		1		1		1.057	
14	1		1		1		1		1.06	
13	1		1		1		1		1.065	
12	1		1		1		1		1.067	
11	1		1		1		1		1.071	
10	1	1	1	1	1	1	1	1	1.068	1.077
9	1	1	1	1	1	1	1	1	1.071	1.047
8	1	1	1	1	1	1	1	1	1.077	1.048
7	1	1	1	1	1	1	1	1	1.098	1.077
6	1	1	1	1	1	1	1	1	1.106	1.083
5	1	1	1	1	1	1	1	1	1.104	1.089
4	1	1	1	1	1	1	1	1	1.119	1.112
3	1	1	1	1	1	1	1	1	1.124	1.121
2	1	1	1	1	1	1	1	1	1.099	1.107
1	1	1	1	1	1	1	1	1	1.097	1.031

It is apparent from Table 3.3, that member stability effects are only applicable to the exterior beams. These effects are irrelevant for all other prototype members. Because the exterior beams are flexibly connected to the columns, there will be no significant end moments developed due to sidesway; therefore, the only amplification due to second order effects for these beams is because of member instability. Because of this, ETABS method of directly accounting for the additional second order end moments (P-Δ) in the exterior columns and Vierendeel panels and indirectly accounting for the second order moment amplification in the exterior beams (P-δ) is a reasonable approach for the typical FHTF.

Table 3.4 Comparison of 2nd Order Moment Amplification Factors

Story	Member	ETABS B1 Factor	Amplification Factor from Analysis
8	W24x117	1.077	1.075
6	W24x68	1.106	1.105
3	W24x55	1.124	1.123

3.6 Staged Analysis and Synthesis

To calculate accurate member stresses, the dead load and notional load corresponding to the dead loads were applied in a series of construction stages to the prototype frames. The first stage was comprised of the base level and the first four story frame elements including the first four story planks with topping. Each stage is built on the deformed and stressed members of the previous stage. The corresponding notional loads were applied at the appropriate stages. The next stage was comprised of the fourth, fifth, and sixth story frame elements added to the frame, and then the new levels were planked and

topped. The additional stages were added in a similar manner, three stories at a time, until the entire frame was built. At each stage of the model, ETABS accounts for the geometric nonlinearity between stages by solving the equilibrium equations of the stage considering the complete deformed configuration of the previous stages (CSI, 1984-2004). The live, superimposed dead, wind, and their corresponding notional loads are applied to the completed frame. The staged dead load results were then used in combination with the other loads to determine the maximum member stresses.

At each iteration of the design process, a staged analysis must be performed. Each stage is comprised of certain levels being planked and topped, starting at the lowest level. Therefore, there are as many stages or analysis models as stages of construction. When considering a variety of sequences for the construction, this step-by-step analysis can become excessively time consuming and computationally undesirable. Also the structural designer will not always know the exact erection sequence that will be used. Therefore, a method for synthesizing the dead load staged analysis from a full height instantaneous analysis is proposed.

The relationship between the full height analysis and staged analysis is dependent on the force in the diagonals. With a few assumptions, all of the axial forces in the other members at each stage can be resolved by equilibrium once the diagonal forces are known. First, the gravity loads are collected at the panel points based on the tributary areas of the verticals. The members are then treated as axial only members. The shears in the exterior and Vierendeel columns are neglected in the computation of the axial force

in the members at each stage. The additional axial force caused in the beams due to shear difference in the columns can be accounted for after all the stages have been completed.

The gravity loads between the Vierendeel panel points cause joint moments and shear forces in the vertical Vierendeel members. The differences in shear at the Vierendeel panel joints cause an equal and opposite axial force in the horizontal panel members – shown in Figure 3.7. Therefore, even though their quantities are unknown, they will not affect the joint equilibrium equations at each stage, but the additional axial force in the interior bay beams caused by the shears in the Vierendeel columns can be accounted for in the completed staged model based on the shear results from the instantaneous full height analysis.

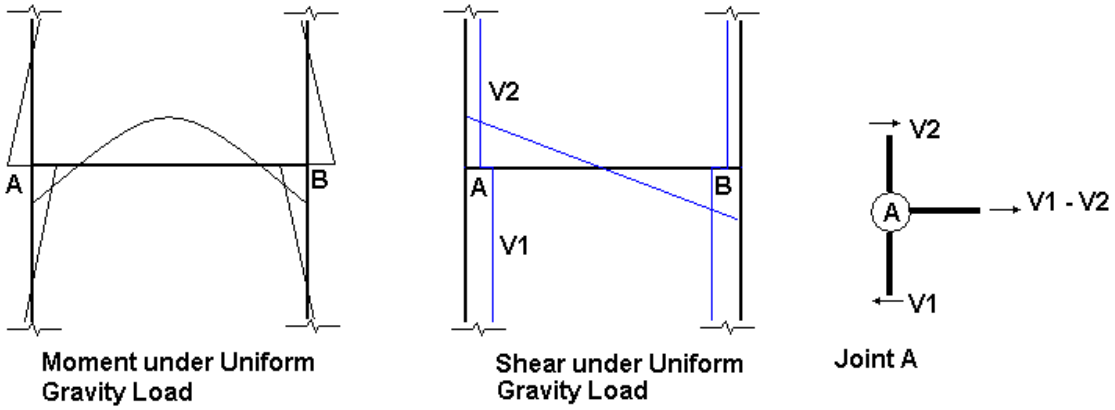

Figure 3.7 Vierendeel Panel Response to Uniform Gravity Load

The major difference in Vierendeel joint moments from the staged analysis and the full height analysis result from the stages where the level being loaded is only supported by panels below. Less moment will be created in these joints because there is less rigidity

due to the absence of the panels above the joint. The joint moments under combined loading will control the flexure design of the corridor beams. Therefore, assuming the joint moments calculated from the full height analysis are equal to those of a staged analysis is conservative.

The exterior columns above the second level can be considered gravity only members because negligible amounts of shear are introduced as the diagonals transfer the gravity loads to the exterior columns. Therefore, the difference between the shears and moments due to the staged analysis are insignificant except in the lowest two exterior columns. The shear and moment in these columns are caused by the compression force in the lowest beam. This compression force is caused by the elongation of the lowest corridor beam, effectively pressing the lowest beams into the exterior columns. This is illustrated in Figure 3.8.

If the frame and loading across the level is symmetric, the left and right diagonal will be equally tensioned. If the loading is not symmetrical, both the left and right side must be analyzed. The method being outlined can be applied to each side of the frame individually if needed. For the purposes of the synthesis, a stage is considered to be the planking or loading of one level. Thus, a ten story building will have ten stages. The load carried by one side of diagonals at a stage can be calculated based on the tributary area of the vertical at the level of loading and the angle of the brace. The force collected at the vertical (V_m) is carried to the exterior columns by all of the diagonals as illustrated in Figure 3.9.

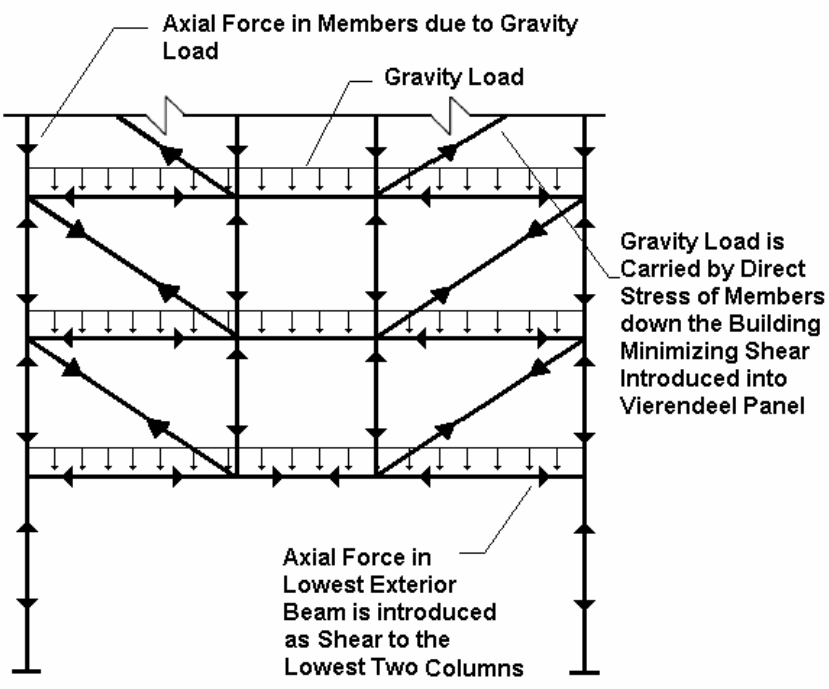

Figure 3.8 Joint forces due to Gravity Loads

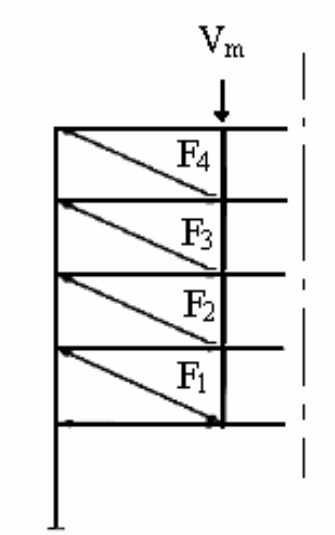

Figure 3.9 Force at Vertical Transferred to Exterior Column

The axial deformations of the diagonals will be insignificant compared to their lengths, thus axial effects can be neglected in regards to a diagonal's stiffness. The deformation of the staged frame at each stage of the construction sequence will be greater than that of the full height frame under the same loading, but in both instances the effect of the deformation on the stiffness of the frame are negligible. The deformation of the staged frame will be larger due to fewer diagonals to distribute the gravity load; therefore, more tension will be added to each diagonal thus each diagonal will elongate more. But, the diagonals carry the load in direct stress thus the deformations are small, causing minimal effect on the frame's stiffness.

For instance, the structures in Figure 3.10 are identical, except structure one has an additional level. Because the lengths, spans, configuration, and members are the same, the stiffnesses of same level diagonals will be the same. From the stiffness equation, it can be shown the diagonal forces in structure two can be calculated from the diagonal forces in structure one, given the deflections of both diagonals.

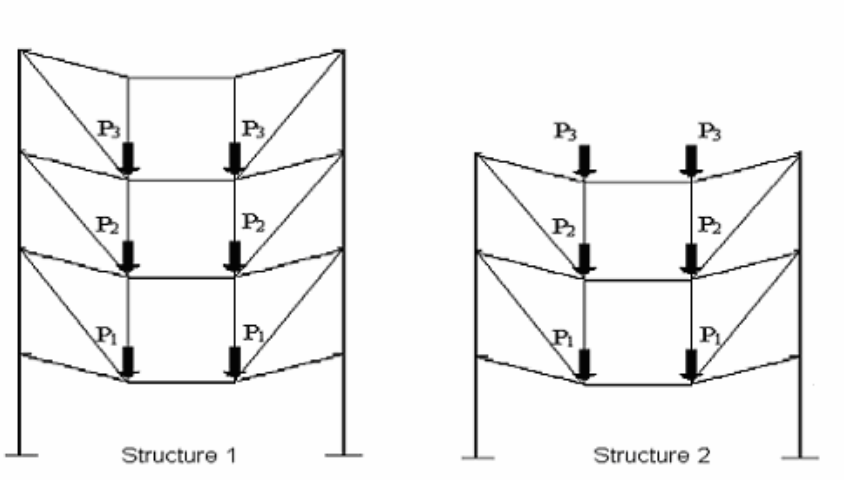

Figure 3.10 Truss Deformations under Dead Load

$$K_i = (K_i)_1 = (K_i)_2 \tag{3-20}$$

where

K = stiffness of ith level diagonal of either structure 1 or 2, kips per inch.

The stiffness of a diagonal can be written as the force it carries divided by its deflection.

$$\left(\frac{F_i}{\Delta_i}\right)_1 = K = \left(\frac{F_i}{\Delta_i}\right)_2 \tag{3-21}$$

where

F = tension force in the ith level diagonal, kips

Δ = axial deflection of the ith level diagonal, inches

Equation 3-21 can be rearranged.

$$(F_i)_2 = \frac{(\Delta_i)_2}{(\Delta_i)_1}(F_i)_1 \tag{3-22}$$

Without an analysis, the actual displacements of the diagonals from either structure cannot be known. If this ratio is assumed to be constant at each level, the force in structure two can be calculated from the force in structure one. This is analogous to approximating the ratio of actual displacements at a level by a ratio of "average" displacements.

As the levels of the FHTF increase, the deviation of actual deflections from the average will increase. Deflections greater than the average occur in the lower levels and those less than the average in the upper levels. More levels result in a greater range of deflections. Additionally, as the FHTF staged model approaches the full height model in number of levels, the ratio of average deflection and actual deflection at a level will approach 1. Therefore, when comparing the full height to the staged model, the staged model will have fewer levels thus the difference between the average and actual deflections at each level will be smaller. This will result in the ratio of average deflections of the staged to the full height being slightly larger than the similar ratio of actual deflections. Consequently, this will conservatively overestimate the force to diagonals, particular in the early stages.

The ratios of average deflection will be the same at each level and thus a constant.

$$\frac{\Delta_2}{\Delta_1} \approx \frac{\overline{\Delta}_2}{\overline{\Delta}_1} = k \tag{3-23}$$

where

k = constant relating diagonal force in structure 1 to the force in the same diagonal of structure 2

$\overline{\Delta}$ = average deflection at all levels of the structures, inches

The sum of the diagonal forces of the staged model can be written as:

$$\left(\sum_{1}^{n} F\right)_2 = \sum_{1}^{n_2} kF_1 \tag{3-24}$$

where

n_2 = the number of diagonals from structure 2

Equation 3-24 can be reduced to:

$$\left(\sum_{1}^{n} F\right)_2 = k\sum_{1}^{n_2} F_1 \tag{3-25}$$

By dividing the both sides of Equation 3-25 by the sum of force in the diagonals from structure 1, the constant *k* can be shown to equal a known value:

$$\frac{\left(\sum_{1}^{n} F\right)_2}{\left(\sum_{1}^{n} F\right)_1} = \frac{k\sum_{1}^{n_2} F_1}{\left(\sum_{1}^{n} F\right)_1} \tag{3-26}$$

This can be further reduced by observing that the sum of the forces in the diagonals for both structures will equal due to equal loading.

$$\left(\sum_{1}^{n} F\right)_2 = \left(\sum_{1}^{n} F\right)_1 \tag{3-27}$$

By substituting equation 3-27 into 3-26 and solving for *k*:

$$k = \frac{\sum_{1}^{n_1} F_1}{\sum_{1}^{n_2} F_1} \tag{3-28}$$

where

n_1 = the number of diagonals from structure 2

At each stage, the frames of the full height and staged models are similar in configuration and members; therefore by applying equation 3-28, the diagonal forces from the full height model can be used to approximate the diagonal forces in the staged model when the frames are similarly loaded. This is shown in Figure 3.11.

$$\left(F_i\right)_m^{STAGED} = \left(\frac{\sum_{1}^{n_1} F_{FULL\ HEIGHT}}{\sum_{1}^{n_2} F_{FULL\ HEIGHT}} \right)_m \left(F_i\right)_m^{FULL\ HEIGHT} \qquad (3\text{-}29)$$

where

m = loading stage

n_1 = the number of diagonals from the full height model

n_2 = the number of diagonals from the staged model

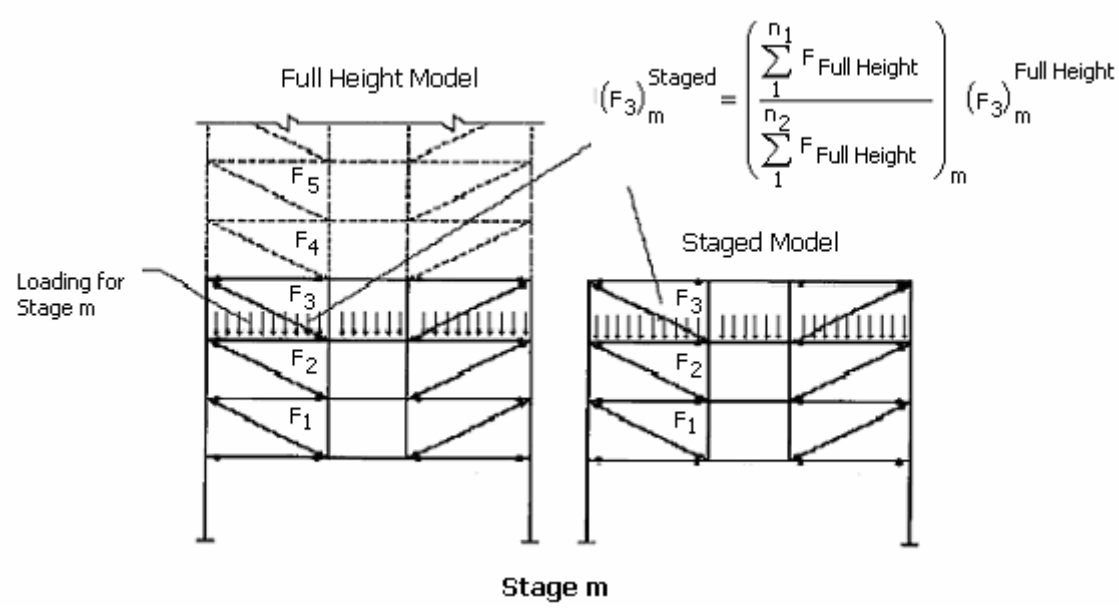

Figure 3.11 Relating Diagonal Forces from Full Height to Staged Analysis

The constant relating the full height diagonal forces to the staged diagonal forces can be calculated at each stage using the known diagonal forces in the full height model. This constant cannot be greater than one, thus the staged diagonal forces will be equal to or greater than the full height diagonal forces.

$$k_m = \left(\frac{\sum_{1}^{n_1} F_{FULL\ HEIGHT}}{\sum_{1}^{n_2} F_{FULL\ HEIGHT}} \right)_m \tag{3-30}$$

$$\left(F_i\right)_m^{STAGED} = k_m \left(F_i\right)_m^{FULL\ HEIGHT} \tag{3-31}$$

where

k_m = "force" factor, the sum of the full height diagonal forces of all the diagonals of the full height model divided by the sum of the full height diagonal forces of the diagonals present in the staged model

Equation 3-31 applies to the diagonal forces of a discrete stage loading. The full height diagonal forces due to loading individual stages are unknown. But the forces at a stage can be approximated by the known full height diagonal force distribution and the loading at each stage because distribution of force to the diagonals will not significantly change as the different levels are loaded. Meaning, that a given diagonal will not be stressed significantly more or less if level five is loaded compared to level fifteen. Table 3.5 gives the diagonal force distributions (tension in a diagonal divided by the sum of tension in all of the diagonals) of a ten story FHTF model when only one level is loaded. Every member of the frame is the same, and the configuration of the members is identical to the prototype models. Each stage in the table corresponds to only one level being loaded:

stage one to level one, stage two to level two, and so on. The average distribution over all the stages will be equal to the full height instantaneous distribution if the construction loadings at each stage are similar.

Table 3.5 Distribution of Load Between the Diagonals of a Full Height Model at Different Stages

Story	Stage 1	Stage 2	stage 3	stage 4	Stage 5	Stage 6	Stage 7	Stage 8	Stage 9	Stage 10	Average	Maximum Deviation From Average
10	0.065	0.066	0.067	0.070	0.073	0.077	0.082	0.091	0.090	0.074	0.076	0.016
9	0.076	0.077	0.078	0.081	0.085	0.089	0.098	0.095	0.090	0.105	0.087	0.018
8	0.082	0.084	0.085	0.089	0.092	0.101	0.096	0.091	0.100	0.094	0.091	0.009
7	0.091	0.093	0.094	0.098	0.105	0.100	0.094	0.102	0.095	0.098	0.097	0.008
6	0.103	0.105	0.106	0.114	0.107	0.101	0.108	0.101	0.102	0.103	0.105	0.009
5	0.119	0.121	0.126	0.119	0.112	0.118	0.110	0.111	0.111	0.112	0.116	0.010
4	0.140	0.145	0.136	0.128	0.134	0.125	0.125	0.124	0.125	0.126	0.131	0.014
3	0.165	0.158	0.143	0.150	0.140	0.139	0.138	0.138	0.138	0.139	0.145	0.021
2	0.158	0.150	0.163	0.153	0.151	0.150	0.149	0.149	0.149	0.150	0.152	0.011

The diagonal forces in the full height model at a stage can be calculated by the known instantaneous results and the loading of the stage.

$$V_m = D_m A_T \tag{3-32}$$

$$\left(\sum_{1}^{n} F \right)^{Full\ HEIGHT} = \frac{V_m}{\sin\theta} \tag{3-33}$$

$$C_i = \left(\frac{F_i}{\sum_{1}^{n} F} \right)^{FULL\ HEIGHT} \tag{3-34}$$

$$\left(F_i\right)_m^{FULL\ HEIGHT} = C_i \frac{V_m}{\sin\theta} \tag{3-35}$$

where

C_i = distribution factor

V_m = gravity load delivered to diagonals at mth stage, kips

D_m = dead load added at mth stage, psf

A_T = tributary area of interior Vierendeel column, ft^2

θ = angle between diagonal and horizontal

Finally, equation 3-37 can be substituted into 3-31 to give:

$$\left(F_i\right)_m^{STAGED} = k_m C_i \frac{V_m}{\sin\theta} \tag{3-36}$$

The final staged tension force in the diagonal is the sum of the individual tension forces at each stage.

$$\left(F_i\right)^{STAGED} = \left(\sum_1^m F_i\right)^{STAGED} \tag{3-37}$$

This process can be done using a spread sheet to approximate the diagonal forces due to the construction stages. An example of the methodology is illustrated in Table 3.6 for a six story FHTF. The sequence was arbitrarily chosen and can be broken down in terms of diagonals as follows: stages 1, 2, and 3 include the second and third story diagonals, stage 4 includes the second through fourth story diagonals, stage 5 includes the second through fifth story diagonals, and stage 6 includes all. Stage 1 corresponds to the first level being loaded, stage 2 to the second level being load, and so on. The sequence is shown in Figure 3.12. The instantaneous full height diagonal forces were arbitrarily chosen.

Table 3.5 is broken into three sections. The first section is the list of the diagonal forces from the instantaneous full height analysis and distribution factors for the completed structure. Each force corresponds with a different story diagonal. The second section and third sections are divided into the stages of construction. In the second section, the gravity load collected at the interior vertical, and the "force" factors *k* are listed for each stage. The third section is the calculation of the force added to the diagonals at each stage of construction. These forces are summed to calculate the final forces in each diagonal of the staged model. The detailed calculations involved in this example are shown in Appendix A.

Now that the staged forces in the diagonals can be calculated, all member axial forces except for the lowest level outer bay beam can be calculated by equilibrium at the joints for each analysis stage assuming pin connections and axial only members. The amount of compression force added to the lowest level exterior bay beam at each stage can be approximated based on the proportion of final compression in this beam to the tension in the lowest corridor beam obtained from the full height analysis. This compression is a result of the elongation of the lowest corridor beam. This beam's axial deflection compresses the connected exterior bay beams into the exterior columns. The resulting compression is directly related to the stiffness of the lowest exterior bay beams and corridor beam. Because these members are identical in both models:

$$\left(F_{BB}\right)_1^{STAGED} = \left(\frac{F_{BB1}}{F_{CB1}}\right)^{Full\ \ Height} F_2^{STAGED} \tag{3-38}$$

Where

F_{BB} = axial force in outer (exterior) bay beams, kips

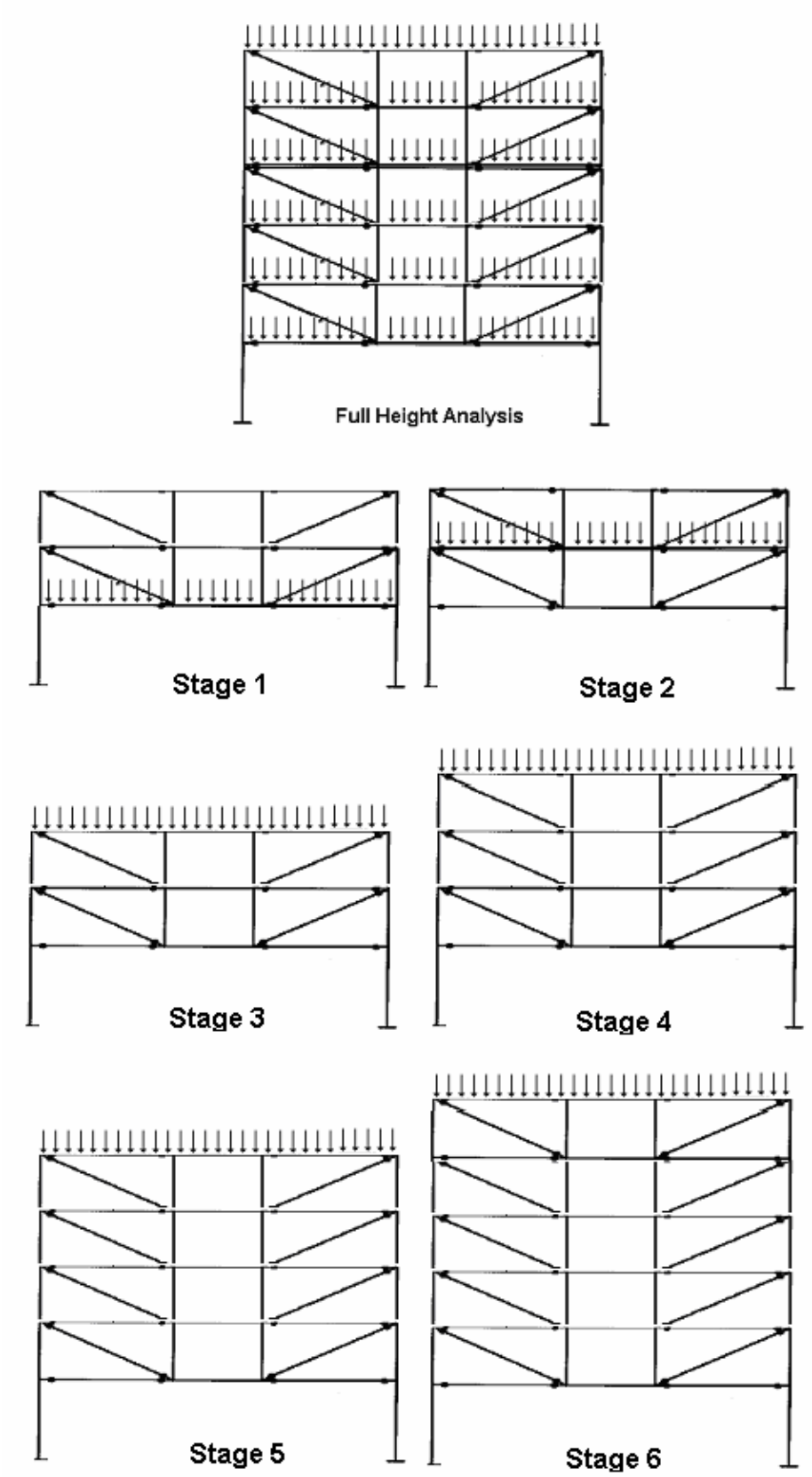

Figure 3.12 Full Height and Staged Models from Example

Table 3.6 Illustration of Synthesis Method on a 6 Story FHTF

Story	Tension Force in Diagonal as Calculated by a Full Height Instantaneous Analysis, F (in^2)	Distribution factor , C_i $\left(\frac{F_i}{\sum_1^n F}\right)$
6	37.2	0.067
5	73.2	0.133
4	110.4	0.2
3	147.6	0.267
2	183.6	0.333

	Stage					
	1	**2**	**3**	**4**	**5**	**6**
Loading, V_m $V_m = D_m A_T$	30	30	30	30	30	30
"Force" Factor, k_m $k_m = \left(\frac{\sum_1^{n_1} F_{FULL\ HEIGHT}}{\sum_1^{n_2} F_{FULL\ HEIGHT}}\right)_m$	5	5	5	1.25	1.07	1.00

Diagonal Tension Forces from Staged Model at Each Stage

$$\left(F_i\right)_m^{STAGED} = k_m C_i \frac{V_m}{\sin\theta}$$

	Stage						Sum
Story	**1**	**2**	**3**	**4**	**5**	**6**	
6	0	0	0	0	0	6	**6**
5	0	0	0	0	13	12	**25**
4	0	0	0	23	20	18	**61**
3	41	41	41	31	26	25	**204**
2	51	51	51	38	33	31	**256**

F_{CB} = axial force in corridor beam, kips

By solving for equilibrium in the x-direction at the exterior column panel points (Figure 3.13) and neglecting the shear in the columns:

$$\left(F_{BB}\right)_i = -F_i \cos\theta \tag{3-39}$$

By solving for the equilibrium in y-direction at the exterior column panel points:

At the loading level,

$$\left(F_C\right)_i = -F_i \sin\theta + \left(F_C\right)_{i+1} - (D_m - V_m) \tag{3-40}$$

At n levels above loading,

$$\left(F_C\right)_{i+n} = F_{i+n} \sin\theta + \left(F_C\right)_{i+n+1} \tag{3-41}$$

At n levels below loading,

$$\left(F_C\right)_{i+n} = F_{i-n} \sin\theta + \left(F_C\right)_{i-n+1} \tag{3-42}$$

Where

F_C = axial force in exterior columns, kips

n = number of levels above or below the loading level

By solving the equilibrium in the x-direction at the interior panel points:

$$\left(F_{CB}\right)_i = F_{i+1} \cos\theta - F_i \cos\theta \tag{3-43}$$

Where

F_{CB} = axial force in corridor beam, kips

By solving the equilibrium in y-direction at the interior panel points:

At the loading level,

$$(F_{VV})_i = F_{i+1}\sin\theta + (F_{VV})_{i+1} - V_m \tag{3-44}$$

At n levels above loading,

$$(F_{VV})_{i+n} = F_{i+n+1}\sin\theta + (F_{vv})_{i+n+1} \tag{3-45}$$

At n levels below loading,

$$(F_{VV})_{i+n} = F_{i-n+1}\sin\theta + (F_{vv})_{i-n+1} \tag{3-46}$$

Where

F_{VV} = axial force in vertical Vierendeel member, kips

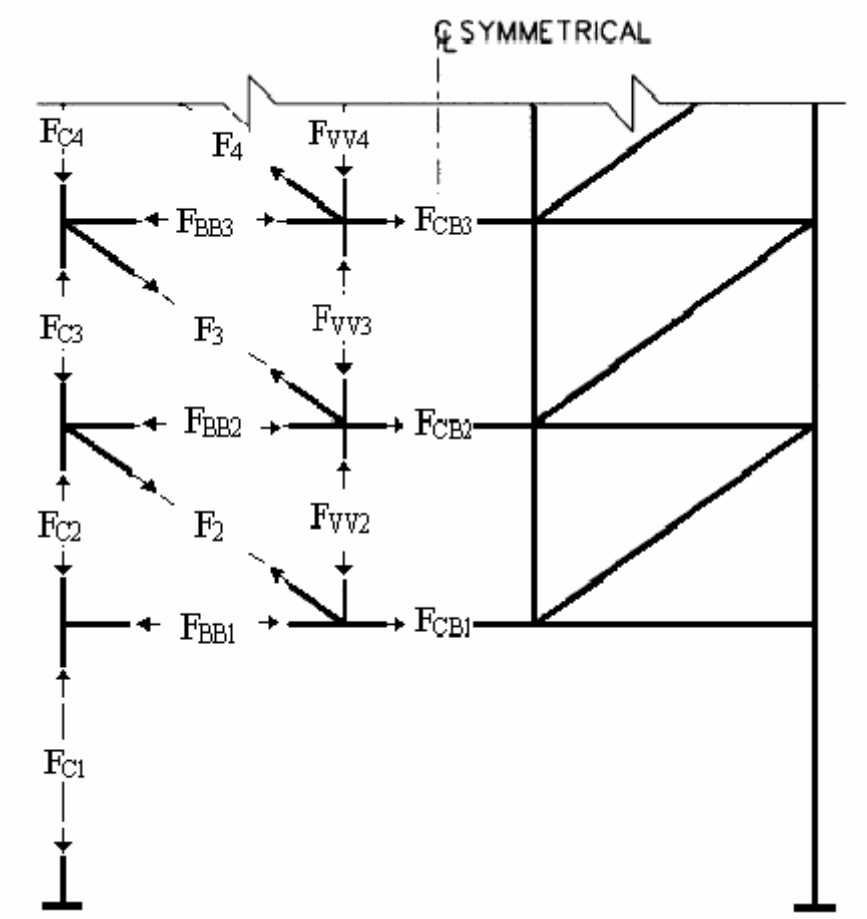

Figure 3.13 Axial Forces at Panel Joints

The final axial forces in all the members can be found by summing the individual axial forces at each stage. The shear force in the lowest two columns under the staged loading is assumed to distribute similarly to the shear in these columns under the full height instantaneous loading. The additional shear due to the staged loading and model causes an increase in moment in the lowest two columns by a factor approximately equal to the ratio of calculated shear to the full height dead load shear:

$$(M_i)^{STAGED} = \frac{(S_i)^{STAGED}}{S_i} M_i \tag{3-47}$$

where

M_i = column end moments at ith level, kip inches

S_i = column shear at ith level, kips

The outer bay beam axial forces above the lowest level can be adjusted by either the addition or subtraction of force due to the difference of the shear in the columns above and below the beams. The additional axial forces in the exterior bay beams can be calculated by differences in the shear force of the columns from the full height analysis modified with the additional shear at the lowest two columns and then summed with the synthesis results. This addition (subtraction) can be particularly large in the second story exterior bay beam. This level is the first exterior column-diagonal connection. Therefore, the shear in the column above the beam is small, but the shear in the column below is large. This is due to the compression in the lowest level beam transferred as shear to the exterior columns as shown in Figure 3.14. Because this compression is caused by the elongation of the lowest corridor beam, increasing this beam's stiffness

will reduce the elongation and consequently the compression in the lowest exterior beams.

In Chapters five and six, this method will be compared with the actual staged results for the 10 and 25 story prototypes. This method can be easily implemented with a computer spread sheet and used to save time during the design stages. This method can quickly recalculate member axial force, shears, and moments when changing member size and construction sequences.

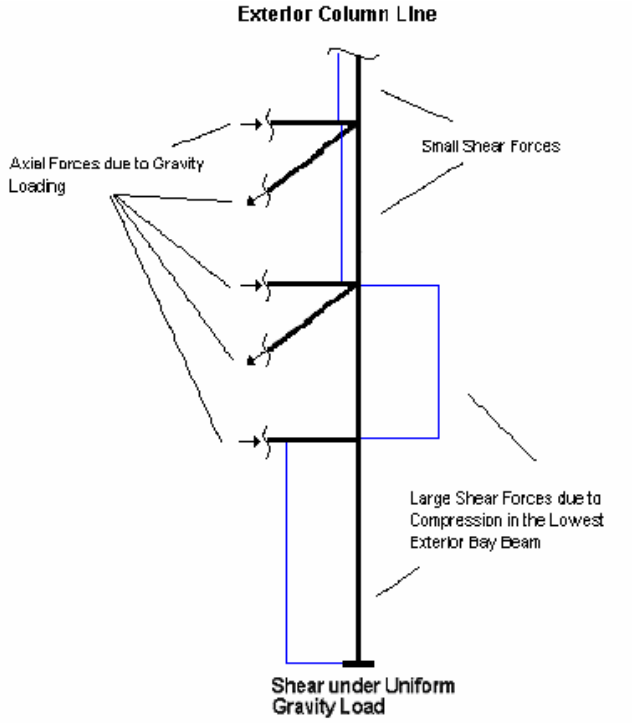

Figure 3.14 Shear in Exterior Columns

3.7 Member Design

Once the member shears, moments, and axial loads were tabulated from analysis for each of the LRFD load combinations, each member was designed as a beam column according

to the current *LRFD Specification for Structural Steel Buildings* (AISC, 2001). The flexural and axial design strength were computed and satisfied AISC interaction equations. Each member was also determined to have adequate shear strength. The connections between frame members were assumed to be adequate for all load cases on the structure; therefore, the connections will not limit the design of the members. The flexural design strength of each W shape can be calculated according to AISC Appendix F:

$$L_b < L_p$$
$$\phi M_n = \phi M_p \qquad \text{(3-48) AISC Eq F1-1}$$

$$L_p < L_b < L_r$$
$$\phi M_n = \phi C_b \left[M_p - \left(M_p - M_r\right)\left(\frac{L_b - L_p}{L_r - L_p}\right)\right] \le \phi M_p \qquad \text{(3-49) AISC Eq. F1-2}$$

$$L_b > L_r$$
$$\phi M_n = \phi M_{cr} = \phi C_b \frac{\pi}{L_b}\sqrt{EI_y GJ + \left(\frac{\pi E}{L_b}\right)^2 I_y C_w} \le \phi M_p \qquad \text{(3-50) AISC Eq.F1-13}$$

where

Φ = reduction factor for flexure = 0.9

L_b = distance between points braced against lateral displacement of compression flange, or between point braces to prevent twist of the cross section, in.

L_p = limiting laterally unbraced length $= 1.76 r_y \sqrt{\frac{E}{F_{yf}}}$, in.

L_r = limiting laterally unbraced length $= \frac{r_y X_1}{F_L}\sqrt{1 + \sqrt{1 + X_2 F_L^2}}$, in.

C_b = modification factor for non-uniform moment diagrams

$$X_1 = \frac{\pi}{S_x}\sqrt{\frac{EGJA}{2}}$$

$$X_2 = \quad 4\frac{C_w}{I_y}\left(\frac{S_x}{GJ}\right)^2$$

M_r = limiting buckling moment = $F_L S_x$, kip-in

M_p = plastic moment = $F_y Z \le 1.5M_y$, kip-in

M_y = moment corresponding to onset of yielding at the extreme fiber from an elastic stress distribution = $F_y S$, kip-in

S_x = section modulus about major axis, in^3

Z = plastic section modulus, in^3

E = modulus of elasticity of steel = 29,000 ksi

G = shear modulus of elasticity of steel = 11200 ksi

F_L = smaller of ($F_{yf} - F_r$) or F_{yw}, ksi

F_r = compressive residual stress in flange = 10 ksi for rolled shapes

F_{yf} = yield stress in flange = 50 ksi

F_{yw} = yield stress in web = 50 ksi

I_y = moment of inertia about y-axis, in^4

C_w = warping constant, in^6

The planking that rests upon the top flange of the beams will act as continuous bracing against lateral-torsional buckling where the bending causes compression in the top flange. For the outer bay beams, the moment caused by gravity loading will always cause compression in the top flange because of the flexible connections on either end; therefore,

it can be assumed that the unbraced lengths of the exterior bay beams are equal to zero. Thus, the nominal moment strength of these members will be equal to the plastic moment. The corridor beam was modeled as a fixed-fixed beam where the top flange is in compression between 0.211L and 0.789L; therefore, the unbraced length was taken as 0.211L (30.38 inches). The nominal strength of the corridor beam will then equal the plastic moment, given that $r_y > 0.641$ inches using the AISC formulation for limiting lateral unbraced length; this will be satisfied for a typical W shape. The planking and orthogonal lateral force resisting system act to brace the columns at each level, thus giving the columns an unbraced length equal to the story height. For each member local buckling was determined not to control the design according to AISC Table 5.1:

Flange Local Buckling,

$$\frac{b}{t} < 0.38\sqrt{\frac{E}{F_{yf}}} \qquad \text{(3-51) Table B5.1}$$

Web Local Buckling,

$$\frac{P_u}{\phi P_y} \le 0.125$$

$$\frac{h}{t_w} = 3.76\sqrt{\frac{E}{F_{yf}}\left(1 - \frac{2.75P_u}{\phi P_y}\right)} \qquad \text{(3-52) Table B5.1}$$

$$\frac{P_u}{\phi P_y} > 0.125$$

$$\frac{h}{t_w} = 1.12\sqrt{\frac{E}{F_{yf}}\left(2.33 - \frac{P_u}{\phi P_y}\right)} \ge 1.49\sqrt{\frac{E}{F_y}} \qquad \text{(3-53) Table B5.1}$$

where

P_u = required axial compressive strength under LRFD load combination, kips

$P_y = AF_y$ = member yield strength, kips

Once the nominal moment capacity for the member was known, the nominal axial capacity was calculated based on an effective length factor of 1 for all frame members. The planking offers continuous bracing against weak axis bucking for every floor beam; therefore, L_y can be assumed to be zero for the corridor and outer bay beams. Because the effective length of the columns in all directions are equal, either weak axis buckling or flexural-torsional buckling will control the column design, but the compression design for the exterior and interior beams will be controlled by either strong axis buckling or flexural-torsional buckling. The nominal axial capacity can be calculated according to AISC Appendix E: Columns and other Compression Members:

$$\phi P_n = \phi A_g F_{cr} \qquad \text{(3-54) AISC Eq. A-E3-1}$$

where

Φ = reduction factor for compression = 0.85

P_n = nominal compression capacity, kips

F_{cr} = nominal critical stress = $\frac{0.877}{\lambda_e^2} f_y$ for $\lambda_e > 1.5$ (3-55) AISC Eq. A-E3-3

$= 0.658^{\lambda_e^2} f_y$ for $\lambda_e \le 1.5$ (3-56) AISC Eq. A-E3-2

$\lambda_e = \sqrt{F_y / F_e}$ (3-57) AISC Eq. A-E3-4

F_y = yield stress = 50 ksi

F_e = larger of the critical flexural torsional elastic buckling stress, F_{ez}; buckling stress by strong axis buckling, F_{ex}; and buckling stress by weak axis buckling, F_{ey}

$$F_{ez} = \left(\frac{\pi^2 E C_w}{(k_z L_y)^2} + GJ \right) \frac{1}{I_{xx} + I_{yy}} \qquad \text{(3-58) AISC Eq. A-E3-5}$$

$$F_{ey} = \frac{\pi^2 E}{\left(k_y l_y / r_y \right)^2} \qquad \text{(3-59) AISC Eq. A-E3-11}$$

$$F_{ex} = \frac{\pi^2 E}{\left(k_x l_x / r_x \right)^2} \qquad \text{(3-60) AISC Eq. A-E3-10}$$

K = Effective length

l = unbraced length, in

Because the connections were assumed to not limit the design, the nominal tension capacity of the each brace is based on its cross-sectional area and the yield limit of the steel. The relationship is given in Chapter D by:

$$\phi P_n = \phi F_y A_g \qquad \text{(3-61) AISC Eq. D1-1}$$

where

Φ = reduction factor for tension = 0.9

P_n = nominal tensile capacity, kips

A_g = gross cross sectional area of member, in^2

Fy = specified minimum yield stress = 50 ksi

Once the axial and bending capacities of the members are known, the capacity under the combined effects is limited to the interaction equation found in Chapter H. The interaction equation is given by:

$$\frac{P_u}{\phi P_n} \geq 0.2$$

$$\frac{P_u}{\phi P_n} + \frac{8}{9}\left(\frac{M_u}{\phi M_n}\right) \leq 1.0 \qquad \text{(3-62) AISC Eq. H1-1a}$$

$$\frac{P_u}{\phi P_n} < 0.2$$

$$\frac{P_u}{2\phi P_n} + \left(\frac{M_u}{\phi M_n}\right) \leq 1.0 \qquad \text{(3-63) AISC Eq. H1-1b}$$

where

P_u = required tension or compression strength, kips

P_n = nominal tensile or compressive strength, kips

Φ = reduction factor for either tension, compression, or flexure

= 0.85 compression

= 0.9 Tension

= 0.9 flexure

M_u = required flexural strength, kip-in

M_n = nominal flexural strength, kip-in

Once the combined effects of flexure and axial load were determined to be acceptable, the shear capacity of each member was checked according Chapter F: Beams and Other Flexural Members. The shear capacity is given by:

$$\frac{h}{t_w} \leq 2.45\sqrt{\frac{E}{F_{yw}}}$$

$$V_n = 0.6F_{yw}A_w \qquad \text{(3-64) AISC Eq. F2-1}$$

$$2.45\sqrt{\frac{E}{F_{yw}}} < \frac{h}{t_w} \le 3.07\sqrt{\frac{E}{F_{yw}}}$$

$$V_n = 0.6F_{yw}A_w\left(\frac{2.45\sqrt{E/F_{yw}}}{h/t_w}\right) \qquad \text{(3-65) AISC Eq. F2-2}$$

$$3.07\sqrt{\frac{E}{F_{yw}}} < \frac{h}{t_w} \le 260$$

$$V_n = A_w\left(\frac{4.52E}{(h/t_w)^2}\right) \qquad \text{(3-66) AISC Eq. F2-3}$$

The composite columns were designed according to *Steel Design Guide Series: Load and Resistance Factor Design of W-Shapes Encased in Concrete* (AISC, 1992). This design guide is based on the 1986 AISC specification. There are four criteria that must be satisfied in order for a concrete encased steel W-shape to qualify under LRFD Specification design procedure. These criteria are outlined in Section I2.1:

1. The cross sectional area of the steel shape must comprise at least four percent of the total composite cross section.
2. Concrete encasement of a steel core shall be reinforced with longitudinal load carrying bars, longitudinal bars to restrain concrete, and lateral ties. Longitudinal load carrying bars shall be continuous at framed levels; longitudinal restraining bars may be interrupted at framed levels. The spacing of ties shall be not greater than two-thirds of the least dimension of the composite cross section. The cross sectional area of the transverse and longitudinal reinforcement shall be at least 0.007 in2 per inch of bar spacing.

The encasement shall provide at least 1 ½ in of clear cover outside of both transverse and longitudinal reinforcement.

3. Concrete shall have a specified compressive strength fc' of not less than 3 ksi nor more than 8 ksi for normal weight concrete, and not less that 4 ksi for lightweight concrete.
4. The specified minimum yield stress of structural steel and reinforcing bars used in calculating the strength of a composite column not exceed 55 ksi.

The design strength of the column is $\phi_c P_n$,

where

$P_n = A_s F_{cr}$, nominal axial strength (3-67) AISC Eq. E2-1 modified

For $\lambda_c \le 1.5$,

$$F_{cr} = \left(0.658^{\lambda_c^2}\right) F_{my} \qquad \text{(3-68) AISC Eq. E2-2 modified}$$

For $\lambda_c > 1.5$,

$$F_{cr} = \frac{0.877}{\lambda_c^2} F_{my} \qquad \text{(3-69) AISC Eq. E2-3 modified}$$

$$\lambda_c = \frac{Kl}{r_m \pi} \left({F_{my}}/{E_m} \right)^{1/2} \qquad \text{(3-70) AISC Eq. E2-4 modified}$$

Φ_c = resistance factor for compression = 0.85

A_s = gross area of steel shape, in^2

$F_{my} = F_y + c_1 F_{yr} \left(A_r / A_s\right) + c_2 f_c' \left(A_c / A_s\right)$, modified yield stress, ksi

F_y = specified yield stress of structural steel column, ksi

E = modulus of elasticity of steel, ksi

K = effective length factor

l = unbraced length of column, in

rm = radius of gyration of steel shape in plane of buckling, except that it shall not be less than 0.3 times the overall thickness of the composite cross section in the plane of bending, in

A_c = net concrete area = $A_g - A_s - A_r$, in^2

A_g = gross area of composite section, in^2

A_r = area of longitudinal reinforcing bars, in^2

E_c = modulus of elasticity of concrete = $57{,}00\sqrt{f_c'}$, ksi

f_c' = specified compressive strength of concrete, ksi

F_{yr} = specified minimum yield stress of longitudinal reinforcing bars, ksi

$c_1 = 0.7$

$c_2 = 0.6$

$c_3 = 0.2$

The nominal moment capacity is calculated based on a plastic analysis of the composite cross-section. The resistance factor for flexure is 0.9 and the interaction between axial compression and flexure is based on equation H1.1-a and H1.1b. The AISC design guide is complete with tabulated capacities of a variety of composite columns. These tables were used to pick and check the composite section used for the design.

In addition to strength concerns, the serviceability was checked against general limitations that guard against deflection related problems for steel structures (Ellingwood, 1989). The deflection at the center spans of beams was limited to L/240 for the

unfactored dead load and L/500 for unfactored live load, where L is the span of the beam. The drift at each floor was checked against H/200, where H is the height of the story. The truss deflection under service load was checked against L/500, where L is the span of the truss. Limiting the deflections and drift to these levels generally preserve the structural and the aesthetic integrity of the building.

CHAPTER 4

10 STORY PROTOTYPE DESIGN RESULTS

The objective of the 10 Story Prototype is to illustrate the economy of the design and to validate the synthesis method for approximating the staged dead load case. The design of the 10 story prototype structure was completed as outlined in Chapter 3. The analysis was done using ETABS Nonlinear v8.4.3 (CSI, 1984-2004). The staged dead load construction results from ETABS were compared to the synthesis results using the full height dead load analysis also performed by ETABS.

4.1 Frame Sections

The frame sections were chosen to result in a lightweight and economical frame that would meet the design criteria and serviceability limits. The total weight of the frame is 71,200 pounds or 3.96 psf. The design results for each member are discussed in Section 4.3, and the serviceability limits are reviewed in Section 4.5.

The outer bay beams and diagonals were designed in groups according to the construction sequence. This sequence is shown in Figure 4.1. The outer bay beams range in depths from 24" to 21" for a typical story and 16" at the roof. The beams are designed with flexible connections. A pin connected beam spanning between two columns results in more moment due to gravity loads than an equal span rigidly connected beam. Designing the FHTF's exterior bay beams with FR connections does not however result in significantly less moment due to the configuration differences.

Therefore, the limited savings in beam weight would be offset by the increased cost of moment connections.

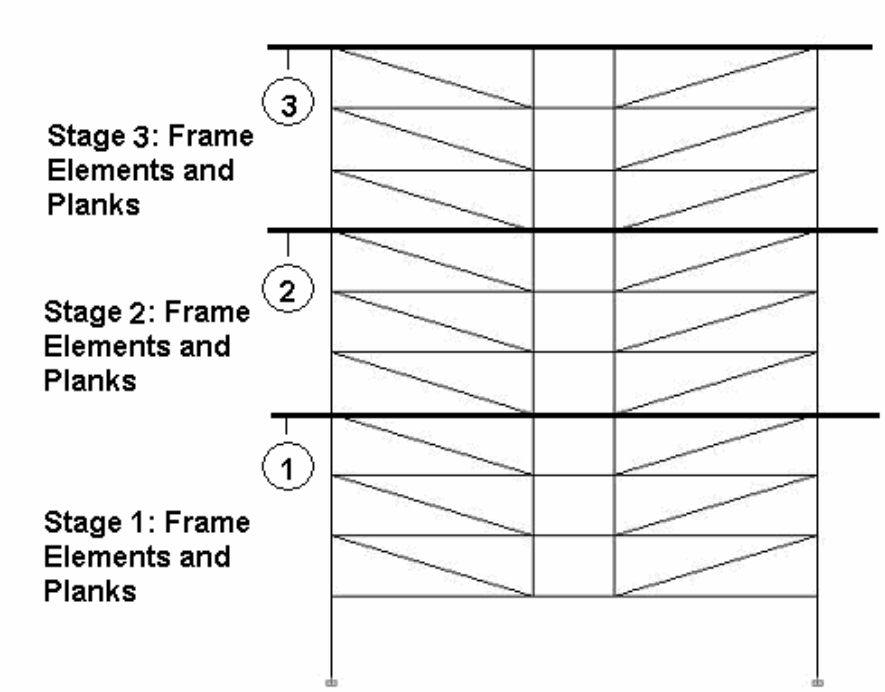

Figure 4.1 Construction Sequence for the 10 Story Prototype

The steel sections used for each member and the configuration of the FHTF are outlined in Figure 4.2. The interior beams, except at the lowest level, were designed to have a maximum depth of 14" to supply the required clearance of 7'. These beams were combined with W10 shape vertical members to form the Vierendeel Panels. The exterior columns were designed on a per story basis while limiting the member to a W14X38.

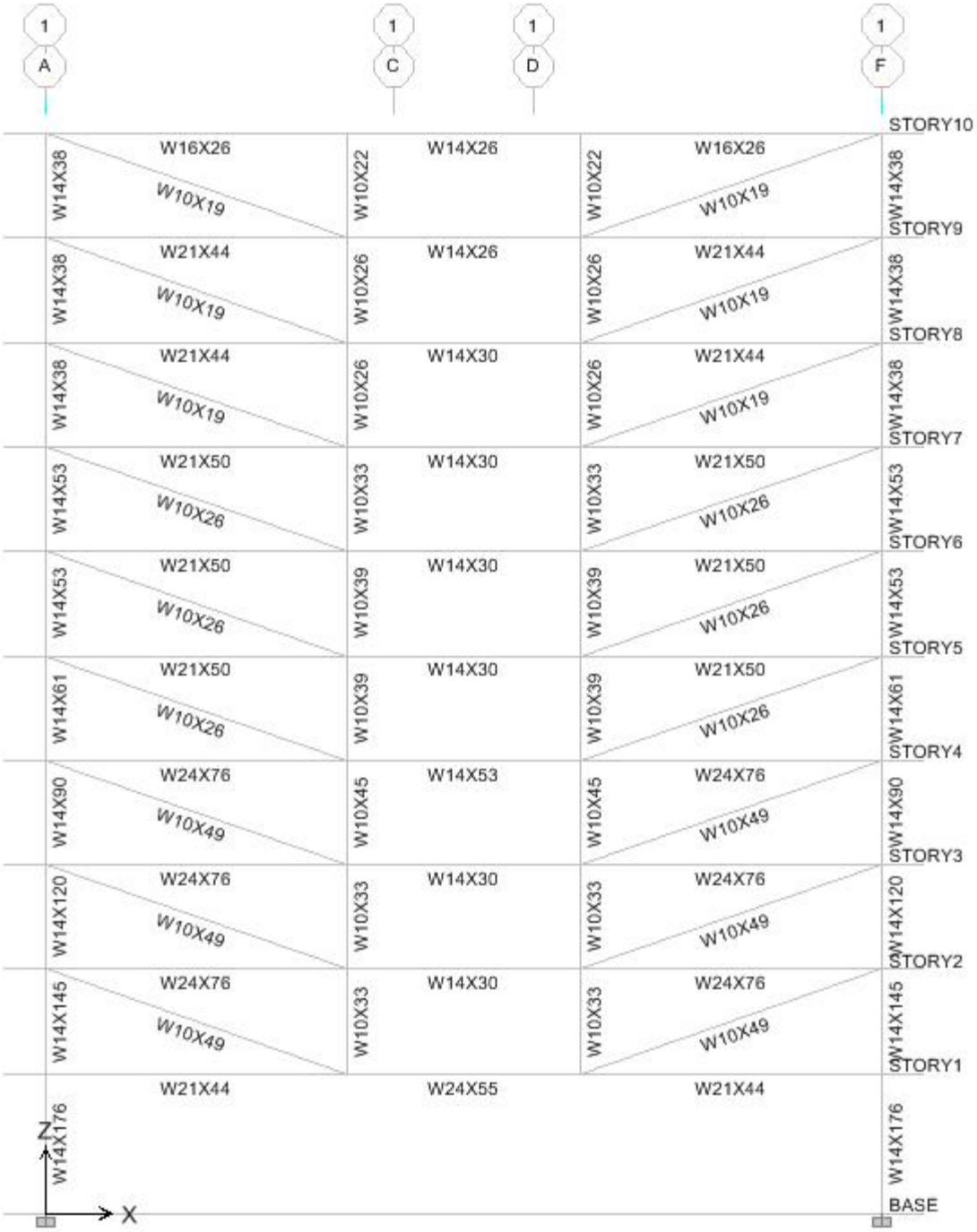

Figure 4.2 Design Sections of the 10 Story Prototype

4.2 Member Stiffness Reduction

The flexural stiffness of the lowest two exterior columns and Vierendeel panels and the axial stiffness of the diagonals, the exterior bay beams, and other exterior columns were reduced according to Appendix 7 of the draft *Specification for Structural Steel Buildings* (AISC, 2004). The axial stiffness (EA) was reduced by a factor of 0.8. The reduction of flexural stiffness is outlined in Table 4.1. The modifier τ did not deviate significantly from 1; therefore, all of the flexural reduction factors were approximated by the value of 0.8 to simplify the analysis model.

4.3 Analysis and Design Results

The capacities of all the frame members were checked in accordance to the methods outlined by section 3.7. The design shears, axial forces, and moments acting on each member were calculated by ETABS under the combined loading of the frame according to chapter 3. The capacity of each member was checked against the interaction equations 3-63 and 3-64. The results of the analysis and capacity check can be found in Table 4.2, 4.3, 4.4, 4.5, and 4.6.

Table 4.1 Flexural Stiffness Reduction Factors – 10 Story Prototype

Member	Story	Pr (k)	Pu	Pu/Pr	τ	Stiffness Reduction
Exterior Columns	2	2135	1274.5	0.60	0.962	0.770
	1	2590	1326.3	0.51	0.999	0.800
Vierendeel Columns	10	324.5	22.04	0.07	1.000	0.800
	9	380.5	89.07	0.23	1.000	0.800
	8	380.5	150.33	0.40	1.000	0.800
	7	485.5	210.19	0.43	1.000	0.800
	6	575	243.41	0.42	1.000	0.800
	5	575	271.72	0.47	1.000	0.800
	4	720	296.38	0.41	1.000	0.800
	3	485.5	203.74	0.42	1.000	0.800
	2	485.5	101.18	0.21	1.000	0.800
Corridor Beams	10	384.5	84.13	0.22	1.000	0.800
	9	384.5	25.07	0.07	1.000	0.800
	8	690	3.63	0.01	1.000	0.800
	7	390	84.17	0.22	1.000	0.800
	6	390	12.45	0.03	1.000	0.800
	5	390	10.67	0.03	1.000	0.800
	4	780	341.47	0.44	1.000	0.800
	3	390	36.93	0.09	1.000	0.800
	2		Tension	NA	1.000	0.800
	1		Tension	NA	1.000	0.800

Table 4.2 Exterior Column Capacity Checks – 10 Story Prototype

Outer Columns	Story	Combo	Mu (k-in)	Pu (k)	Vu (k)	ΦMn (k-in)	ΦPn (k)	ΦVn (k)	Capacity
W14X38	10	2	62.6	40.0	1.0	532.4	355.4	156.9	0.17
W14X38	9	2	91.6	119.7	1.8	532.4	355.4	156.9	0.49
W14X38	8	2	48.8	201.6	1.0	532.4	355.4	156.9	0.65
W14X53	7	2	126.0	309.6	2.9	966.4	549.4	239.4	0.66
W14X53	6	2	82.3	425.9	1.5	966.4	549.4	239.4	0.85
W14X61	5	2	119.2	545.0	2.4	1445.9	677.3	290.0	0.88
W14X90	4	2	171.1	781.7	2.3	3370.3	1069.8	463.3	0.78
W14X120	3	2	1036.2	1030.6	12.8	4545.9	1430.2	621.8	0.92
W14X145	2	5	4123.9	1115.3	45.9	11700.0	1738.6	271.7	0.96
W14X176	1	5	7032.0	1159.8	75.0	14400.0	2020.3	340.6	1.01*

Table 4.3 Vierendeel Column Capacity Checks – 10 Story Prototype

Vierendeel Columns	Story	Combo	Mu (k-in)	Pu (k)	Vu (k)	ΦMn (k-in)	ΦPn (k)	ΦVn (k)	Capacity
W10X22	10	5	640.6	24.0	11.0	1170.0	177.1	66.1	0.62
W10X26	9	5	849.2	86.8	15.7	1408.5	222.1	72.3	0.93
W10X26	8	5	538.5	144.9	11.5	1408.5	222.1	72.3	0.99
W10X33	7	5	839.3	201.0	17.1	1746.0	343.2	76.2	1.01*
W10X39	6	5	914.3	232.1	16.7	2106.0	409.2	84.4	0.95
W10X39	5	5	797.2	258.0	15.5	2106.0	409.2	84.4	0.97
W10X45	4	5	1041.0	282.6	20.1	2470.5	481.2	95.5	0.96
W10X33	3	5	817.9	196.7	14.5	1746.0	347.6	76.2	0.98
W10X33	2	5	1304.1	99.8	21.3	1746.0	347.6	76.2	0.95

Table 4.4 Diagonal Capacity Checks – 10 Story Prototype

Diagonals	Story	Combo	Mu (k-in)	Tu (k)	Vu (k)	ΦMn (k-in)	ΦTn (k)	ΦVn (k)	Capacity
W10X19	10	2	24.6	80.2	0.3	170.3	252.9	68.9	0.45
W10X19	9	2	24.6	98.0	0.3	170.3	252.9	68.9	0.52
W10X19	8	2	24.6	102.8	0.3	170.3	252.9	68.9	0.54
W10X26	7	2	33.3	184.9	0.4	422.9	342.5	72.3	0.61
W10X26	6	2	33.3	199.6	0.4	422.9	342.5	72.3	0.65
W10X26	5	2	33.3	213.6	0.5	422.9	342.5	72.3	0.69
W10X49	4	2	63.0	570.9	0.8	2147.1	648.0	91.6	0.91
W10X49	3	2	63.0	600.8	0.9	2147.1	648.0	91.6	0.95
W10X49	2	2	63.0	590.2	0.9	2147.1	648.0	91.6	0.94

Table 4.5 Corridor Beam Capacity Checks – 10 Story Prototype

Corridor Beams	Story	Combo	Mu (k-in)	Pu (k)	Vu (k)	ΦMn (k-in)	ΦPn (k)	ΦVn (k)	Capacity
W14X26	10	5	581.4	61.0	13.3	1809.0	267.5	95.7	0.51
W14X26	9	5	1527.6	20.8	42.6	1794.8	267.5	95.7	0.89
W14X30	8	5	1596.2	1.9	42.6	2128.5	324.8	100.6	0.75
W14X30	7	5	1584.5	81.1	42.8	2128.5	324.8	100.6	0.91
W14X30	6	5	1771.9	14.8	42.8	2128.5	324.8	100.6	0.86
W14X30	5	5	1823.2	11.3	42.9	2128.5	324.8	100.6	0.87
W14X53	4	5	1978.2	316.6	42.2	3919.5	576.8	138.9	1.00
W14X30	3	5	1824.1	36.7	43.0	2128.5	398.3	100.6	0.91
Corridor Beams	**Story**	**Combo**	**Mu (k-in)**	**Tu (k)**	**Vu (k)**	**ΦMn (k-in)**	**ΦTn (k)**	**ΦVn (k)**	**Capacity**
W14X30	2	5	1824.2	40.5	42.9	2128.5	398.3	100.6	0.91
W24X55	1	2	2159.8	507.8	0.4	6075.0	733.5	251.7	1.01*

Table 4.6 Outer Bay Beam Capacity Checks – 10 Story Prototype

Outer Bay Beams	Story	Combo	Mu (k-in)	Pu (k)	Vu (k)	ΦMn (k-in)	ΦPn (k)	ΦVn (k)	Capacity
W16X26	10	3	1238.5	53.5	16.1	1953.6	263.3	98.8	0.77
W21X44	9	2	3599.0	93.3	47.1	4245.8	485.2	193.0	0.94
W21X44	8	2	3591.8	96.3	47.2	4244.1	485.2	193.0	0.95
W21X50	7	2	3624.7	176.0	47.3	4950.0	551.1	213.4	0.97
W21X50	6	2	3628.9	187.7	47.3	4950.0	551.1	213.4	0.99
W21X50	5	2	3613.6	202.6	47.2	4903.5	551.6	213.4	1.02*
W24X76	4	2	3613.3	539.1	47.2	8720.0	872.2	283.9	0.99
W24X76	3	2	3626.0	578.0	47.2	8658.6	872.2	283.9	1.03
W24X76	2	2	3608.0	516.4	47.2	8751.4	872.2	283.9	0.96
W21X44	1	2	3593.1	62.2	47.0	4293.0	484.9	193.0	0.90

* Member deemed acceptable by the author because it is within a small margin ($\pm$3%) of maximum allowable compression and flexure interaction

4.4 Staged Synthesis Results

The staged dead load synthesis results were calculated using the full height dead load axial results and the stiffnesses of the diagonals according to the methods outlined in Section 3.6. A comparison between the full height and the staged results under dead loading for the diagonals performed by computer analysis is shown in Table 4.7. From Table 4.7, it is clear that a staged analysis is needed for an accurate design; the full height results are approximately 30 percent unconservative in the lower levels where the strength of the diagonals is most crucial. The axial force results compared in this section are those of the right side frame members. The synthesized axial forces from the right side diagonal forces can be used to approximate the axial forces in the left side due to the symmetry of the frame members, construction, and dead loading. If this symmetry does not exist, the axial force in the left side can be calculated independently.

Table 4.7 Full Height and Staged Analysis Results for Diagonal – 10 Story Prototype

Story	Sequential (k)	Full Height (k)	Percent Difference
10	23	71	214%
9	26	90	242%
8	26	96	270%
7	80	120	50%
6	88	128	46%
5	92	141	53%
4	333	234	-30%
3	352	245	-31%
2	345	243	-30%

The dead load is not perfectly symmetrical because of the small notional lateral load applied in the positive x-direction to the left side column floor nodes. This lateral force results in a slightly unequal force distribution. The overturning moment caused by the notional load is resisted by a tension-compression couple in the exterior columns. This causes a slight discrepancy in axial force in the exterior columns shown in Figure 4.8. The lateral force also causes joint moments in the Vierendeel panels. But these irregularities can be ignored in regards the staged synthesis of the axial forces, but later accounted for by the results of full height analysis.

The shear forces in the lowest two columns were used to calculate the increase in moment, resulting in a conservative approximation for both the right and left side exterior column shown in Figure 4.9 & 4.10. In order to calculate the shear addition, the synthesis process must be done for both sides of the frame to approximate the respective shear increase due to the lowest level exterior bay beams. The mechanism of this shear

increase is illustrated in Figure 4.3. All the synthesized results are compared to the results calculated by ETABS using the construction sequence shown in Figure 4.1.

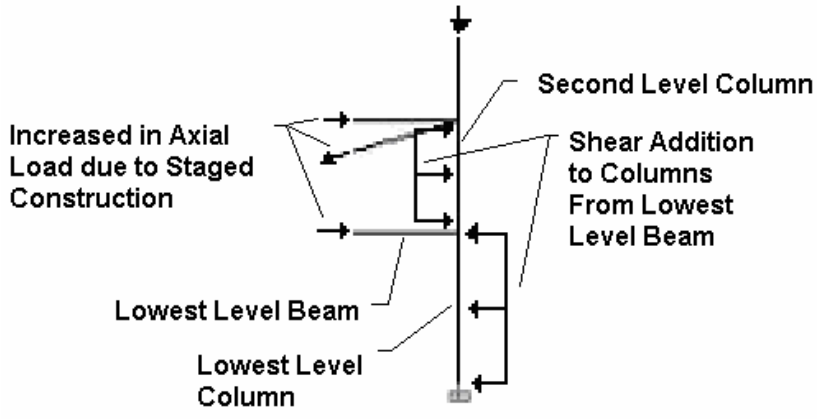

Figure 4.3 Illustration of Shear Increase in the Lowest Level Columns

The differences between the synthesis results and ETABS are small. For this frame, the synthesis gives conservative results for the lower diagonals but underestimates the force in the upper diagonals as shown in Table 4.8. Although the percent difference is large in the upper levels, the magnitude of force is small thus the actual difference is also small. Furthermore, the members in the upper levels were selected for a minimum stiffness and far surpass the ultimate stress criteria as shown in Table 4.4.

These deviations occur due to the assumption that the full height instantaneous diagonal forces can be used to calculate the force in the diagonals at each stage of the construction model and assuming the ratio of actual diagonal displacement at a level is constant at each stage. In all stages, the latter assumption results in conservative force addition to the diagonals; however, as the number of levels in the staged model approach the full

height, both the actual and average (constant) deflection ratios approach one. Meaning, the effects are only apparent in the beginning stages when the difference in levels is the greatest.

Table 4.8 Comparison of Axial Force in Diagonal – 10 Story Prototype

Story	Synthesis (k)	ETABS Results (k)	Difference (k)	Percent Difference
10	18.0	22.66	-4.7	-20.64%
9	22.8	26.3	-3.5	-13.37%
8	24.3	26	-1.7	-6.41%
7	78.2	79.96	-1.7	-2.18%
6	83.5	87.61	-4.1	-4.69%
5	91.6	91.94	-0.4	-0.41%
4	344.3	333.25	11.1	3.32%
3	359.7	352.31	7.4	2.09%
2	356.9	345.18	11.7	3.39%

The full height instantaneous diagonal forces were used to estimate the force added to each diagonal at each stage. Essentially, it has been assumed that the loading of any one floor can be equally divided and spread across all present floors. In reality as each stage or floor is loaded, the distribution will deviate from the previous stages. Generally, the diagonals closer to the loading level will be stressed more than members further from the loading thus using the average distribution at each stage would not affect the final results of a full height model where all the diagonals are present at each stage. However, this is not true for a staged model where not all diagonals are present in each stage.

For the diagonals that are not present in all stages, particularly those added in the final few, the average distribution will result in less force calculated to the upper diagonals.

As the upper levels are loaded, the upper level diagonals will be stressed proportionately more than when the lower levels are loaded. Therefore, approximating the results in the upper levels with the average will underestimate force in the stages where the upper levels are loaded, and because these diagonals are only present as these levels are being loaded, the sum of the force added to these diagonals will be less than the actual force. Therefore, when applying the average addition at each stage to the staged construction model, the synthesis method will accurately tabulate the total force addition to the lower level diagonals, which are present in all the stages, but underestimate the tension in the upper level diagonals, which are present in only a few of the stages.

The consequences of these approximations are apparent in all of the axial forces calculated from equilibrium based on the synthesized diagonal tension forces. From the Figures it can be seen that the synthesis method overestimates force in the lower levels and underestimates the forces in the upper, except for the Vierendeel columns. The synthesis model directs more load to the lower level diagonals through the Vierendeel columns; therefore, extra load accumulates in these columns as the force is transferred to the foundation.

Another cause of difference can be attributed to the tributary area method of calculating the gravity load carried to the exterior and Vierendeel columns. The load that is carried to interior is resisted by the collection of diagonals connected by the Vierendeel columns. The actual force transferred to the interior verticals can be slightly different at each level.

When examining the corridor beam comparison in Figure 4.6, part of fluctuation is in part due to assuming a pin connection between the Vierendeel vertical and the corridor beam. In reality this connection is designed as fixed. This complicates the relationship between the connecting members by allowing shear force to be introduced to both Vierendeel columns at the joint. For design purposes, only the corridor beams that were part of the upper or lower truss chord, at a level between a change in diagonal size, or both will see a significant amount of axial load. In the case of the prototype, these will be the first, the fourth, the seventh, and the tenth floor corridor beams. All other corridor beams will have an insignificant amount of axial load.

4.5 Serviceability

The serviceability is of equal importance to strength in the final design of a structure. In evaluating the serviceability criteria of the ten story prototype, three aspects of the frame deflection were considered: the drift due to lateral load and the individual beam and truss section deflections due to the gravity load. The serviceability criteria used to evaluate the prototype frame are standard limits that in the past have prevent damage to the structures and discomfort to their occupants (Ellingwood, 1989).

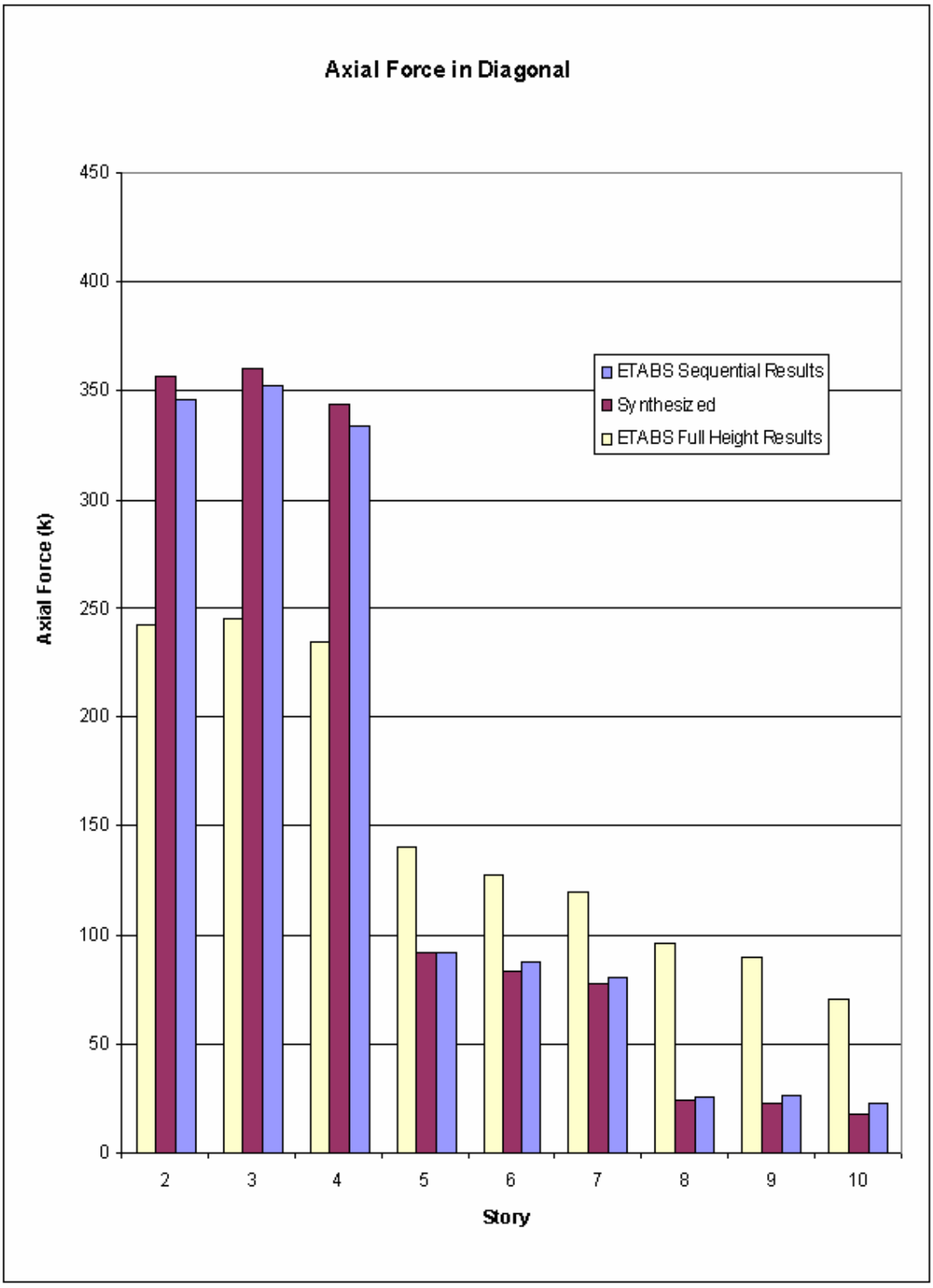

Figure 4.4 Axial Force in Diagonals due to Staged Load – 10 Story Prototype

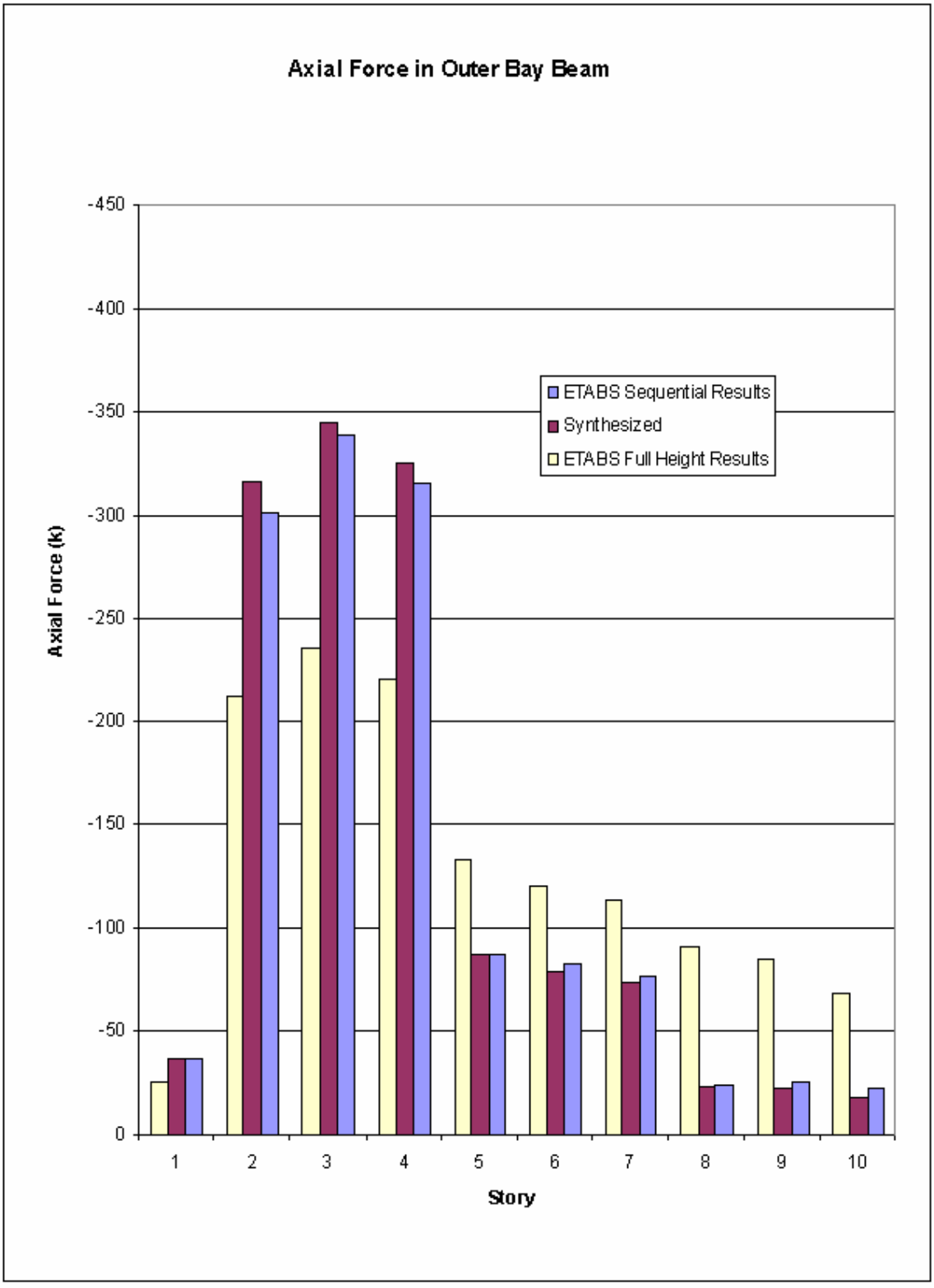

Figure 4.5 Axial Force in Outer Bay Beams due to Staged Load – 10 Story Prototype

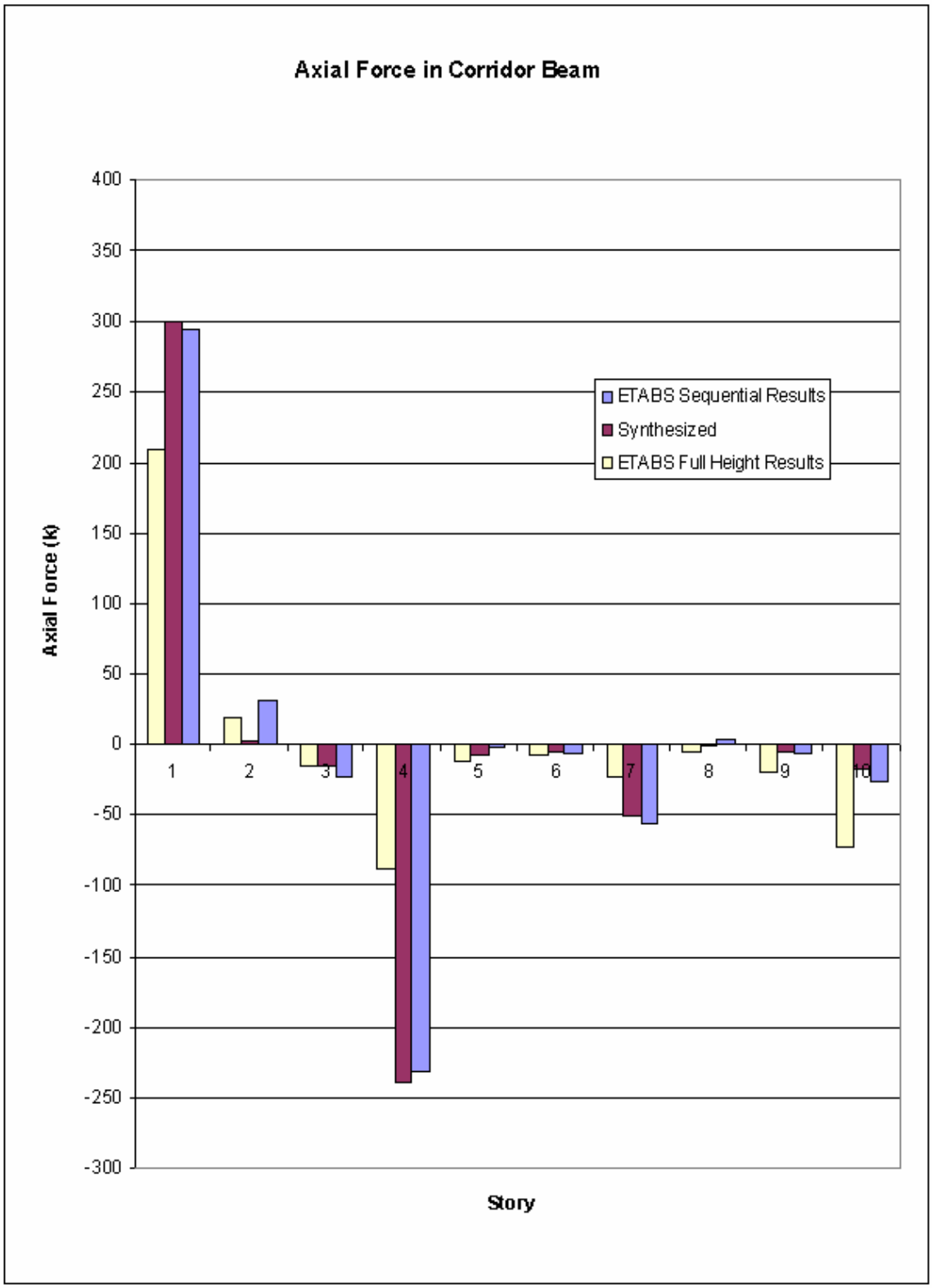

Figure 4.6 Axial Force in Corridor Beams due to Staged Load – 10 Story Prototype

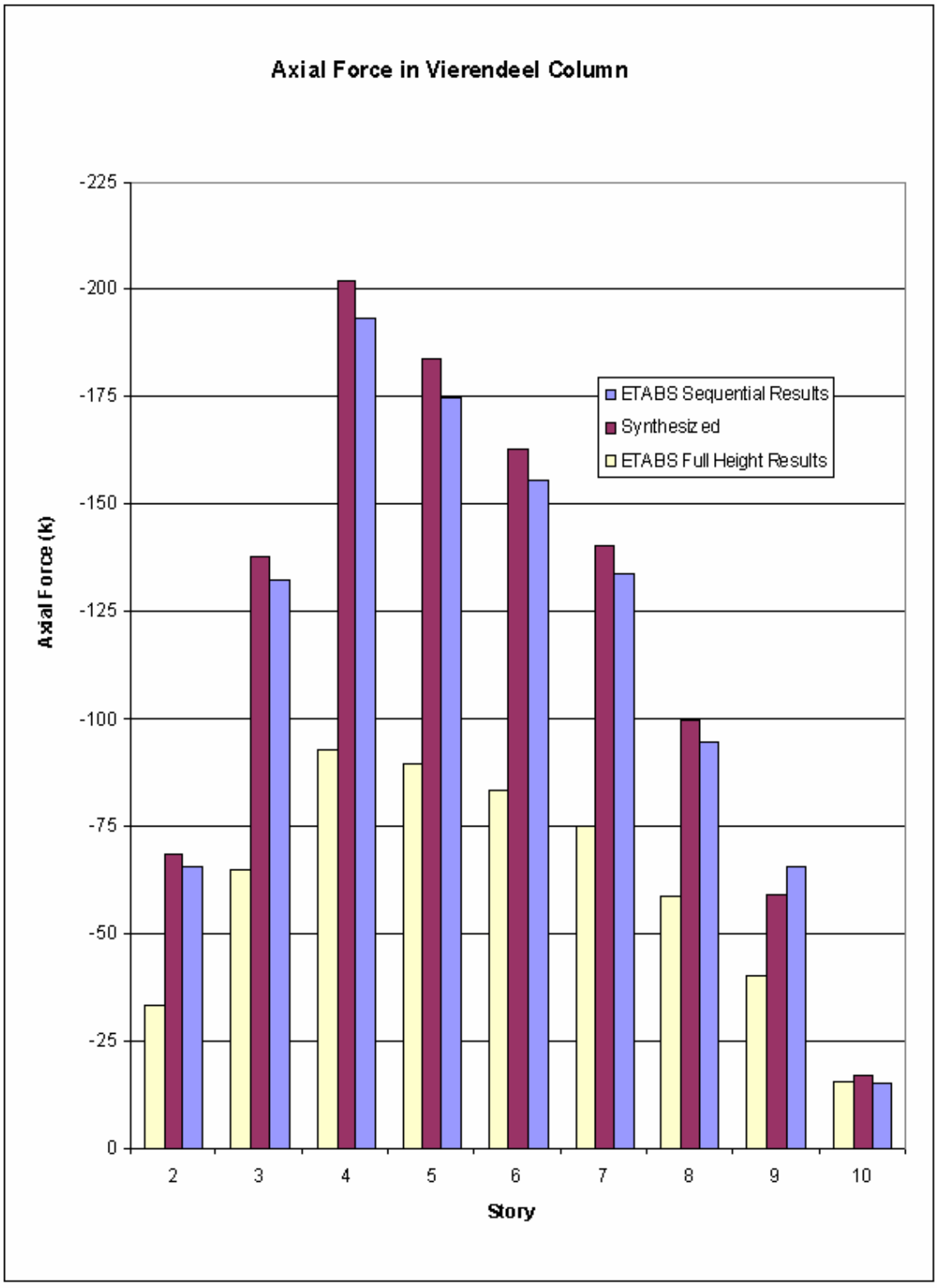

Figure 4.7 Axial Force in Vierendeel Columns due to Staged Load – 10 Story Prototype

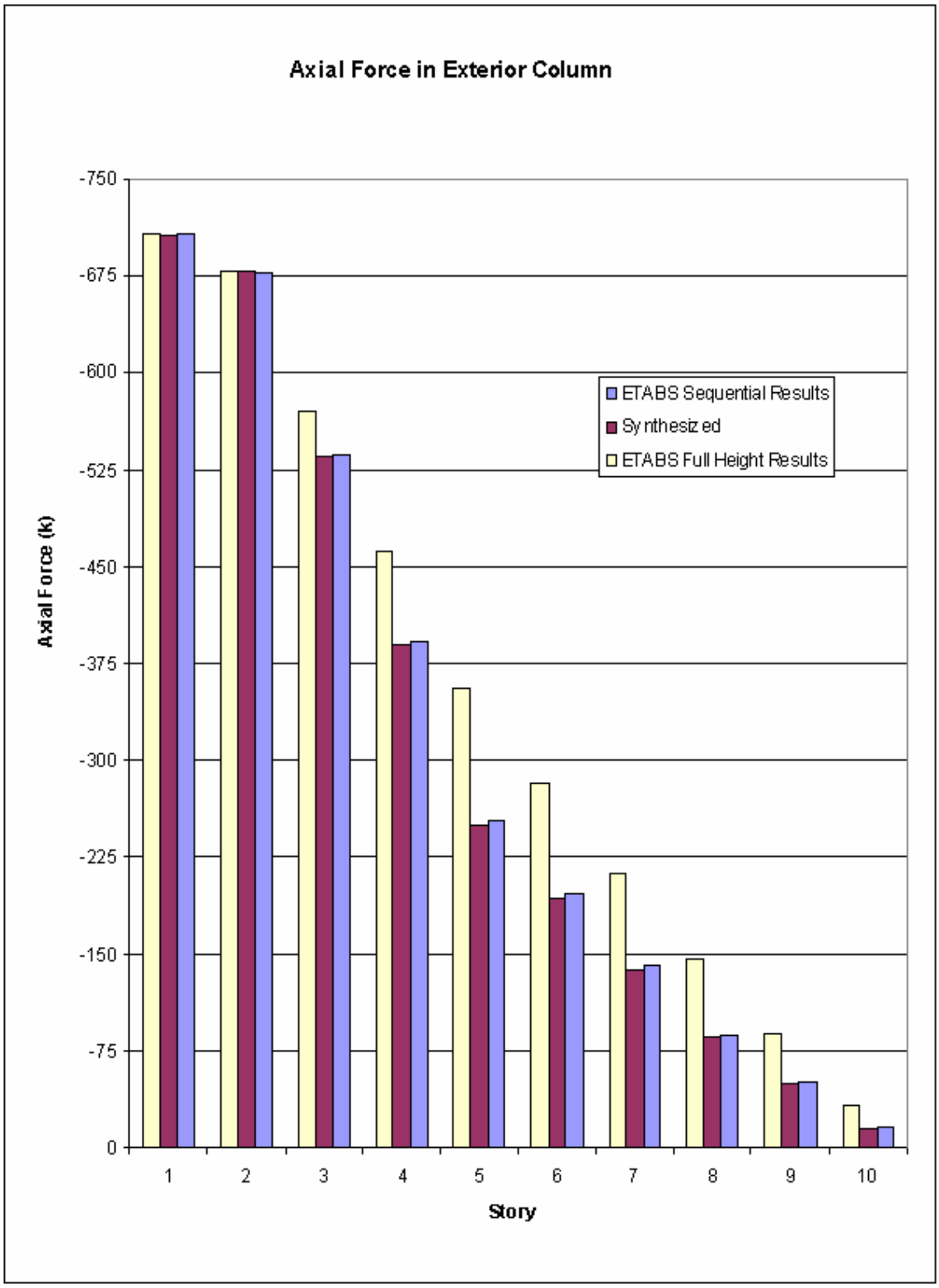

Figure 4.8 Axial Force in Exterior Columns due to Staged Load – 10 Story Prototype

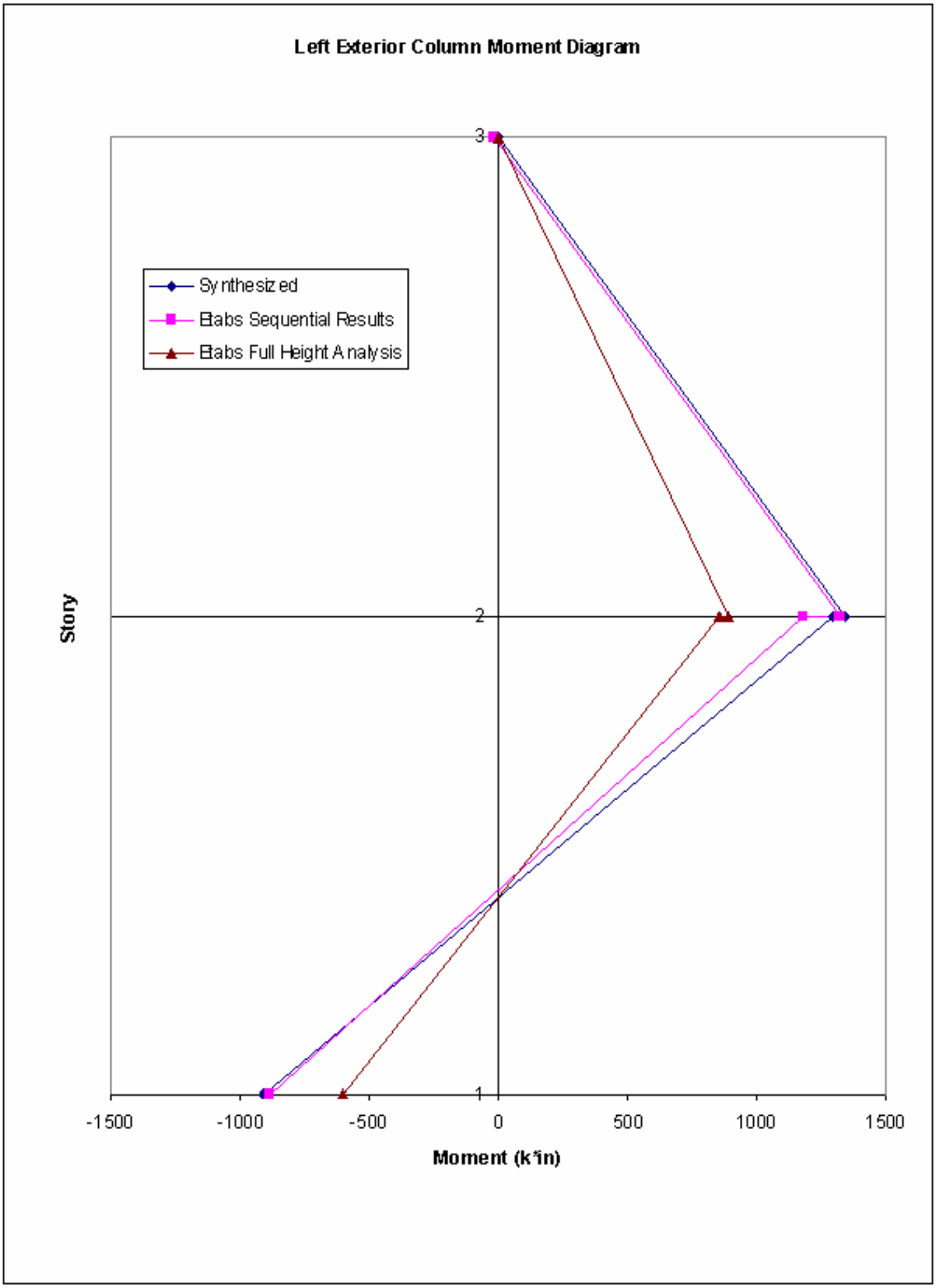

Figure 4.9 Moment in Lowest Two Left Exterior Columns due to Staged Load – 10 Story Prototype

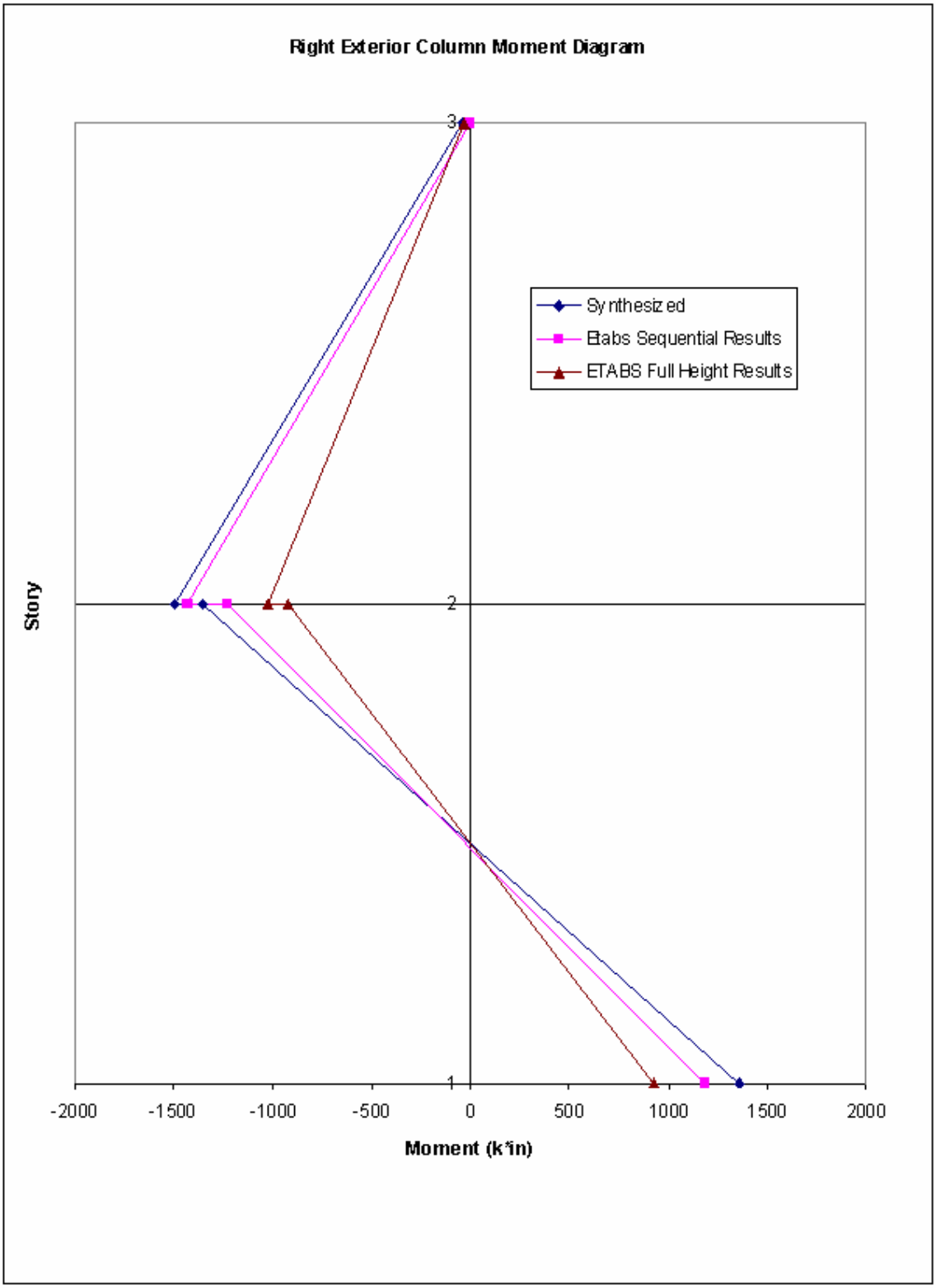

Figure 4.10 Moment in Lowest Two Right Exterior Columns due to Staged Load – 10 Story Prototype

One of the advantages of the FHTF is its stiffness to lateral loading. The ten story prototype structure underwent minimal drift due to the wind load. The drift along each exterior column line at each floor is recorded in Table 4.9. A sizable portion of the drift was due to the bending of the base columns; on all levels above these columns, the lateral load is primarily carried by direct stress in the diagonals and beams resulting in small inter-story drift. The total drift of the frame was approximately 1.5 inches; this surpasses the stricter criterion of H/400, where H is the total building height. The inter-story drift did not surpass H/200, where H is the height of each floor. It is not necessary to stiffen the base columns in this case, but if their deflection is greater than desired, a composite column or an additional lateral system to take the lateral load from the lowest level into the foundation can be introduced. It should be noted that if the end (exterior) FHTFs of the building were braced at the lowest level then part of the lateral load delivered to the lowest level columns of the interior frames could be transferred to the bracing in the end frames by the diaphragm action of the planks. This would reduce the bending and thus the deflection of the frames at the lowest levels where the drift is the greatest.

The deflection at the center span of the floor beams were checked against standard deflection limitations. The dead load deflection was limited to L/240 and the live load deflection to L/500, where L is the span of the beam. All beams meet this requirement. Therefore, member camber is unnecessary, but camber can be used if the engineer desires. The deflections for each beam at each story level are recorded in Table 4.10.

Table 4.9 FHTF Drift – 10 Story Prototype

Story	Column Line A Drift (in)	Column Line E Drift (in)	Maximum Inter-Story Drift (in)	H/200 (in)	H/400 (in)
10	1.48	1.26	0.13	0.54	0.27
9	1.35	1.21	0.10	0.54	0.27
8	1.25	1.12	0.11	0.54	0.27
7	1.23	1.01	0.13	0.54	0.27
6	1.1	0.9	0.12	0.54	0.27
5	0.99	0.78	0.13	0.54	0.27
4	1.04	0.65	0.17	0.54	0.27
3	0.87	0.54	0.18	0.54	0.27
2	0.69	0.44	0.37	0.54	0.27
1	0.32	0.414	0.414	0.72	0.36

The deflection of the truss at its interior panel points was limited to L/500 under the service load condition, where L is the span of the truss. This limits the truss to 1.73 inches at its joints. The greatest deflection of the truss occurred on the first truss section erected, and under service load conditions underwent a downward deflection of approximately 2 inches. The least deflection of the truss occurred on the third and final truss section and totaled approximately 0.7 inches under service load conditions. The service load deflection of the second truss section erected was approximately 1.1 inches. Therefore, during the erection of the first truss section, the floor trusses must be assembled with a camber to offset these deflections. The truss deflections at the interior panel points are shown in Table 4.11.

Table 4.10 Beam Deflection at Center Span – 10 Story Prototype

	Beam Deflection					
	Exterior Beam			Interior Beam		
Story	Dead (in)	Sdead (in)	Live (in)	Dead (in)	Sdead (in)	Live (in)
10	0.71		0.33	0.13		0.07
9	0.80	0.15	0.20	0.31	0.06	0.19
8	0.80	0.15	0.20	0.25	0.05	0.14
7	0.68	0.12	0.17	0.25	0.05	0.15
6	0.68	0.12	0.17	0.24	0.04	0.14
5	0.68	0.12	0.17	0.23	0.04	0.13
4	0.32	0.06	0.08	0.14	0.03	0.08
3	0.32	0.06	0.08	0.24	0.04	0.14
2	0.32	0.06	0.08	0.26	0.05	0.15
1	0.80	0.15	0.20	0.13	0.02	0.07

Table 4.11 Truss Deflection at Interior Joints – 10 Story Prototype

	Deflection at Interior Joints			
Story	Seq. Dead (in)	Super dead (in)	Live (in)	Total
10	0.27	0.14	0.27	0.68
9	0.27	0.14	0.27	0.68
8	0.26	0.14	0.27	0.67
7	0.65	0.15	0.27	1.07
6	0.64	0.15	0.29	1.08
5	0.63	0.16	0.29	1.08
4	1.46	0.17	0.31	1.94
3	1.46	0.17	0.32	1.95
2	1.46	0.18	0.33	1.97
1	1.49	0.19	0.34	2.02

4.6 Economy

The economy of the FHTF is due to a lightweight frame and the simplicity of configuration, fabrication, and erection. All design members are commonly fabricated sections that are erected using conventional stick erection practices. The majority of connections are designed as shear connections which result in less expensive assembly. Shop fabricating parts of the Vierendeel panels can result in further savings. The ten story prototype FHTF achieved a 9' floor to floor height, provided a column free first level, and carried all wind loads to the foundation without a secondary lateral system.

The ten story prototype was compared to a similar staggered truss model using ETABS staggered truss template and design function. The staggered truss frame and sections are illustrated in Figure 4.11. The ETABS design included an additional lateral bracing system for taking the wind load from the lowest truss to the foundation to avoid excessive column shear and moment. The result of the design was a staggered truss frame weighing 67,000 pounds or an average of 3.72 psf over the ten stories. The FHTF weighs an additional 4,000 pounds, but the cost of the materials can be made up by the fabrication savings and the absence of an extra lateral force resisting systems. Typically, fabricating the FHTF's simple members will cost less than fabricating the complete trusses used in the staggered truss frame.

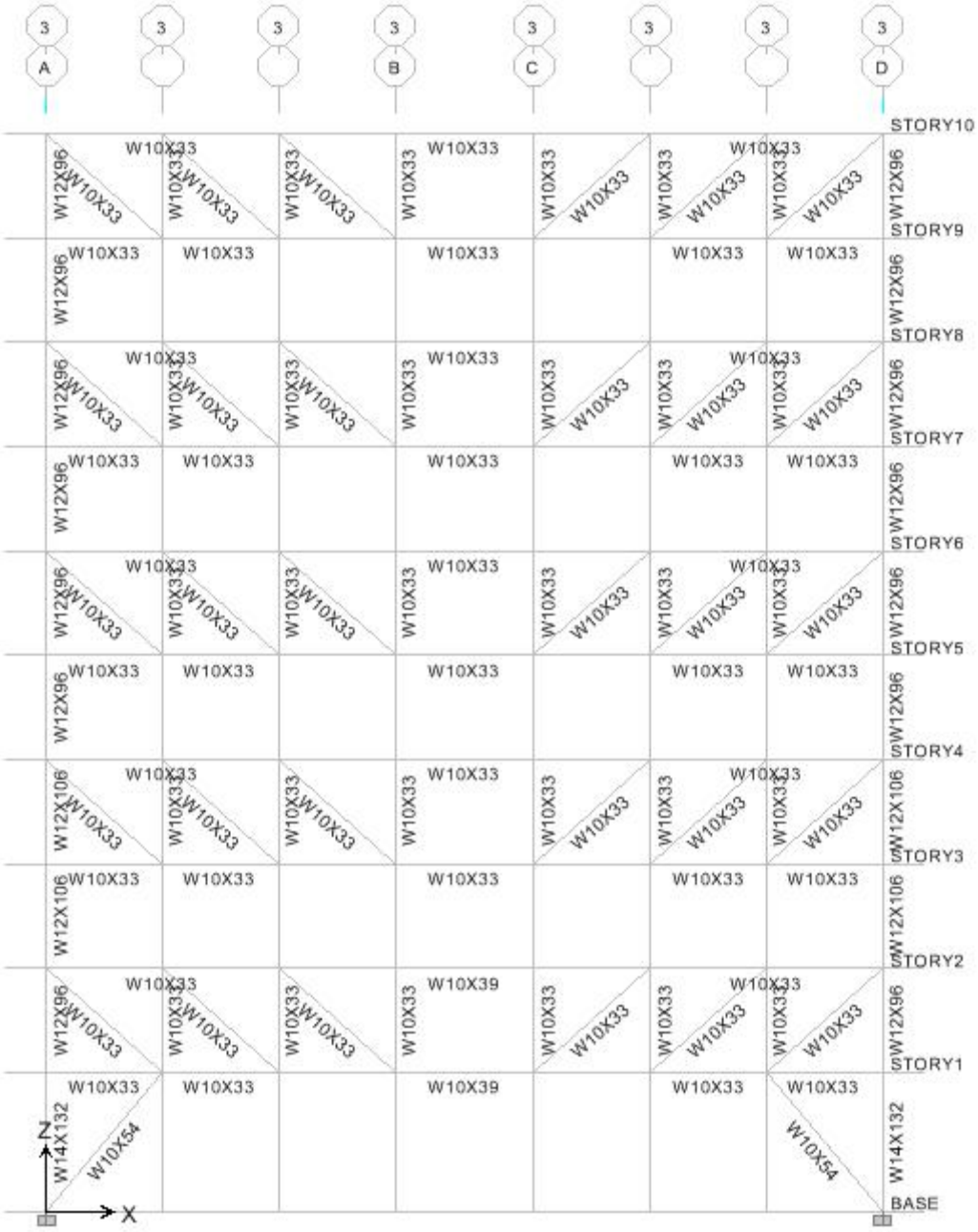

Figure 4.11 Staggered Truss Sections from ETABS Design

CHAPTER 5

25 STORY PROTOTYPE DESIGN RESULTS

The objective of the 25 Story Prototype is similar to the 10 story in its intent to illustrate the economy of its design and to validate the synthesis method for approximating the staged dead load case. In addition to this, the 25 story model demonstrates the viability of the FHTF as a mid to high rise framing system. The design of the 25 story prototype structure was completed as outlined in Chapter 3 and was similar to the 10 story prototype except for the composite columns used in the first truss section. The analysis with a computer analysis program, and the staged dead load results from the computer analysis were compared to the synthesis results.

5.1 Frame Sections

The frame section selection was performed according to outlined design and serviceability criteria. The frame sections were chosen to result in a lightweight and economical frame configuration. The total weight of the frame was 312,200 pounds or 6.94 psf. The volume of concrete used in the composite columns was 19.08 cubic yards. The concrete was assumed to weigh 150 pounds per cubic foot or 4,050 pounds per cubic yard, the total weight of the concrete is 77,700 pounds. Therefore, the total weight of the steel was 234,500 pounds or 5.21 psf. This is an increase of 1.25 psf of steel compared to the weight of the 10 story prototype. A comparison of the weight of steel used in the 10 story prototype to the 25 story prototype is shown in Table 5.1. This increase in steel

weight is largely due to the increase in size of the exterior and Vierendeel columns due to the added gravity load from the additional floors.

The average weight of the exterior columns was 114.9 pounds per linear foot, and that of the Vierendeel columns was 85.5 pounds per linear foot. This is an increase of 34 for the exterior columns and 52.6 pounds per linear foot for the Vierendeel columns compared to the 10 story prototype. The column increases total 0.87 psf, accounting for almost 70% of the increase in steel weight.

The remaining increase in steel tonnage is due to the beams and diagonals. The average weight of the exterior bay beams was 57.8 compared to 53.6 pounds per linear foot of the 10 story prototype. The average weight of the corridor beam was 50.4 pounds per linear foot, an increase of 16.4 pounds per linear foot when compared to the 10 story prototype. The average weight of the diagonals was 33.63 pounds per linear foot, an increase of 2.3 pounds per linear foot. These account for a total increase of 0.37 psf.

Table 5.1 Average Member Weights

	Average Weight (lbs/ft unless noted)		
Member	**10 Story Prototype**	**25 Story Prototype**	**Percent Increase**
Exterior Bay Beam	53.6	57.8	7.8
Interior Corridor Beam	34	50.4	48.2
Diagonal	31.33	33.63	7.3
Vierendeel Column	27.7	85.5	209
Exterior Column	80.9	114.9	42
Total Weight	3.96 psf	5.21 psf	31.6

The steel sections used for each member and the configuration of the FHTF are shown in Figure 5.2. The outer bay beams and diagonals were designed in groups according to the construction sequence. The diagonals were designed as W10 shapes. Because they are exclusively tension members, they could be any shape of the appropriate area of steel. The exterior bay beams were wide flange shapes ranging in depth from 21" to 24", the latter being at the lower more stressed levels. The interior corridor beams, except at the lowest level, were designed to have a maximum depth of 14" to supply the required clearance of 7'. These beams were combined with W14 shape vertical members to form the Vierendeel Panels. The exterior columns were designed on a per story basis while limiting the member to a W14X38. The first four exterior columns, part of the first truss section erected, were designed as 32" by 32" composite columns of an encased W-Shape in high strength normal weight concrete with one #10 60ksi steel reinforcing bar in each corner as shown in figure 5.1. The composite columns were design using an AISC guide (AISC, 1992); these columns were not checked against ACI spacing and transverse steel provisions and will require further detailing.

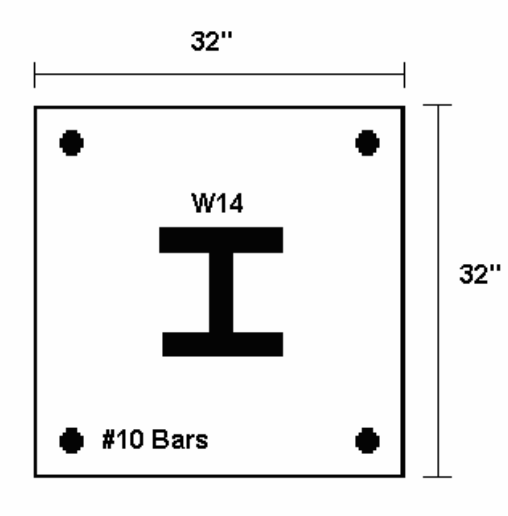

Figure 5.1 Composite Column Section

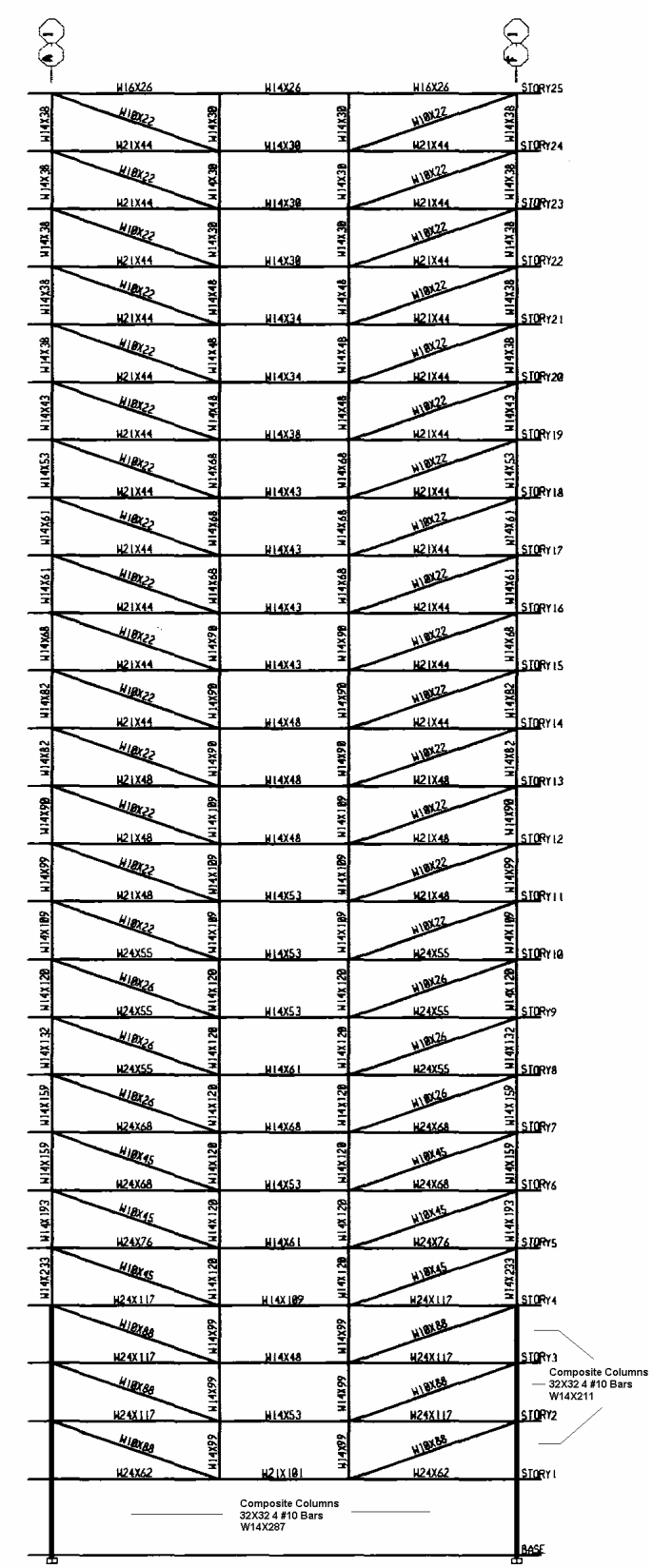

Figure 5.2 Design Sections of the 25 Story Prototype

5.2 Member Stiffness Reduction

The flexural stiffness of the lowest two outer columns and Vierendeel panels and the axial stiffness of the diagonals, exterior columns above the second level, and the outer bay beams were reduced according Appendix 7 of the draft *Specification for Structural Steel Buildings* (AISC, 2004). The stiffness of the axial members (EA) was reduced by a factor of 0.8. The flexural reduction is outlined in Table 5.2. The modifier, τ, did not deviated significantly from 1; therefore, all of the flexural reduction factors were approximated by the value of 0.8 in order simplify the analysis model.

5.3 Analysis and Design Results

The capacities of all the frame members were checked according to the methods outlined in Section 3.7. The design shears, axial forces, and moments acting on each member were calculated by ETABS under the combined loading of the frame according to Chapter 3. The results of the analysis and capacity check can be found in Table 5.3, 5.4, 5.5, 5.6, and 5.7.

Table 5.2 Flexural Stiffness Reduction Factors – 25 Story Prototype

	Exterior Column		Vierendeel Columns		Interior Corridor Beam	
Story	τ	Stiffness Reduction	τ	Stiffness Reduction	τ	Stiffness Reduction
25			1.000	**0.800**	1.000	**0.800**
24			1.000	**0.800**	1.000	**0.800**
23			1.000	**0.800**	1.000	**0.800**
22			1.000	**0.800**	1.000	**0.800**
21			1.000	**0.800**	1.000	**0.800**
20			0.984	**0.787**	1.000	**0.800**
19			1.000	**0.800**	1.000	**0.800**
18			0.995	**0.796**	1.000	**0.800**
17			0.961	**0.769**	1.000	**0.800**
16			1.000	**0.800**	1.000	**0.800**
15			0.993	**0.794**	1.000	**0.800**
14			0.972	**0.777**	1.000	**0.800**
13			0.999	**0.799**	1.000	**0.800**
12			0.992	**0.794**	1.000	**0.800**
11			0.981	**0.785**	1.000	**0.800**
10			0.994	**0.795**	1.000	**0.800**
9			0.990	**0.792**	1.000	**0.800**
8			0.987	**0.790**	1.000	**0.800**
7			0.984	**0.787**	1.000	**0.800**
6			0.995	**0.796**	1.000	**0.800**
5			1.000	**0.800**	1.000	**0.800**
4			0.987	**0.790**	1.000	**0.800**
3			1.000	**0.800**	1.000	**0.800**
2	1.000	**0.800**	1.000	**0.800**	Tension	**0.800**
1	1.000	**0.800**			Tension	**0.800**

Table 5.3 Exterior Column Capacity Checks – 25 Story Prototype

Outer Columns	Story	Combo	Mu (k-in)	Pu (k)	Vu (k)	ΦMn (k-in)	ΦPn (k)	ΦVn (k)	Capacity
W14X38	25	2	67.3	-27.3	1.0	532.4	-343.4	156.9	0.17
W14X38	24	2	98.2	-92.8	1.8	532.4	-355.4	156.9	0.43
W14X38	23	2	45.2	-158.8	0.9	532.4	-355.4	156.9	0.52
W14X38	22	2	94.1	-228.6	2.0	532.4	-355.4	156.9	0.80
W14X38	21	2	94.8	-299.1	1.4	532.4	-355.4	156.9	1.00
W14X43	20	2	81.5	-370.4	1.4	762.8	-441.0	190.8	0.94
W14X53	19	2	106.5	-447.8	2.2	966.4	-549.2	239.4	0.91
W14X61	18	2	137.9	-526.5	2.5	1445.9	-677.1	290.0	0.86
W14X61	17	2	71.1	-606.1	1.3	1445.9	-677.1	290.0	0.94
W24X68	16	2	127.0	-692.8	2.8	1633.5	-757.6	324.0	0.98
W14X82	15	2	128.6	-782.8	2.2	1978.2	-911.1	388.6	0.92
W14X82	14	2	78.9	-873.3	1.6	1978.2	-911.1	388.6	0.99
W14X90	13	2	189.5	-973.9	4.1	3370.3	-1065.7	463.3	0.96
W14X99	12	2	140.6	-1078.7	2.7	3717.1	-1172.2	512.5	0.95
W14X109	11	2	134.4	-1185.5	3.0	4133.2	-1290.1	565.0	0.95
W14X120	10	2	182.9	-1312.5	3.5	4545.9	-1429.7	612.8	0.95
W14X132	9	2	138.1	-1443.1	0.9	5032.7	-1573.9	681.3	0.94
W14X159	8	2	387.2	-1580.3	6.9	6473.1	-1903.3	835.4	0.88
W14X159	7	2	211.1	-1779.1	1.6	6473.1	-1903.5	835.4	0.96
W14X193	6	2	580.1	-1990.1	4.1	8005.4	-2320.2	1017.4	0.92
W14X233	5	2	1622.8	-2212.2	23.3	9764.2	-2801.3	1230.7	0.94
Composite W14X211	4	2	2092	-2638		24840	-6450		0.49
Composite W14X211	3	2	7497	-3056		24840	-6540		0.74
Composite W14X211	2	2	10745	-3500		24960	-6540		0.92
Composite W14X283	1	5	23899	-3432		38040	-7350		1.03*

Table 5.4 Vierendeel Column Capacity Checks – 25 Story Prototype

Vierendeel Columns	Story	Combo	Mu (k-in)	Pu (k)	Vu (k)	ΦMn (k-in)	ΦPn (k)	ΦVn (k)	Capacity
W14X30	25	5	889.9	-26.7	16.3	2128.5	-264.6	100.6	0.47
W14X30	24	5	1065.0	-103.4	19.3	2128.5	-264.6	100.6	0.82
W14X30	23	5	564.2	-175.6	12.2	2128.5	-264.6	100.6	0.88
W14X48	22	5	1159.0	-246.9	23.8	3528.0	-495.0	126.7	0.79
W14X48	21	5	1245.9	-315.8	21.7	3528.0	-495.0	126.7	0.95
W14X48	20	5	767.3	-381.8	16.0	3528.0	-495.0	126.7	0.97
W14X68	19	5	1415.3	-447.2	28.4	5175.0	-757.6	156.9	0.83
W14X68	18	5	1505.7	-509.2	26.1	5175.0	-757.6	156.9	0.93
W14X68	17	5	1002.5	-568.0	20.3	5175.0	-757.6	156.9	0.92
W14X90	16	5	1528.6	-624.6	30.5	7065.0	-1065.8	166.3	0.78
W14X90	15	5	1702.4	-674.7	28.6	7065.0	-1065.8	166.3	0.85
W14X90	14	5	1266.4	-723.1	24.8	7065.0	-1065.8	166.3	0.84
W14X109	13	5	1741.0	-769.1	33.7	8640.0	-1290.1	202.7	0.76
W14X109	12	5	1890.2	-806.0	31.9	8640.0	-1290.1	202.7	0.82
W14X109	11	5	1671.9	-840.7	30.7	8640.0	-1290.1	202.7	0.82
W14X120	10	5	1884.4	-872.7	34.7	9540.0	-1429.7	231.0	0.79
W14X120	9	5	2034.5	-885.1	34.8	9540.0	-1429.7	231.0	0.81
W14X120	8	5	2457.2	-896.2	41.5	9540.0	-1429.7	231.0	0.86
W14X120	7	5	1771.9	-907.0	32.9	9540.0	-1429.7	231.0	0.80
W14X120	6	5	1798.0	-852.7	32.9	9540.0	-1429.7	231.0	0.76
W14X120	5	5	3444.7	-791.0	52.6	9540.0	-1429.7	231.0	0.87
W14X99	4	5	1672.3	-739.9	34.6	7785.0	-1177.0	185.9	0.82
W14X99	3	5	1456.7	-489.7	27.4	7785.0	-1177.0	185.9	0.58
W14X99	2	5	5051.3	-239.8	66.7	7785.0	-1177.0	185.9	0.78

Table 5.5 Diagonal Capacity Checks – 25 Story Prototype

Diagonals	Story	Combo	Mu (k-in)	Pu (k)	Vu (k)	ΦMn (k-in)	ΦPn (k)	ΦVn (k)	Capacity
W10X22	25	2	28.4	44.5	0.4	301.8	292.1	66.1	0.17
W10X22	24	2	28.4	52.6	0.4	301.8	292.1	66.1	0.19
W10X22	23	2	28.4	55.0	0.4	301.8	292.1	66.1	0.19
W10X22	22	2	28.4	64.8	0.4	301.8	292.1	66.1	0.31
W10X22	21	2	28.4	67.7	0.5	301.8	292.1	66.1	0.32
W10X22	20	2	28.4	70.9	0.5	301.8	292.1	66.1	0.33
W10X22	19	2	28.4	87.1	0.5	301.8	292.1	66.1	0.39
W10X22	18	2	28.4	91.5	0.5	301.8	292.1	66.1	0.42
W10X22	17	2	28.4	95.9	0.5	301.8	292.1	66.1	0.46
W10X22	16	2	28.4	115.9	0.5	301.8	292.1	66.1	0.54
W10X22	15	2	28.4	123.3	0.6	301.8	292.1	66.1	0.58
W10X22	14	2	28.4	128.9	0.6	301.8	292.1	66.1	0.61
W10X22	13	2	28.4	156.7	0.6	301.8	292.1	66.1	0.72
W10X22	12	2	28.4	166.6	0.7	301.8	292.1	66.1	0.76
W10X22	11	2	28.4	174.6	0.7	301.8	292.1	66.1	0.80
10X26	10	2	33.3	235.5	0.8	422.9	342.5	72.3	0.86
10X26	9	2	33.3	249.9	0.9	422.9	342.5	72.3	0.90
10X26	8	2	33.3	261.7	1.5	422.9	342.5	72.3	0.92
W10X45	7	2	58.2	452.8	1.5	1586.1	598.5	95.4	0.82
W10X45	6	2	58.2	488.7	1.6	1586.1	598.5	95.4	0.88
W10X45	5	2	58.2	520.0	1.7	1586.1	598.5	95.4	0.90
W10X88	4	2	113.3	1104.3	3.2	5085.0	1165.5	176.4	0.97
W10X88	3	2	113.3	1084.0	3.1	5085.0	1165.5	176.4	0.95
W10X88	2	2	113.3	1155.4	3.3	5085.0	1165.5	176.4	1.01*

Table 5.6 Corridor Beam Capacity Checks – 25 Story Prototype

Corridor Beams	Story	Combo	Mu (k-in)	Pu (k)	Vu (k)	ΦMn (k-in)	ΦPn (k)	ΦVn (k)	Capacity
W14X26	25	5	865.0	-36.7	14.4	1809.0	-267.5	95.7	0.55
W14X30	24	5	1924.8	-14.7	42.2	2128.5	-326.3	100.6	0.93
W14X30	23	5	1888.8	0.1	42.2	2128.5	398.3	100.6	0.89
W14X30	22	5	1997.4	-25.2	42.0	2128.5	-326.3	100.6	0.98
W14X34	21	5	2303.8	-5.1	42.6	2457.0	-370.4	107.7	0.94
W14X34	20	5	2279.2	-2.4	42.5	2457.0	-370.4	107.7	0.93
W14x38	19	5	2493.1	-29.7	44.6	2767.5	-415.6	118.0	0.94
W14x43	18	5	2806.9	-6.6	47.1	3132.0	-466.7	112.8	0.90
W14x43	17	5	2800.7	-2.6	47.1	3132.0	-466.7	112.8	0.90
W14x43	16	5	2886.0	-33.1	48.0	3132.0	-466.7	112.8	0.96
W14x43	15	5	3048.6	-7.9	49.1	3132.0	-466.7	112.8	0.98
W14X48	14	5	3256.7	-4.4	51.1	3528.0	-523.1	126.7	0.93
W14X48	13	5	3319.8	-39.9	51.9	3528.0	-523.1	126.7	0.98
W14X48	12	5	3461.9	-8.9	52.8	3528.0	-523.1	126.7	0.99
W14X53	11	5	3707.5	-8.3	55.0	3919.5	-579.7	138.9	0.95
W14X53	10	5	3699.9	-62.1	55.2	3919.5	-579.7	138.9	1.00
W14X53	9	5	3780.6	-11.4	55.7	3919.5	-579.7	138.9	0.97
W14X61	8	5	4200.3	-18.7	59.3	4590.0	-668.0	140.7	0.93
W14X68	7	5	4332.2	-156.2	60.7	5175.0	-747.3	156.9	0.95
W14X53	6	5	3655.3	-27.1	54.6	3919.5	-579.8	138.9	0.96
W14X61	5	5	4107.7	-54.7	58.1	4590.0	-668.0	140.7	0.94
W14X109	4	5	5432.9	-481.3	70.7	8640.0	-1205.9	202.7	0.96
W14X48	3	5	3208.7	-33.1	51.0	3528.0	-523.2	126.7	0.94
W14X53	2	5	3556.2	121.3	54.8	3919.5	702.0	138.9	0.99
W21X101	1	5	5051.3	720.7	73.9	11385.0	1341.0	288.9	0.93

Table 5.7 Exterior Bay Beam Capacity Checks – 25 Story Prototype

Exterior Beams	Story	Combo	Mu (k-in)	Pu (k)	Vu (k)	ΦMn (k-in)	ΦPn (k)	ΦVn (k)	Capacity
W16X26	25	3	1206.1	-27.3	15.9	1989.0	-264.0	98.8	0.66
W21X44	24	2	3519.8	-50.4	46.7	4293.0	-486.0	193.0	0.87
W21X44	23	2	3520.1	-50.9	46.7	4293.0	-486.0	193.0	0.87
W21X44	22	2	3526.7	-62.2	46.7	4293.0	-486.0	193.0	0.89
W21X44	21	2	3527.3	-63.2	46.7	4293.0	-486.0	193.0	0.89
W21X44	20	2	3514.9	-66.8	46.6	4293.0	-486.0	193.0	0.89
W21X44	19	2	3521.4	-83.0	46.6	4251.4	-486.0	193.0	0.91
W21X44	18	2	3500.6	-86.5	46.5	4249.5	-486.0	193.0	0.91
W21X44	17	2	3502.2	-89.3	46.5	4248.0	-486.0	193.0	0.92
W21X44	16	2	3515.0	-110.8	46.5	4235.6	-486.0	193.0	0.97
W21X44	15	2	3516.8	-115.7	46.5	4232.6	-486.0	193.0	0.98
W21X44	14	2	3519.9	-120.9	46.5	4229.4	-486.0	193.0	0.99
W21X48	13	2	3474.7	-150.5	46.3	4742.2	-532.0	192.6	0.93
W21X48	12	2	3476.2	-155.6	46.3	4739.0	-532.0	192.6	0.95
W21X48	11	2	3481.1	-164.9	46.3	4733.0	-532.0	192.6	0.96
W24X55	10	2	3481.7	-223.0	46.5	5915.5	-628.8	246.4	0.88
W24X55	9	2	3485.4	-233.0	46.6	5905.8	-628.8	246.4	0.90
W24X55	8	2	3481.8	-252.3	46.6	5886.0	-629.0	246.4	0.93
W24X68	7	2	3519.5	-422.4	47.1	7697.0	-781.9	265.6	0.95
W24X68	6	2	3527.7	-454.9	47.2	7650.8	-781.9	265.6	0.99
W24X76	5	2	3532.4	-516.4	47.4	8751.3	-873.7	283.9	0.95
W24X117	4	2	3404.5	-1031.1	47.6	14715.0	-1357.5	360.9	0.97
W24X117	3	2	3409.9	-1069.4	47.6	14715.0	-1357.5	360.9	1.00
W24X117	2	2	3383.0	-873.6	47.3	14715.0	-1357.5	360.9	0.85
W24X62	1	5	2942.3	-361.0	45.4	6748.4	-708.0	275.2	0.90

* Member deemed acceptable by the author because it is within a small margin ($\pm$3%) of the maximum allowable compression flexure interaction

5.4 Staged Synthesis Results

The staged dead load synthesis results were calculated using the full height dead load axial results according to methods outlined in Section 3.6. The full height dead load results for the diagonals are compared with the sequential results in Table 5.8. The comparison of the 25 story prototype shows the same trends as the 10 story prototype. The synthesis results compared were the axial forces from the right side of the frame. These results can be applied to the left side due to symmetry, or the left side axial forces in the members can be synthesized independently using the same method. A graphical comparison of the axial force in each member at each level is shown in Figures 5.3 through 5.9.

Similar to the 10 story prototype, the differences in magnitude between the synthesis results and ETABS are small. For the 25 story frame, the synthesis gives more conservative results for the lower diagonals but underestimates the force in the upper diagonals. From Table 5.9, the diagonal forces in the lower levels are much larger, and design is based upon strength criteria; therefore conservative results are more desirable than the opposite. For the upper level members, the forces are small and though the synthesis yields unconservative estimates, the magnitudes are not as significant because these diagonals were designed based on a minimum stiffness and surpass the strength requirements by a wide margin. From Table 5.5, diagonals above the tenth story are loaded at or less than 80% of ultimate capacity. An additional 6 or 7 kips would only account for 2% of the total capacities of the W10x22 diagonals in these levels.

When comparing the 10 story prototype results with the 25 story, it is clear that the synthesis gives more accurate approximations for the diagonal forces from the FHTF with fewer levels. The magnitudes of the differences from the 10 story prototype ranged from 5 to 11 kips and the percent differences ranged from 21 in the upper levels to 4 percent in the lower. As predicted, the synthesis model yielded less accurate results for the 25 story prototype due to ratio of average deflection being increasingly greater than the ratio of actual deflection as the number of levels increases between the full height and staged model. But, the synthesis still predicts reasonable tension forces in the diagonal for design. The percent differences ranged from 55 percent at the top level to 8 percent at the bottom level. The large percent differences in the upper levels are deceiving; the differences are small, approximately 5 kips, but the forces in the diagonals are along the same order of magnitudes. As has been noted, accuracy in these levels is not as important because the diagonals are chosen based on a minimum area, and they will not be stressed near ultimate capacity.

Table 5.8 Full Height and Staged Analysis Results for Diagonal – 25 Story Prototype

Story	Sequential (k)	Full Height (k)	Percent Difference
25	9	42	357%
24	9	52	505%
23	9	54	483%
22	17	54	217%
21	18	57	212%
20	19	60	211%
19	30	64	111%
18	32	68	113%
17	33	72	115%
16	47	77	63%
15	50	83	64%
14	52	88	68%
13	71	95	33%
12	76	102	34%
11	79	109	38%
10	116	131	12%
9	123	140	13%
8	127	150	18%
7	239	230	-4%
6	259	249	-4%
5	270	275	2%
4	646	461	-29%
3	634	454	-28%
2	676	486	-28%

Table 5.9 Comparison of Axial Force in Diagonal – 25 Story Prototype

Story	Synthesis (k)	ETABS Results (k)	Difference (k)	Percent Difference
25	4.1	9.15	-5.0	-54.72%
24	5.2	8.67	-3.5	-40.07%
23	5.3	9.2	-3.9	-42.17%
22	12.5	17.16	-4.6	-27.07%
21	13.0	18.19	-5.2	-28.32%
20	13.7	19.19	-5.5	-28.46%
19	23.6	30.36	-6.8	-22.37%
18	25.0	31.84	-6.9	-21.54%
17	26.4	33.37	-7.0	-20.87%
16	39.7	47.23	-7.5	-15.96%
15	42.5	50.41	-7.9	-15.71%
14	45.0	52.26	-7.2	-13.84%
13	63.9	71.37	-7.4	-10.41%
12	68.6	75.84	-7.3	-9.60%
11	73.2	78.75	-5.6	-7.10%
10	111.4	116.39	-5.0	-4.26%
9	119.1	123.36	-4.2	-3.43%
8	127.9	127.41	0.5	0.35%
7	244.3	239.28	5.0	2.08%
6	264.5	258.59	5.9	2.28%
5	292.5	269.56	22.9	8.51%
4	692.0	646.07	46.0	7.12%
3	682.0	633.68	48.3	7.62%
2	728.5	675.82	52.7	7.79%

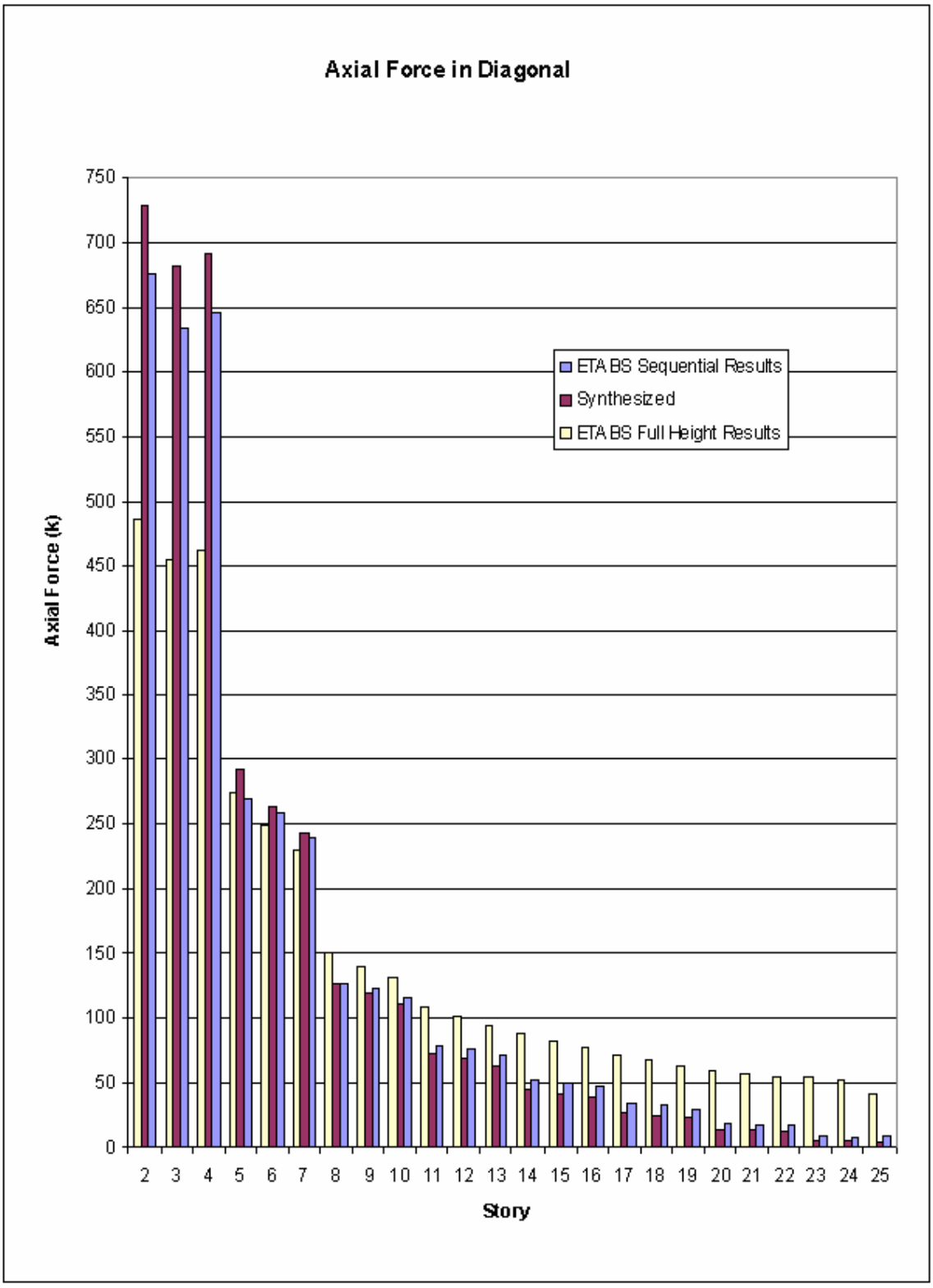

Figure 5.3 Axial Force in Diagonals due to Staged Load – 25 Story Prototype

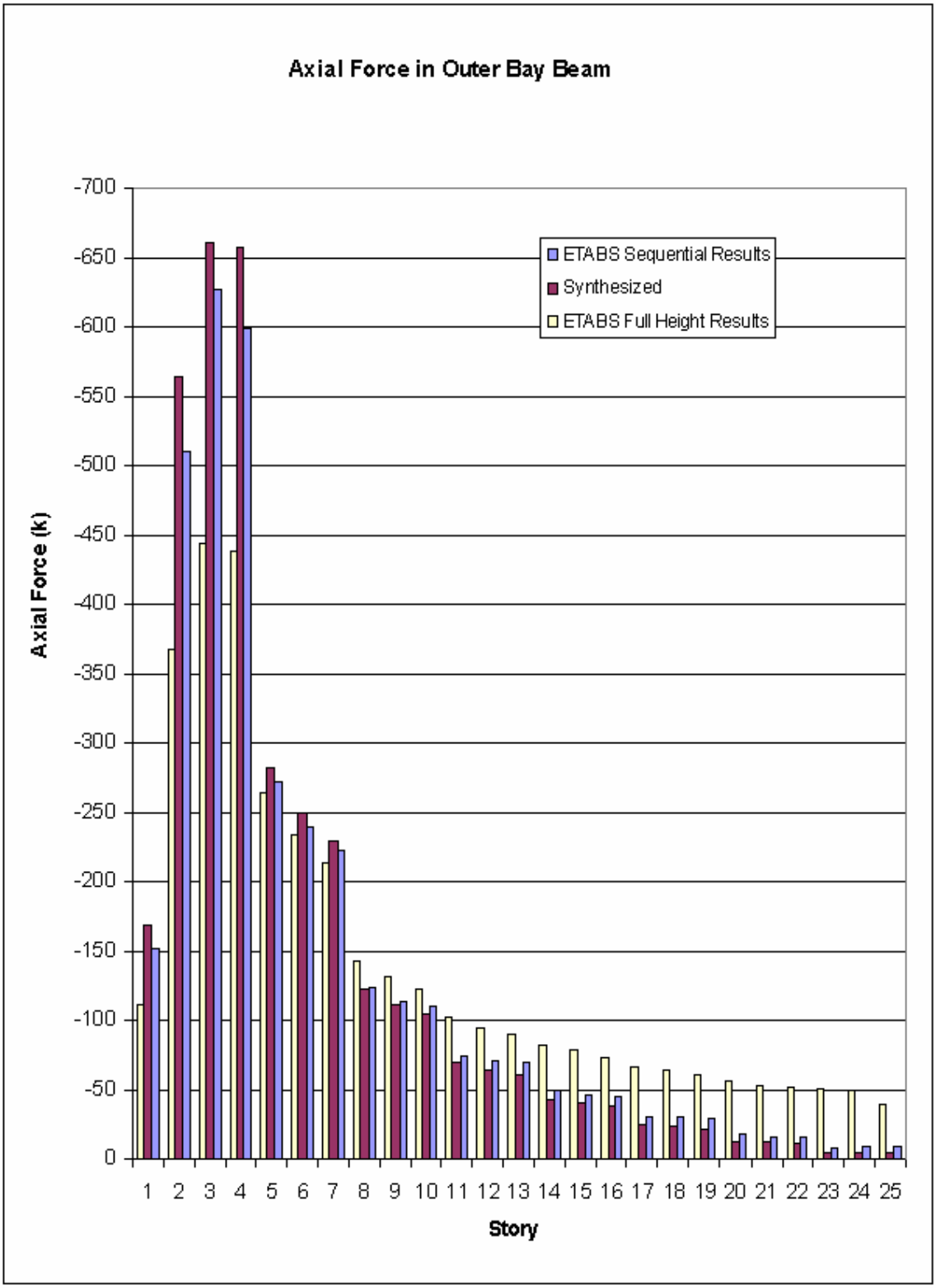

Figure 5.4 Axial Force in Outer Bay Beams due to Staged Load – 25 Story Prototype

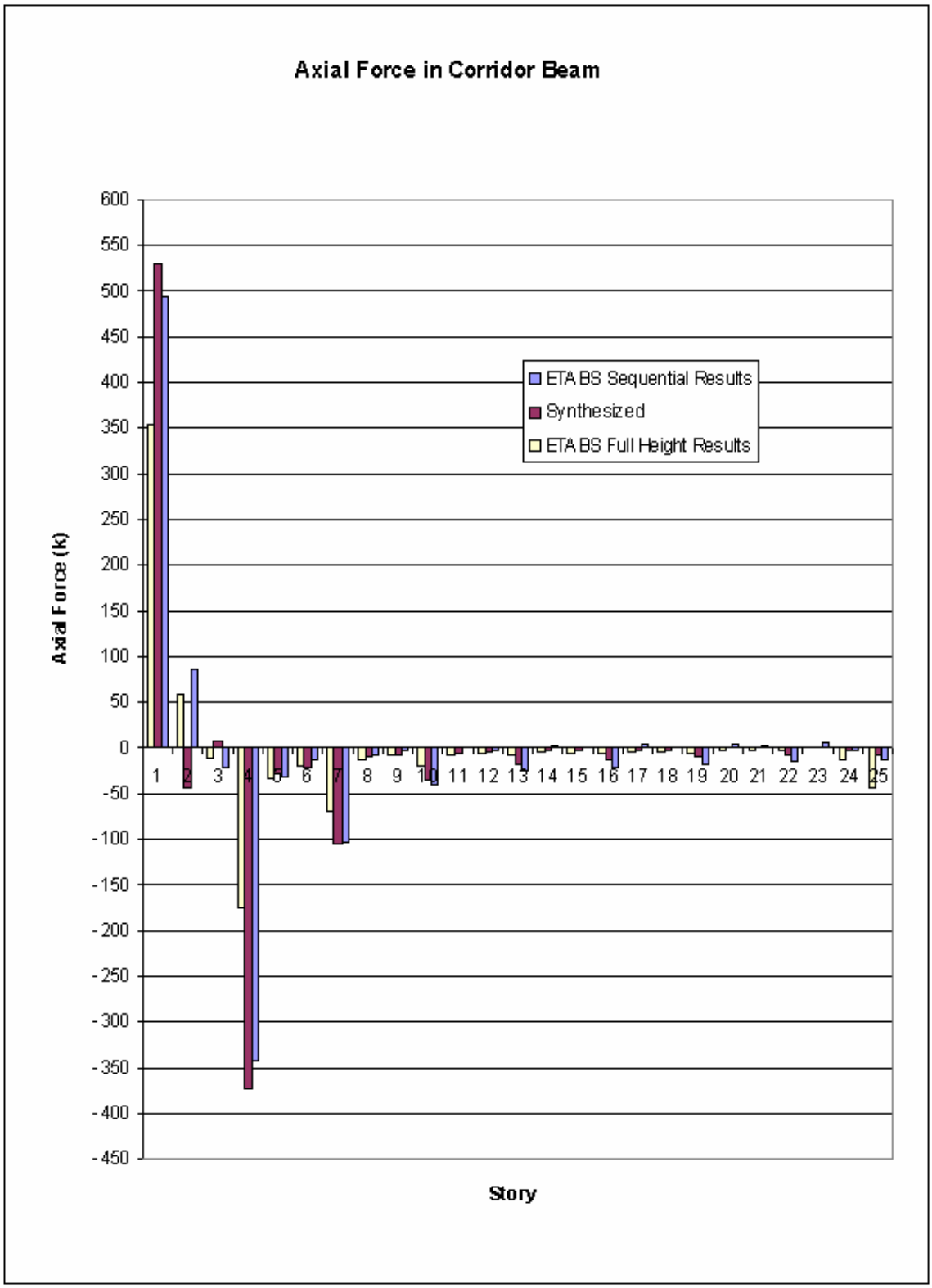

Figure 5.5 Axial Force in Corridor Beams due to Staged Load – 25 Story Prototype

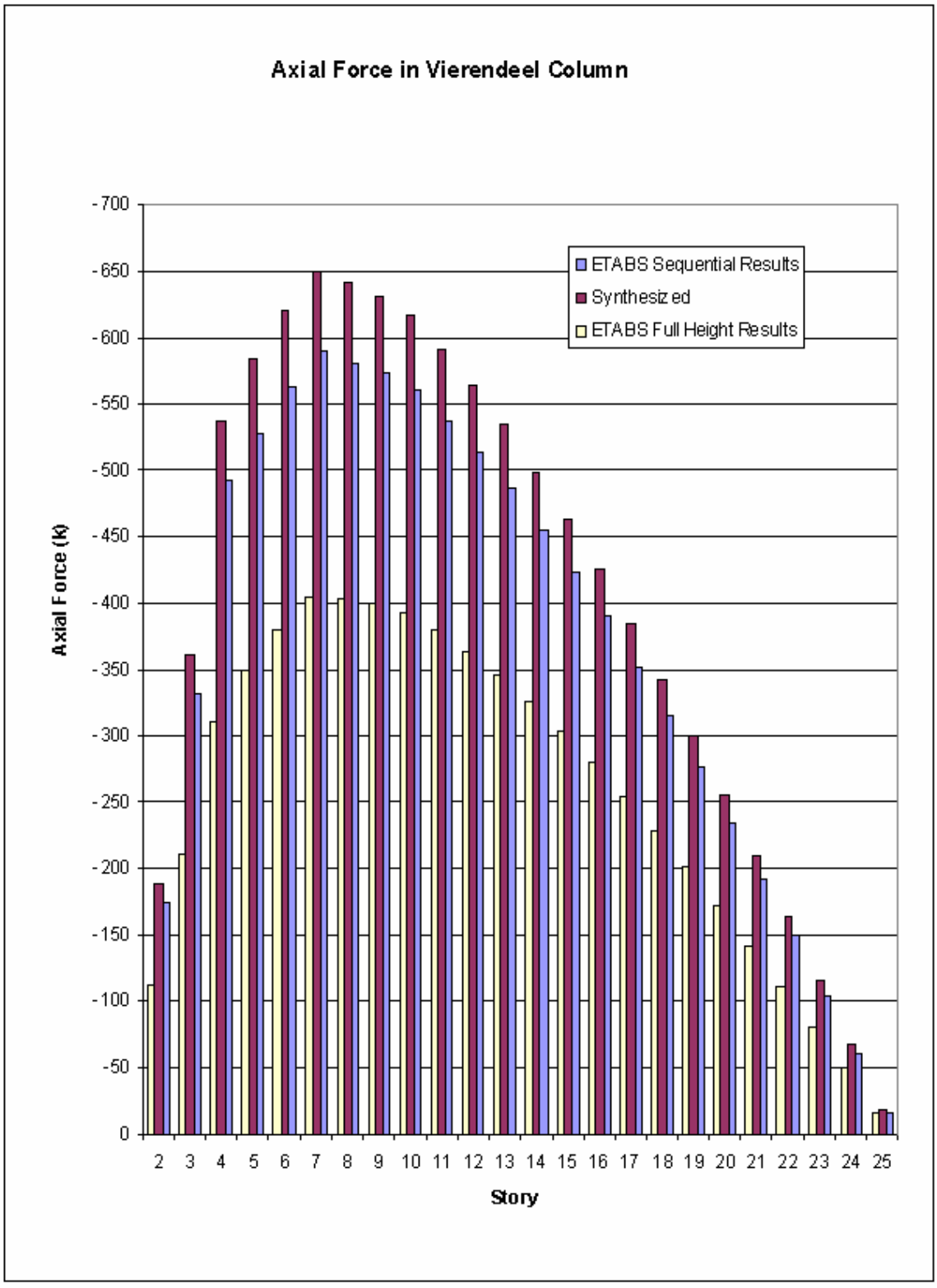

Figure 5.6 Axial Force in Vierendeel Columns due to Staged Load – 25 Story Prototype

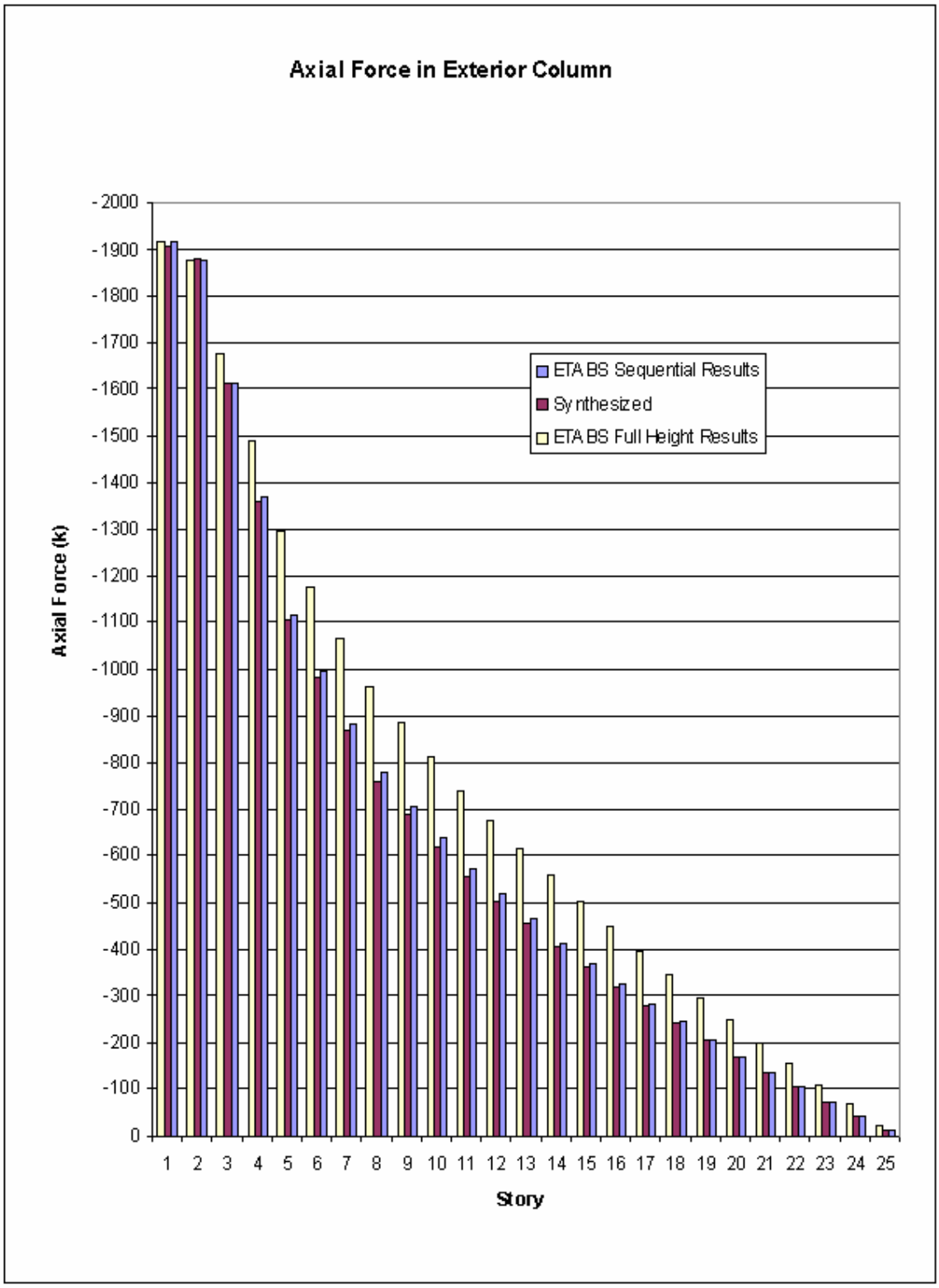

Figure 5.7 Axial Force in Exterior Columns due to Staged Load – 25 Story Prototype

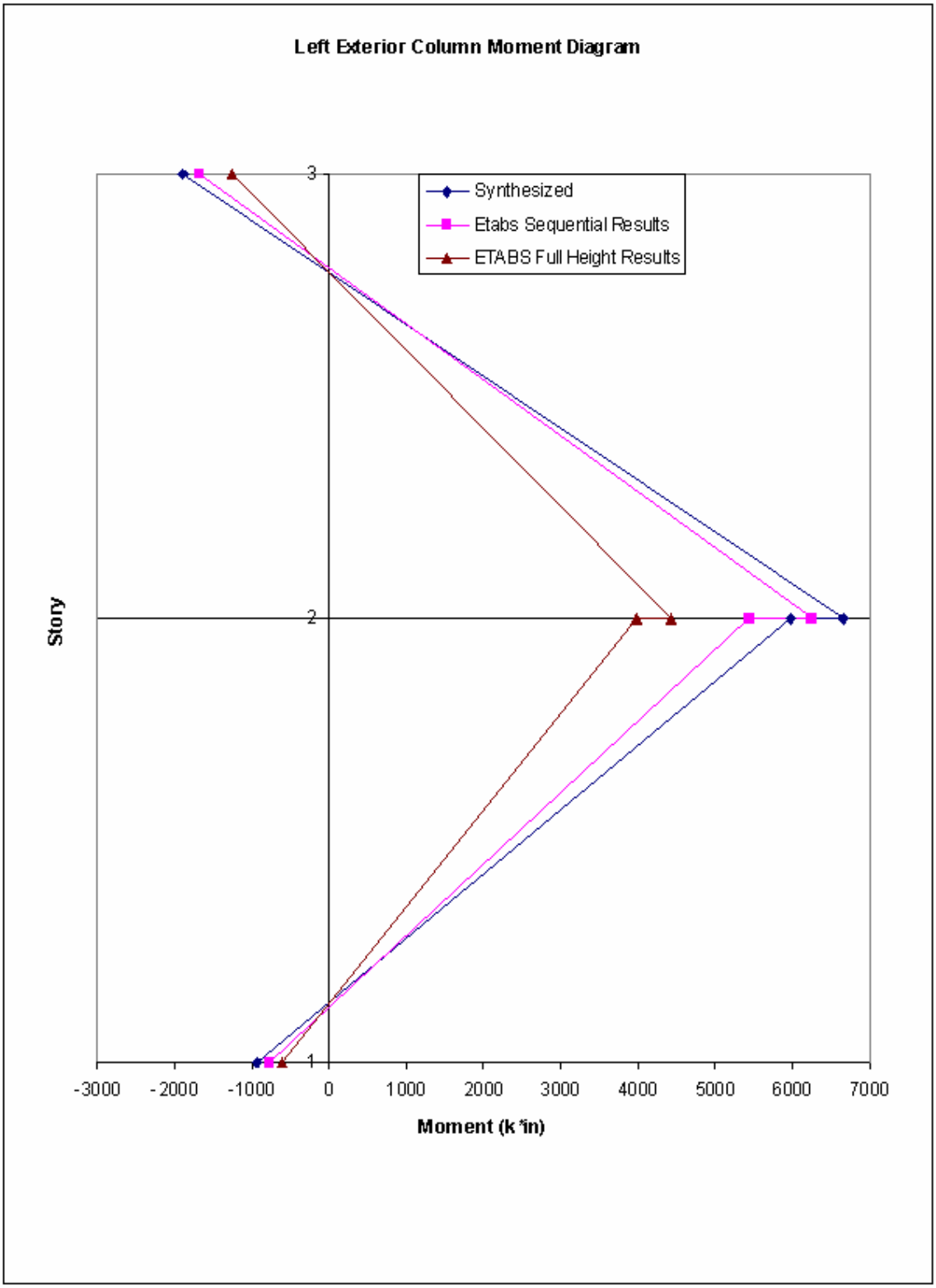

Figure 5.8 Moment in Lowest Two Left Exterior Columns due to Staged Load – 25 Story Prototype

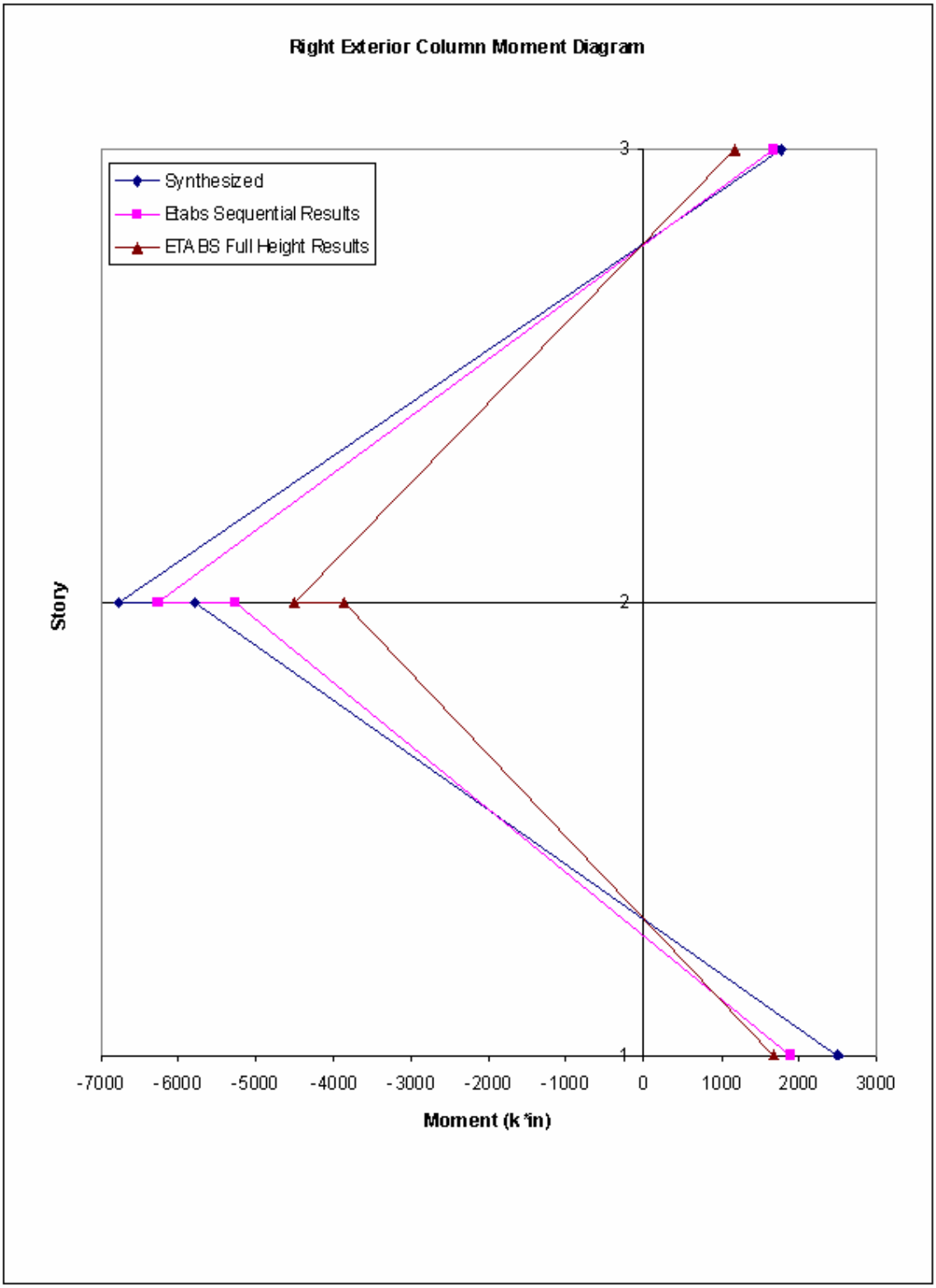

Figure 5.9 Moment in Lowest Two Right Exterior Columns due to Staged Load – 25 Story Prototype

5.5 Serviceability

When evaluating the serviceability criteria of the 25 story prototype, three aspects of the frame deflection were considered: the drift due to lateral load, the individual beam deflection due to gravity load, and the truss section deflections due to the gravity load. The drift results of the 25 story FHTF illustrate its impressive stiffness to lateral load. A typical limitation put on a building's drift is its height divided by a factor of 200. For a 25 story building with a height of 228 ft, this would limit the drift to approximately 14 inches. The 25 story FHTF prototype drifts approximately 5 ½ inches far surpassing common criteria and the more restrictive criterion of H/400. The drift along each exterior column line at each floor is recorded in Table 5.10. The largest inter-story drift was at the first and second level due to the bending of the composite columns; however, the composite columns limit this drift to less than H/200, where H is the column height. This bending in these columns could be reduced by the addition of bracing at the lowest level in the exterior FHTFs of the building. Some of the lateral loads would be redirected to this bracing by the rigid diaphragm of the planking floor system.

The deflection at the center span of the floor beams were checked against standard deflection limitations. The dead load deflection was limited to L/240 and the live load deflection to L/500, where L is the span of the beam. This limits dead load deflection to 1.3 inches for the exterior bay beams and 1 inch for the interior corridor beams. The live load deflections of the exterior and interior beams are limited to 0.62 inches and 0.5 inches. All beams meet these requirements, therefore member camber is unnecessary,

but the engineer might desire cambering against the dead load. The deflections for each beam at each story level are recorded in Table 5.11.

The deflection of the truss at its interior panel points was limited to L/500 under the service load condition, where L is the span of the truss. This limits the truss to a downward deflection of 1.73 inches at its interior joints. The greatest deflection of the truss occurred on the first truss section erected, and under service load conditions underwent a downward deflection of approximately 2.1 inches. This deflection is almost identical to the maximum deflection observed in the 10 story FHTF. The least deflection of the truss occurred on the eighth and final truss section and totaled approximately 0.4 inches under service load conditions. The service load deflection of the second through seventh truss section erected varied between 0.5 inches at the seventh truss section and 1.7 inches at the second truss section. Therefore, during the erection of the first stage truss, the floor truss must be assembled with camber from the exterior panel point to the interior panel point. The truss deflections at the interior panel points are shown in Table 5.12.

Table 5.10 FHTF Drift – 25 Story Prototype

Story	Drift Column Line A (in)	Drift Column Line B (in)	Maximum Inter-Story Drift (in)	H/200	H/400
25	5.52	5.39	0.17	0.54	0.27
24	5.35	5.27	0.17	0.54	0.27
23	5.18	5.12	0.14	0.54	0.27
22	5.08	4.98	0.19	0.54	0.27
21	4.89	4.80	0.20	0.54	0.27
20	4.69	4.61	0.19	0.54	0.27
19	4.54	4.42	0.22	0.54	0.27
18	4.32	4.21	0.23	0.54	0.27
17	4.09	3.98	0.24	0.54	0.27
16	3.91	3.74	0.25	0.54	0.27
15	3.66	3.50	0.26	0.54	0.27
14	3.40	3.24	0.27	0.54	0.27
13	3.18	2.98	0.27	0.54	0.27
12	2.91	2.72	0.28	0.54	0.27
11	2.63	2.44	0.30	0.54	0.27
10	2.40	2.14	0.28	0.54	0.27
9	2.12	1.88	0.27	0.54	0.27
8	1.86	1.61	0.27	0.54	0.27
7	1.68	1.34	0.25	0.54	0.27
6	1.43	1.11	0.22	0.54	0.27
5	1.21	0.89	0.21	0.54	0.27
4	1.11	0.68	0.23	0.54	0.27
3	0.88	0.50	0.28	0.54	0.27
2	0.60	0.34	0.37	0.54	0.27
1	0.23	0.18	0.23	0.72	0.36

Table 5.11 Beam Deflection at Center Spans – 25 Story Prototype

	Beam Deflection					
	Exterior Beam			Interior Corridor Beam		
Story	Dead (in)	Sdead (in)	Live (in)	Dead (in)	Sdead (in)	Live (in)
25	0.70		0.32	0.09		0.05
24	0.79	0.14	0.19	0.22	0.04	0.14
23	0.79	0.14	0.19	0.23	0.04	0.13
22	0.79	0.14	0.19	0.20	0.04	0.12
21	0.79	0.14	0.19	0.17	0.03	0.10
20	0.78	0.14	0.19	0.17	0.03	0.10
19	0.78	0.14	0.19	0.15	0.03	0.09
18	0.77	0.14	0.19	0.14	0.03	0.08
17	0.77	0.14	0.19	0.14	0.03	0.08
16	0.77	0.14	0.19	0.13	0.02	0.08
15	0.77	0.14	0.19	0.13	0.02	0.08
14	0.77	0.14	0.19	0.12	0.02	0.07
13	0.67	0.12	0.16	0.12	0.02	0.07
12	0.67	0.12	0.16	0.12	0.02	0.07
11	0.67	0.12	0.16	0.1	0.02	0.06
10	0.47	0.09	0.11	0.1	0.02	0.06
9	0.47	0.09	0.11	0.1	0.02	0.06
8	0.47	0.09	0.11	0.08	0.02	0.05
7	0.35	0.06	0.09	0.08	0.01	0.05
6	0.35	0.06	0.09	0.1	0.02	0.06
5	0.31	0.06	0.09	0.08	0.02	0.05
4	0.17	0.03	0.04	0.05	0.01	0.03
3	0.17	0.03	0.04	0.13	0.02	0.07
2	0.17	0.03	0.04	0.12	0.02	0.06
1	0.41	0.07	0.1	0.06	0.01	0.03

Table 5.12 Truss Deflection at Interior Joints – 25 Story Prototype

	Deflection at Interior Joints			
Story	Seq. Dead (in)	Super dead (in)	Live (in)	Total (in)
25	0.12	0.08	0.16	0.36
24	0.11	0.08	0.17	0.36
23	0.10	0.08	0.17	0.35
22	0.21	0.08	0.17	0.46
21	0.21	0.09	0.18	0.48
20	0.20	0.09	0.18	0.47
19	0.32	0.10	0.19	0.61
18	0.32	0.10	0.20	0.62
17	0.31	0.11	0.21	0.63
16	0.46	0.11	0.22	0.79
15	0.46	0.12	0.23	0.81
14	0.46	0.13	0.24	0.83
13	0.63	0.13	0.25	1.01
12	0.64	0.14	0.26	1.04
11	0.64	0.15	0.28	1.07
10	0.85	0.16	0.29	1.30
9	0.85	0.16	0.30	1.31
8	0.86	0.17	0.31	1.34
7	1.11	0.18	0.32	1.61
6	1.11	0.18	0.33	1.62
5	1.12	0.20	0.34	1.66
4	1.60	0.20	0.35	2.15
3	1.56	0.19	0.34	2.09
2	1.55	0.19	0.34	2.08
1	1.55	0.20	0.35	2.10

5.6 Economy

The 25 Story prototype derives its economic advantage for the same reasons as the 10 Story Prototype: the lightweight frame and the simplicity of the configuration, fabrication, and erection. Both the 10 story and 25 story prototypes achieved a 9' floor to floor height, provided a column free first level, and carried all wind loads to the foundation without an additional lateral system.

The 25 story prototype was compared to a similar 25 story staggered truss model using ETABS staggered truss template and AISC LRFD-99 design function. The staggered truss frame and sections are illustrated in Figure 5.10. The ETABS design included an additional lateral bracing system for taking the wind load from the lowest truss to the foundation to avoid excessive column shear and moment. The staggered truss model did not incorporate any composite columns; the lowest four columns are heavy steel W14 members. The result of the design was a staggered truss frame weighing 232,720 pounds or an average of 5.125 psf. The FHTF weighs an additional 1,780 pounds in steel and uses 19.08 cubic yards of high strength concrete weighing 77,700 pounds. With the concrete, the prototype weighed 6.94 psf; without the concrete, the average weight of steel was 5.21 psf. The cost of the increase in material of the FHTF can be offset by truss fabrication costs of the staggered truss.

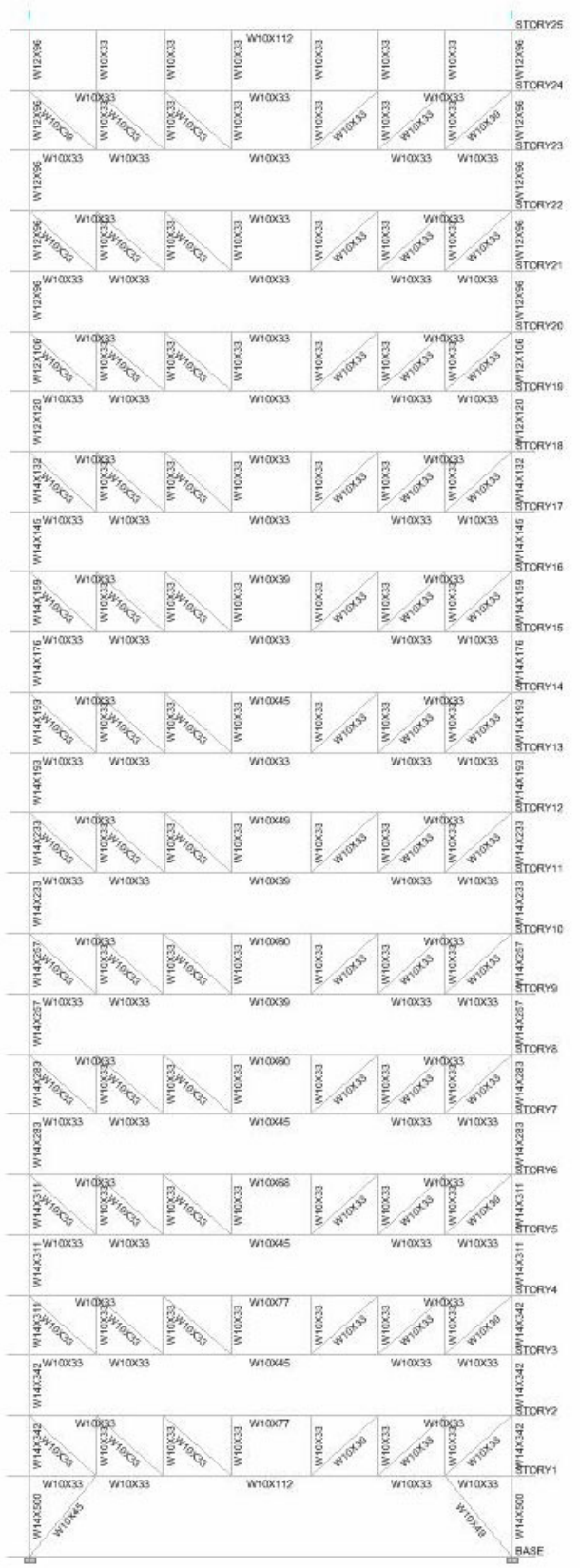

Figure 5.10 Staggered Truss Sections from ETABS Design

CHAPTER 6

CONCLUSION

This chapter addresses the conclusions that were reached as a result of the research related to the design and analysis of the FHTF. Also discussed is additional research concerning the design of FHTF systems that needs to be completed.

6.1 Research Conclusions

First, FHTF systems can be designed using preexisting design procedure. The FHTF is comprised of traditional steel shapes that can be designed according to tested capacity and interaction equations. This results in an economical frame that performs beyond standard serviceability limits.

Given the constraints of a typical residential multi-story building, the FHTF can perform as a low floor to floor height structural steel system. The FHTF can accommodate the floor plan requirements of apartment towers, hotel buildings, and other residential builds utilizing units serviced by a central corridor. The units are separated at each frame line thus only limiting the depth of the corridor beam between the two outer bay beams. The diagonals, columns, and other beams are hidden within the walls of the units. If needed, alterations can be made to the frame to allow for doorway connections between desired units.

The FHTF performs as an adequate lateral system for resisting wind forces. The prototype frames exhibited the framing system's strong lateral stiffness. Inter-story drift calculated was below conventional limits. Above the first story, the lateral load is carried down the structure by direct stress in the diagonal members, but at the lowest level the exterior column carries the load in bending to the foundation. For this reason, high strength composite columns were used in the lower levels of the 25 story model to increase the flexural stiffness. If needed or desired, additional lateral systems can be introduced to carry the load from the last diagonal to the foundation.

The numerical method as outlined in Chapter 3 of estimating the sequential construction loads on the FHTF can be used as a time saving feature in place of a correctly modeled sequential analysis. The comparison between the synthesized and the ETABS analysis for both prototypes showed a fair convergence of the results. This makes the synthesized method a valuable tool for predicting the frame behavior under dead load due to any sequence of construction to optimize the framing element construction sequence versus the planking sequence.

Lastly, The FHTF is competitive with the staggered truss in terms of material usage, fabrication, and construction. The FHTF is comprised of traditional rolled steel shapes and connections; no special member fabrication is needed. It can be built using conventional stick construction practices. The FHTF can be a viable framing system for use in a variety of buildings.

6.2 Future Work

More work can be done to facilitate the design and analysis of FHTFs, encourage their use in the industry, and to better understand their behavior. In no deliberate order, this work includes:

- Establish the lateral response of the FHTF to earthquake loads.
- Improve sequential modeling in computer analysis tools.
- Establish collapse mechanisms to insure adequate margins of safety.
- Investigate framing details between the planking and exterior bay beams to minimize the impact of their large depths.
- Investigate framing and connections details between planking and beams to develop composite action.
- Establish economical shapes to use for various elements of the FHTF.
- Compare economy of system with flat plate concrete systems.

APPENDIX A

SYNTHESIS EXAMPLE

The force in the diagonals after the structure has been erected is dependent on the sequence of construction shown in Figure A.1.

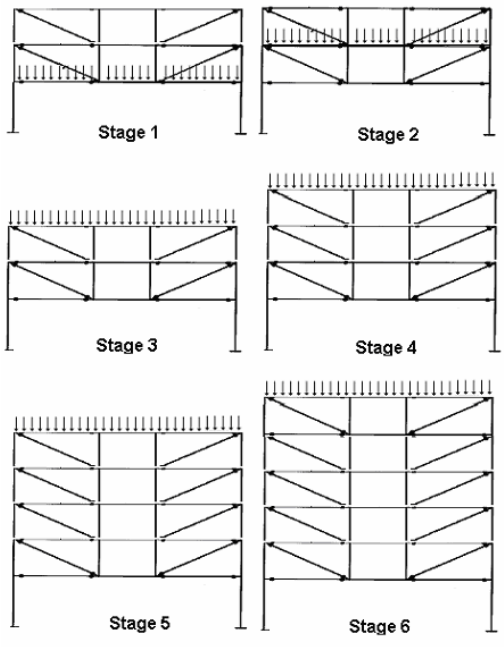

Figure A.1 Construction Sequence

At each construction stage, dead loads due to the weight of the new frame members and the weight of the floor system are added. The load at each stage is given in Table A.1 in terms of pounds per square foot.

Table A.1 Dead Load Applied at Each Stage

	Stage					
	1	**2**	**3**	**4**	**5**	**6**
Dead Load Applied at Each Stage, D_m (psf)	80	80	80	80	80	80

The tributary area of the interior column can be calculated from the frame configuration shown in Figure A.2.

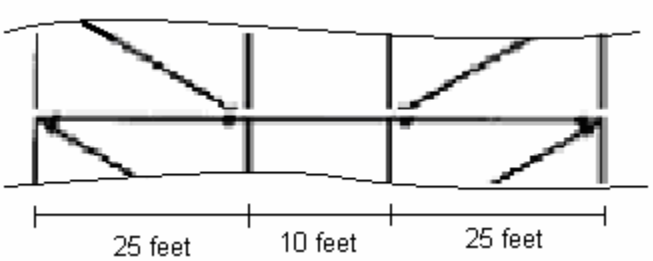

Figure A.2 Frame Configuration

The Frame spacing is 21.4 feet in and out of the page. The tributary area of the interior verticals is then:

$$A_T = \left(25'/2 + 10'/2\right)\ 21.4' = 374.5\ ft^2$$

By multiplying the tributary area of the interior vertical with the dead load applied at each stage, the dead load collected at the interior columns to be carried by the diagonals can be calculated for each stage as shown in Table A.2.

Table A.2 Dead Load Collected at Interior Vertical

	Stage					
	1	**2**	**3**	**4**	**5**	**6**
Dead Load Collected at Interior Vertical, $V_m = D_m A_T$ **(K)**	30	30	30	30	30	30

The full height diagonal forces at each stage can be calculated by the distribution of tension in the diagonals and the total load carried by the diagonals at a stage. Figures

A.3, A.4, and A.5 illustrate this calculation. The full height diagonal forces at each stage are tabulated in Table A.3.

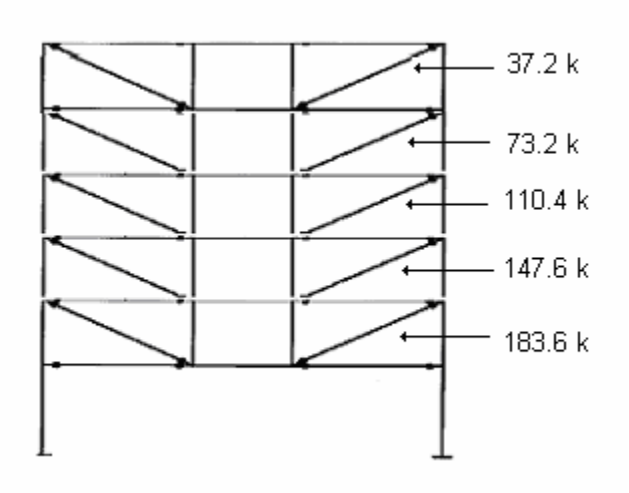

Figure A.3 Full Height Diagonal Forces

To calculate the distrubtion of force between the diagonal, the tension carried by a diagonal is divided by the sum of tension carried by all diagonals.

Story 6 $$\frac{37.2}{37.2+73.2+110.4+147.6+183.6}=0.067$$

Story 5 $$\frac{73.2}{37.2+73.2+110.4+147.6+183.6}=0.133$$

Story 4 $$\frac{110.4}{37.2+73.2+110.4+147.6+183.6}=0.2$$

Story 3 $$\frac{147.6}{37.2+73.2+110.4+147.6+183.6}=0.267$$

Story 2 $$\frac{183.6}{37.2+73.2+110.4+147.6+183.6}=0.333$$

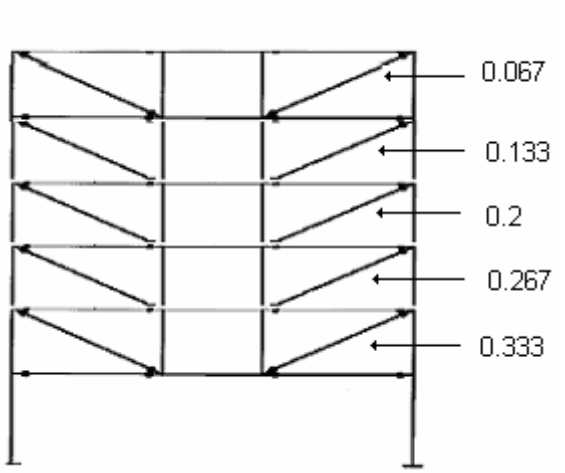

Figure A.4 Distribution of Force Between Diagonals

By multiplying these distribution factors with the sum of the tension force in all diagonals at each stage, the tension in each diagonal can be approximated at each stage. Take stage 3 where 30 kips in the downward direction are collected at each interior vertical.

Story 6: $$0.067\left(\frac{30}{\sin(19)}\right) = 6.2 \ k$$

Story 5: $$0.133\left(\frac{30}{\sin(19)}\right) = 12.2 \ k$$

Story 4: $$0.2\left(\frac{30}{\sin(19)}\right) = 18.4 \ k$$

Story 3: $$0.267\left(\frac{30}{\sin(19)}\right) = 24.6 \ k$$

Story 2: $$0.333\left(\frac{30}{\sin(19)}\right) = 30.6 \ k$$

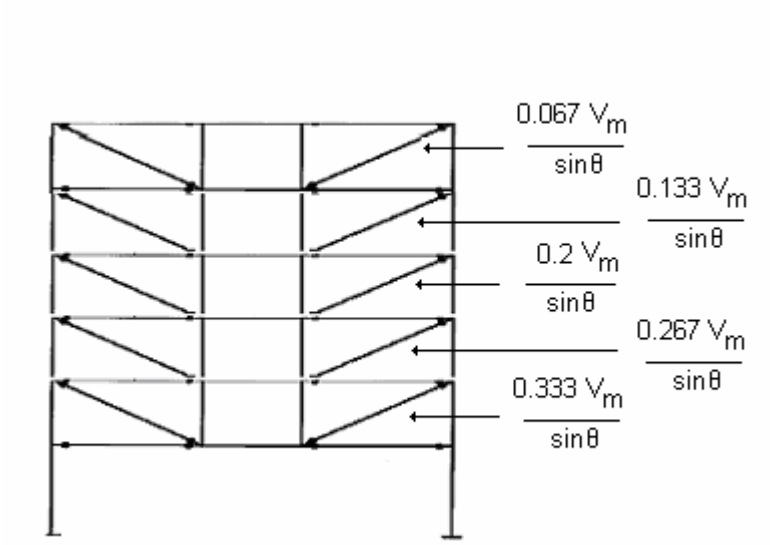

Figure A.5 Full Height Diagonal Forces due to a Stage Loading

Table A.3 Full Height Diagonal Forces at Each Stage

Story	Full Height Diagonal Forces at Stage (k)					
	1	2	3	4	5	6
6	6.2	6.2	6.2	6.2	6.2	6.2
5	12.2	12.2	12.2	12.2	12.2	12.2
4	18.4	18.4	18.4	18.4	18.4	18.4
3	24.6	24.6	24.6	24.6	24.6	24.6
2	30.6	30.6	30.6	30.6	30.6	30.6

The force values shown in Table A.3 are an approximation of the full height diagonal forces at each stage. These forces multiplied by the "force" factor *k* result in the sequential diagonal force. The "force" factor is calculated at each stage and is the sum of full height diagonal forces of all diagonals divided by the sum of full height diagonal forces of the diagonals present in the staged model. Figures A.6 through A.11 are a comparison between the full height and staged model.

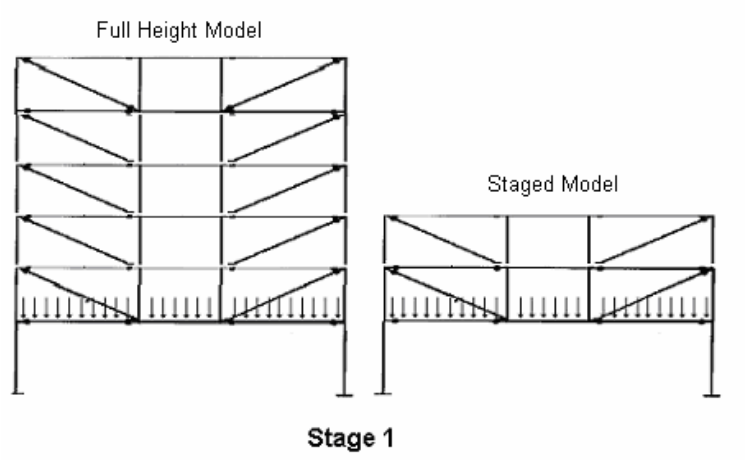

Figure A.6 Stage One

Using the forces from Table A.3 for stage one and considering the models in Figure A.6:

$$k_1 = \frac{30.6 + 24.6 + 18.4 + 12.2 + 6.2}{30.6 + 24.6} = 1.67$$

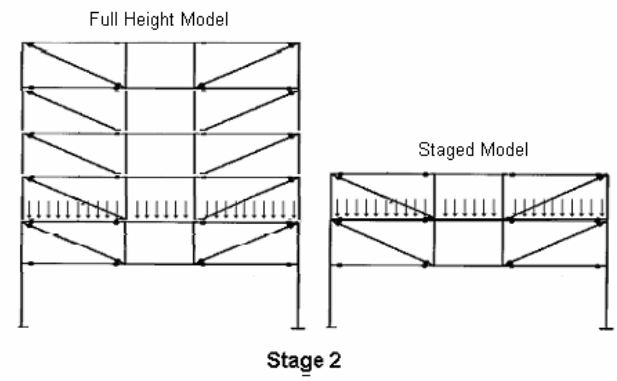

Figure A.7 Stage Two

Using the forces from Table A.3 for stage two and considering the models in Figure A.7:

$$k_2 = \frac{30.6 + 24.6 + 18.4 + 12.2 + 6.2}{30.6 + 24.6} = 1.67$$

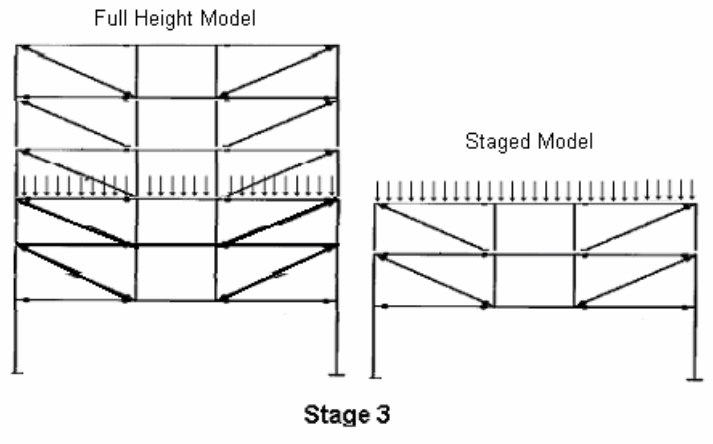

Figure A.8 Stage Three

Using the forces from Table A.3 for stage three and considering the models in Figure A.8:

$$k_3 = \frac{30.6 + 24.6 + 18.4 + 12.2 + 6.2}{30.6 + 24.6} = 1.67$$

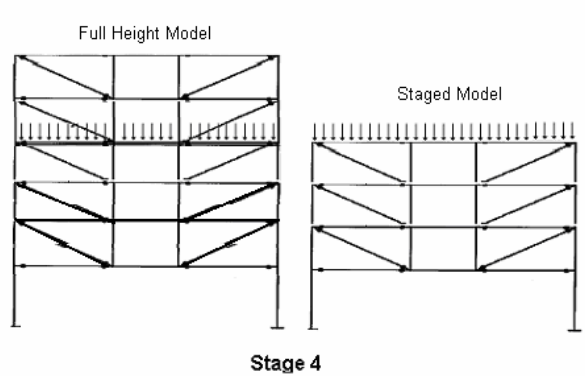

Figure A.9 Stage Four

Using the forces from Table A.3 for stage four and considering the models in Figure A.9:

$$k_4 = \frac{30.6 + 24.6 + 18.4 + 12.2 + 6.2}{30.6 + 24.6 + 18.4} = 1.25$$

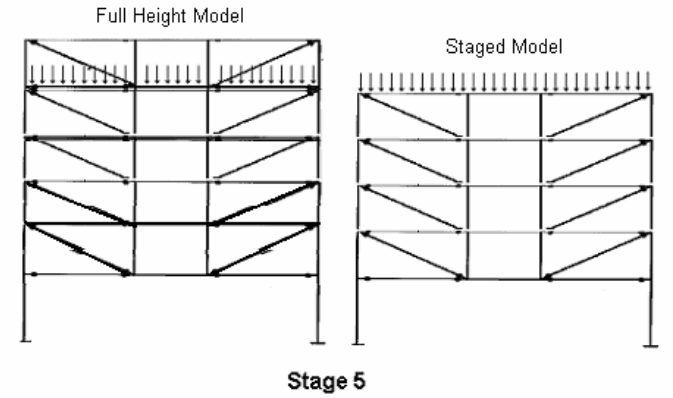

Figure A.10 Stage Five

Using the forces from Table A.3 for stage five and considering the models in Figure A.10:

$$k_5 = \frac{30.6 + 24.6 + 18.4 + 12.2 + 6.2}{30.6 + 24.6 + 18.4 + 12.2} = 1.07$$

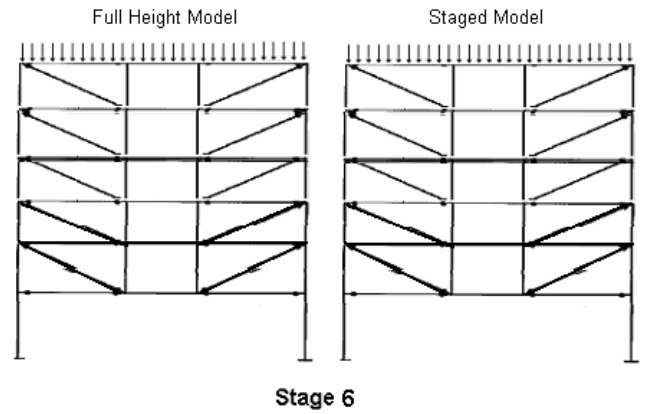

Figure A.11 Stage Six

Using the forces from Table A.3 for stage six and considering the models in Figure A.10:

$$k_6 = \frac{30.6 + 24.6 + 18.4 + 12.2 + 6.2}{30.6 + 24.6 + 18.4 + 12.2 + 6.2} = 1$$

Table A.4 is a collection of the "force" factor at each stage.

Table A.4 "Force" Factors Tabulated at Each Stage

	Stage					
	1	**2**	**3**	**4**	**5**	**6**
"Force" Factor, k_m $k_m = \left(\frac{\sum_{1}^{n_1} F_{FULL\ HEIGHT}}{\sum_{1}^{n_2} F_{FULL\ HEIGHT}} \right)_m$	1.67	1.67	1.67	1.25	1.07	1.00

Now the staged diagonal forces at each stage can be calculated by multiplying the full height diagonal forces for each stage from Table A.3 by the force factor.

Stage One:

Story 3: $1.67(24.6) = 41\,\text{k}$

Story 2: $1.67(30.6) = 51\ \text{k}$

Stage Two:

Story 3: $1.67(24.6) = 41\,\text{k}$

Story 2: $1.67(30.6) = 51\ \text{k}$

Stage Three:

Story 3: $1.67(24.6) = 41\,\text{k}$

Story 2: $1.67(30.6) = 51\ \text{k}$

Stage Four:

Story 4: 1.25(18.4) = 23 k

Story 3: 1.25(24.6) = 31 k

Story 2: 1.25(30.6) = 38 k

Stage Five:

Story 5: 1.07(12.2) = 13 k

Story 4: 1.07(18.4) = 20 k

Story 3: 1.07(24.6) = 26 k

Story 2: 1.07(30.6) = 33 k

Stage Six:

Story 6: 1(6.2) = 6.2 k

Story 5: 1(12.2) = 12.2 k

Story 4: 1(18.4) = 18.4 k

Story 3: 1(24.6) = 24.6 k

Story 2: 1(30.6) = 30.6 k

These force values are tabulated in Table A.5 by stage and summed to calculate the final tension forces due to the staged loading and model.

Table A.5 Diagonal Forces in Staged Model at Each Stage

	Diagonal Tension Forces in Staged Model at Each Stage						
	Stage						
Story	**1**	**2**	**3**	**4**	**5**	**6**	**Sum**
6	0	0	0	0	0	6	**6**
5	0	0	0	0	13	12	**25**
4	0	0	0	23	20	18	**61**
3	41	41	41	31	26	25	**204**
2	51	51	51	38	33	31	**256**

REFERENCES

American Institute of Steel construction (AISC). (1992). Steel Design Guide Series: Load and Resistance Factor Design of W-Shapes Encased in Concrete.

American Institute of Steel Construction (AISC). (2001). Manual of Steel Construction. Load and Resistance Factor Design for Structural steel Buildings (LRFD). Third edition.

American Institute of Steel construction (AISC). (2002). Steel Design Guide Series: Staggered Truss Framing Systems.

American Institute of Steel Construction (AISC). (2004a). Specification for Structural Steel Buildings. Draft.

American Institute of Steel Construction (AISC). (2004b). Commentary to The Specification for Structural Steel Buildings. Draft.

American Society of Civil Engineers (ASCE). (2003). Minimum Design Loads for Buildings and Other Structures. (ASCE 7-02). ASCE, Reston, VA.

Brazil, Aine. (2000). "Staggered Truss System Proves Economical for Hotels." Modern Steel Construction. September

Cheong-Siat-Moy, Francois. (1997). "K-factors for Braced Frames." Engineering Structures. V 19 n 9. pp760-763.

Choi, C. -K. and Kim, E. -D. (1985). "Multistory Frames Under Sequential Gravity Loads." Journal of Structural Engineering, v 111. ASCE. pp2373-2384.

Choi, C. -K; Chung H. -K.; Lee, D. -G and Wilson, E. L. (1992). "Simplified Building Analysis with Sequential Dead Loads - CFM." Journal of Structural Engineering, v 118, n 4. ASCE. Pp944-954.

Choi, C. -K and Chung, H. -K. (1993). "Correction Factor Method for Building Analysis Under Sequential Dead Loads." Structural Engineering in Natural Hazards Mitigation. pp1095-1100.

Cohen, Michael P. (1986). "Design Solutions Utilizing the Staggered-steel Truss System." Engineering Journal. Third Quarter. AISC. pp97-106.

Computers and Structures, Inc (CSI). (1984-2004). ETABS Nonlinear Version 8.4.3: Extended 3D Analysis of Building Structures. Berkeley, CA.

Cross, John. (2003). "Coordinated Construction." Modern Steel Construction. July.

Ellingwood, Bruce (1989). "Serviceability Guidelines for Steel Structures." Engineering Journal. First Quarter. AISC. pp.1-8.

Faraone, Tom. (2003). "Real-Life Adventures in Staggered Truss Framing." Modern Steel Construction. May.

Faraone, Tom and Marstellar Bobbi. (2002). "Anatomy of a Staggered Truss." Modern Steel Construction. September.

Girder-Slab Technologies, LLC. (2005). Design Guide Version 1.2.

LeMessurier, WM. J. (1976). "A Practical Method of Second Order Analysis: Part 1 – Pin Joints." Engineering Journal. Fourth Quarter. AISC. pp89-96.

LeMessurier, WM. J. (1977). "A Practical Method of Second Order Analysis: Part 2 – Rigid Frames." Engineering Journal. Second Quarter. AISC. pp49-67.

Levy, Matthys. (2000) "Staggered Truss System Earns an A^{+}." Modern Steel Construction. Novermber

Lui, Eric M. (1988). "A Practical P-Delta Analysis Method for Type FR and PR Frames." Engineering Journal. Third Quarter. AISC. pp85-98

Maleck, A. E. and White, Donald W. (2003a), "Alternative Approaches for Elastic Analysis and Design of Steel Frames. I: Overview." ASCE *Journal of Structural Engineering, submitted for review.*

Maleck, A. E. and White, Donald W. (2003b), "Alternative Approaches for Elastic Analysis and Design of Steel Frames. II: Verification Studies." ASCE *Journal of Structural Engineering, submitted for review.*

Maleck, A. E. and White, Donald W. (2003c), "Direct Analysis Approach for the Assessment of Frame Stability: Verification Studies," ASCE *Journal of Structural Engineering, submitted for review.*

Naccarato, Peter A. (1999). "New Alternative to Flat Plate Construction." Modern Steel Construction. December.

Naccarato, Peter A. (2000). "Superstructure Completed in Just Eight Weeks." Modern Steel Construction. September.

Naccarato, Peter A. (2001). "Steel and Precast Slab Construction System for Mid and High-Rise Residential Buildings." Modern Steel Construction. May.

Pollak, Beth. (2003). "Staggered Truss Solution." Modern Steel Construction. July.

Pouangare, C. C. and Connor, J. J. (1995). "New Structural Systems for Tall Buildings: The Space-Truss Concept." The Structural Design of Tall Buildings, Vol. 4. pp155-168.

Scalzi, John B. (1971). "The Staggered Truss System – Structural Considerations." Engineering Journal. October. AISC. pp138-143.

Taranath, Bungale S. (1997). Steel, Concrete, and Composite Design of Tall Buildings. Second Edition. McGraw-hill, New York.

Veitas, Rimas. (2002). "Slab Solution." Modern Steel construction. May.

White, Donald W. and Hajjar, Jerome F. (1991). "Application of Second-Order Elastic Analysis in LRFD – Research to Practive." Engineering Journal. Fourth Quarter. AISC. pp133-148.

Ziemain, Ronald D. and McGuire, William. (1992). "A Method for Incorporating Live Load Reduction Provisions in Frame Analysis." Engineering Journal. First Quarter. AISC. pp1-3.

Ziemain, Ronald D. and McGuire, William. (2000). MASTAN2 Version 1.0.